José António Breyer Rodrigues Vieira
Licenciado em Engenharia Biotecnológica

Valorization of Pumpkin Residue by Supercritical Extraction of Added-Value Compounds

Dissertação para a obtenção do Grau de Mestre
em Engenharia Química e Bioquímica

Orientador: Dr. Alexandre Paiva, Investigador Post-Doc, FCT UNL
Co-Orientador: Prof. Dr. Pedro Simões, Professor Auxiliar, FCT UNL

Júri:

Presidente: Prof. Dr. José Paulo Mota
Arguente: Dr. Ana Vital Nunes
Vogal: Dr. Alexandre Paiva

FACULDADE DE CIÊNCIAS E TECNOLOGIA
UNIVERSIDADE NOVA DE LISBOA

Março 2014

Valorization of Pumpkin Residue by Supercritical Extraction of Added-Value Compounds

À MINHA FAMÍLIA.

"Wer andere bezwingt, ist kraftvoll. Wer sich selbst bezwingt, ist unbezwingbar."

Laotse "O Velho"

Acknowledgments

Na realização deste projeto contei com a ajuda de várias pessoas, sem as quais não seria possível atingir a sua conclusão. Gostaria de agradecer a todos aqueles que, contribuindo com o seu conhecimento, apoio, ânimo e constante disponibilidade, permitiram-me enriquecer como pessoa, tanto a nível intelectual como pessoal.

Ao Doutor Alexandre Paiva expresso o meu profundo agradecimento pela orientação e apoio incondicional que permitiu elevar os meus conhecimentos neste mundo que são os fluidos supercríticos. Um muito obrigado pelos conselhos dados e todo o apoio prestado!

O meu sincero agradecimento ao Professor Doutor Pedro Simões, pelo tempo disponibilizado e esclarecimentos técnicos a nível de engenharia prestados. Obrigado por fazer este trabalho de estudante algo mais real e "engenheiral".

Agradeço igualmente à Professora Susana Barreiros, responsável pelo laboratório 427, por aceitar a minha entrada e pela ajuda prestada ao longo deste período. Muito obrigado.

À Carmen, agradeço por toda a ajuda que me deste ao longo deste árduo trabalho académico. Sem ti, teria sido mais difícil orientar-me na instalação de fluidos supercríticos. Tornaste-te uma pessoa muito importante no meu dia-a-dia. Agradeço-te muito pela disponibilidade e dedicação!

Ao Pedro Lisboa, um sincero agradecimento pela dedicação e tempo disponibilizado na realização do modelo matemático, por todo o conhecimento transmitido. Conhecimento esse que foi essencial para que chegasse ao fim deste trabalho com enorme sentimento de satisfação.

A todo o pessoal do laboratório 427, um grande agradecimento, pelo ótimo ambiente de trabalho, espírito de equipa e toda a ajuda prestada no decorrer deste projeto.

A todos os meus amigos, agradeço pelos intermináveis desabafos e pela partilha de bons e menos bons momentos. Pela amizade, companhia, pelo apoio nos momentos de maior angustia, e pela confiança que em mim depositam.

À minha namorada, Filipa, muito obrigado pela confiança e valorização sempre tão entusiasta do meu trabalho, transmitindo-me desta forma, coragem para ultrapassar e finalizar este árduo percurso. Quero agradecer sobretudo pela pessoa que és, e por todo o teu carinho, amizade e paciência que tens comigo. Muito obrigado tótó ;)

À minha família, em especial aos meus pais e à minha irmã, um enorme obrigado por acreditarem sempre em mim, assim como todos os ensinamentos de vida que me têm transmitido. Espero que esta etapa que agora termino, possa de alguma forma, retribuir e compensar todo o carinho, apoio e dedicação que me foi oferecido. A vocês dedico este trabalho.

O meu SINCERO OBRIGADO a todos!

Abstract

The aim of this thesis is the extraction of β-carotene from a renewable source – pumpkin residue, via an environmental friendly extraction process with a supercritical fluid – carbon dioxide. The supercritical carbon dioxide is passed through a packed-bed extractor with the pumpkin residue, which extracts the pumpkin oil containing the added-value compound – β-carotene.

In the first part of this work it was demonstrated, throughout a set of experiments that is possible to extract 66 $\mu g_{\beta\text{-carotene}}/g_{Pumpkin}$, at 325,15 K, 260 bar, and solvent flow rate of 10 g_{CO2}/min. The influence of ethanol, as a co-solvent, was also studied. When the co-solvent was added, a higher yield of extraction was achieved – 533 $\mu g_{\beta\text{-carotene}}/g_{Pumpkin}$ – at 325,15 K, 260 bar, 30 g_{CO2}/min, and a co-solvent flow rate of 3 g_{EtOH}/min.

The mathematical modeling of the oil extraction process was carried out, as a second part of this work. The effective diffusion coefficient (D_e) that predicts the solute diffusion inside the solid particle of the extractor bed, was estimated, varying from 1,12E-16 to 3,73E-16 $m^2.s^{-1}$.

Keywords: β-carotene, Pumpkin Residue, Carbon Dioxide, Supercritical Fluid, Ethanol, Mathematical Modeling, Effective Diffusion Coefficient

Resumo

O objetivo da presente tese consiste na extração de β-caroteno a partir de uma fonte renovável – resíduo de abóbora, através de um processo de extração "verde" com um fluido supercrítico – dióxido de carbono. Neste processo, o dióxido de carbono supercrítico, passa por um extrator empacotado com o resíduo de abóbora, que extraí o óleo da abóbora que contem o composto de valor acrescentado – β-caroteno.

Na primeira fase deste trabalho foi demonstrado, ao longo de um conjunto de experiências, que é possível extrair 66 $\mu g_{\beta\text{-caroteno}}/g_{Abóbora}$, a 325,15K, 260 bar, e com um caudal de solvente de 10 g_{CO2}/min. A influência da presença de um co-solvente (etanol) foi também estudada. Ao adicionar-se o etanol ao processo de extração, o rendimento obtido foi maior – 533 $\mu g_{\beta\text{-caroteno}}/g_{Abóbora}$, nas respetivas condições: 325,15K, 260 bar, 30 g_{CO2}/min, e 3 g_{EtOH}/min.

Como segunda fase desta tese, a modelação matemática do processo de extração de óleo foi feita. O coeficiente de difusão efetivo (D_e) que permite prever a difusão do soluto no interior da partícula sólida do leito do extrator, foi estimado, variando entre 1,12E-16 e 3,73E-16 $m^2.s^{-1}$

Palavras-Chave: β-caroteno, Resíduo de Abóbora, Dióxido de Carbono, Fluido Supercrítico, Etanol, Modelação Matemática, Coeficiente de Difusão Efetiva

Table of Contents

1. Introduction 1
1.1. Motivation 1
1.1.1. Agro-Food Industry – Environmental Safety and Residue Production Management 1
1.1.2. *Cucurbita moschata* – Growth, Characteristics and Properties 5
1.2. Value-Added Compounds 9
1.1.1. Carotenoids 10
1.1.2. Fatty Acids and Triglycerides 18
1.2. Extraction Processes to Obtain Pumpkin Oil 21
1.2.1. Mechanical, Organic Solvent, and Other Extraction Processes 21
1.2.2. Supercritical Fluids 23
2. Materials and Methods 33
2.1. Materials 33
2.1.1. Raw Materials, Chemicals and Compounds 33
2.2. Methods 34
2.2.1. Soxhlet Extraction 34
2.2.2. *Bligh and Dyer* Method 35
2.2.3. Supercritical Fluid Extraction 36
2.2.4. Mathematical Model – Gproms® Software 37
2.3. Experimental Set-Up 38
2.3.1. High-Pressure Installation for Oil Extraction 38
2.4. Sample Analysis 41
2.4.1. Direct Transesterification – Lepage & Roy Method 41
2.4.2. Gas Chromatography 42
2.4.3. High Performance Liquid Chromatography 45
2.4.4. UV Spectrophotometry 46
3. Results and Discussion 47
3.1. Pumpkin Oil Analysis 47
3.1.1. Oil Extraction with Soxhlet Apparatus 47
3.1.2. Oil Extraction by *Bligh and Dyer* Method 48
3.1.3. Oil Extraction with SC-CO_2 49
3.2. Pumpkin Oil Extraction with SC-CO_2 52
3.2.1. Influence of Pumpkin Humidity in scCO_2 Oil and β-carotene Extraction 53

3.2.2. SC-CO_2 Flow Rate Influence in Pumpkin Oil and β-carotene Extraction 55
3.2.3. Influence of Co-solvent Presence in scCO_2 Oil and β-carotene Extraction 59
3.2.4. Understanding Experimental Data with a Mathematical Model 62
3.2.5. β-carotene – Sunflower Oil Natural Additive 74
4. Conclusions and Future Work 75
5. Bibliography 76
6. Annex 81
6.1. Annex A 81
6.2. Annex B 84
6.3. Annex C 85
6.4. Annex D 87

List of Tables

Table 1 - Morphologic characteristics of winter squash *C. moshcata*. [10] 6
Table 2 - Physical characteristics of *C. moschata*. [10] 7
Table 3 - Chemical composition of *C. moschata*. [10,] 8
Table 4 - Chemical name, molecular formula and molecular weight of β-carotene. [34] 14
Table 5 - Critical point for some pure components [49]. 24
Table 6 - Carbon dioxide properties as a liquid, supercritical fluid and vapour. [54] 24
Table 7 - Selected instrument and modified EN 14105 method for the Trace Ultra GC and TriPlus AS (Glycerides) 43
Table 8 - Selected instrument and EN 14103 method for the Trace Ultra GC and TriPlus AS (Fatty acid) 43
Table 9 - Linearization parameters of calibration curves to correlate concentrations and GC peaks areas of methyl esters 44
Table 10 - Experimental parameters for the Soxhlet extraction method. 47
Table 11 - Soxhlet extraction results from HPLC analysis. 47
Table 12 - Experimental parameters for the Bligh and Dyer extraction method. 48
Table 13 - BD extraction method results from HPLC analysis. 48
Table 14 - Experimental conditions used in the $scCO_2$ extraction process. 49
Table 15 - Fatty acid profile for scCO2 oil extraction. 49
Table 16 – Mono-, di-, and triglycerides content in $scCO_2$ extracted oil according to experimental conditions. 51
Table 17 - Experimental results for oil extraction, with $scCO_2$ (325,15K and 260 bar). 52
Table 18 - β-carotene content regarding oil extraction and pumpkin mass. 52
Table 19 - Influence of solvent flow rate on oil extraction from PR according to S/F (325,15K and 260 bar). 56
Table 20 - Extraction yield of b-carotene ($\mu g_{\beta\text{-carotene}}/g_{Pumpkin}$), for different solvent flow rates, at extraction time = 180 min (325,15K and 260 bar). 58
Table 21 - Operating solubility for different solvent flow rates (325,15K and 260 bar). 67
Table 22 - *Gproms*® software key estimated parameters. 68
Table 23 - Measured values vs. predicted values and corresponding standard deviations, for the studied experiments 69
Table 24 - Sunflower oil enrichment parameters. 74
Table 25 - Fatty acid profile of extracted oil with scCO2. 84
Table 26 - Fatty acid chemical structure. 87

List of Figures

Figure 1 - The global concept of food and food related products production. [5] 3
Figure 2 - Production volumes of each commodity group (million tons), in 2007. [6] 3
Figure 3 - Food losses and waste, at consumption and pre-consumption stages (kg), in 2007. [6] 4
Figure 4 - Initial production lost or wasted at different stages of the FSC, for fruits and vegetables, in 2007. [6] 4
Figure 5 - *Cucurbita moschata,* butternut species. [9] 6
Figure 6 - Isoprene group [29]. 10
Figure 7 - Lycopene, carotenoid typical chemical structure.[29] 11
Figure 8 - The s-*cis* and s-*trans* conformations of single bonds in the polyene chain. [31] 11
Figure 9 - The seven different end groups found in natural carotenoids (adapted from [31]). 11
Figure 10 – Structure of β-carotene. [29] 11
Figure 11 – Structure of Lutein. [29] 12
Figure 12 - Structure of Zeaxanthin. [29] 12
Figure 13 - Chemical structure of retinol and retinal (adapted from [32]). 14
Figure 14 - Market value of the major carotenoids. 15
Figure 15 - β-carotene synthesis by the Roche method. [36] 15
Figure 16 - β-carotene synthesis by the BASF Company. [36] 16
Figure 17 - *Murad*®, "beauty pill". [39] 17
Figure 18 - On the left: Saturated fatty acid (C18:0 or stearic acid). On the right: unsaturated fatty acid (C18:1 or oleic acid). [42] 18
Figure 19 - Chemical structure of linoleic acid, ω-6 family. [45] 18
Figure 20 - Chemical structure of heneicosapentaenoic acid, ω-3 family. [45] 19
Figure 21- On the left: Triglyceride (neutral lipid). R', R'' and R''' represent fatty acid chains. On the right: Phospholipid (polar molecule). [42] 19
Figure 22 - Recovery processes for pumpkin bioactive materials. [11] 22
Figure 23 - Supercritical pressure-temperature diagram for carbon dioxide.[49] 23
Figure 24 - Schematic diagram of a typical supercritical fluid extractor with a single separator. [55] 25
Figure 25 - Solvent cycle P-H diagram for the compressor. (adapted from [57]) 27
Figure 26 - Solvent cycle P-H diagram for the liquid pump.(adapted from [57]) 28
Figure 27 - Some industrial reactions carried out with SFCs. [58] 29
Figure 28 - SFC technology distribution in key industries sectors.[58] 29
Figure 29 - D,L-α-tocopherol synthesis with scN_2O. [58] 29
Figure 30 - Terephthalic acid formation using $scCO_2$. [58] 30
Figure 31 - Diagram of a general fixed bed extractor, particle characteristics and concentration profile.[55] 31
Figure 32 - Soxhlet apparatus. 34
Figure 33 - High-pressure installation used for pumpkin oil extraction. 38
Figure 34 - High-pressure installation for pumpkin oil extraction (cont.) 39
Figure 35 - Extraction process installation diagram. 40

Figure 36 - Gas chromatograph on-column Thermo Scientific Trace GC Ultra. 42
Figure 37 - Chromatogram obtained by GC for fatty acid content in $scCO_2$ pumpkin oil extraction. 50
Figure 38 - Typical GC chromatogram obtained for glycerides analysis..... 50
Figure 39 – Yield of extraction (mgOil/gPumpkin) of oil for dry and wet pumpkin (325,15K and 260 bar). 53
Figure 40 - SC-CO_2 extraction yield ($\mu g_{\beta\text{-carotene}}/g_{Pumpkin}$) for β-carotene with wet and dry PR (325,15K and 260 bar). 54
Figure 41 - Extraction yield (%) at different CO_2 flow rates for oil extraction (325,15K and 260 bar). 55
Figure 42 - Amount of extracted oil, at 180 minutes, according to the S/F parameter. 56
Figure 43 - Extraction yield ($mg_{Oil}/g_{Pumpkin}$) vs. solvent consumption (kg_{CO2}), for oil extraction (325,15K and 260 bar). 57
Figure 44 – Extraction yield ($\mu g_{\beta\text{-carotene}}/g_{Pumpkin}$) at different CO2 flow rates for β-carotene extraction (325,15K and 260 bar). 57
Figure 45 - Oil extraction ($mg_{Oil}/g_{Pumpkin}$) with and without co-solvent presence..... 59
Figure 46 - Extraction yield ($mg_{Oil}/g_{Pumpkin}$) for experiment 6 and 7 (325,15K and 260 bar). 60
Figure 47 - Extraction yield ($\mu g_{\beta\text{-carotene}}/g_{Pumpkin}$) with and without co-solvent (325,15K and 260 bar). 60
Figure 48 - Extraction yield ($\mu g_{\beta\text{-carotene}}/g_{Pumpkin}$) for experiment 6 and 7 (325,15K and 260 bar). 61
Figure 49 - Typical extraction curve for pumpkin oil extraction. [13] 66
Figure 50 - Experimental vs. predicted data plot for experiment 2. 69
Figure 51 - Experimental vs. predicted data plot for experiment 5. 70
Figure 52 - Experimental vs. predicted data plot for experiment 7. 70
Figure 53 - Parity plot for experiment 2. 71
Figure 54 - Parity plot for experiment 5. 71
Figure 55 - Parity plot for experiment 7. 72
Figure 56 - Solute concentration variation, along the extractor bed, for experiment 2. 72
Figure 57 - Solute concentration variation, along the extractor bed, for experiment 5. 73
Figure 58 - Solute concentration variation, along the extractor bed, for experiment 7. 73
Figure 59 - Model section code - parameters and distribution domain section. 81
Figure 60 - Model section code - variables section. 81
Figure 61 - Model section code - set and boundary section. 82
Figure 62 - Model section code - equations section (part 1). 82
Figure 63 - Model section code - equations section (part 2). 82
Figure 64 - Process section code - parameters, unit and set sections. 83
Figure 65 - Process section code - assign, initial conditions, solution parameters and schedule sections. 83
Figure 66 - Calibration plot for experiment 1 to 5. 85
Figure 67 - Calibration plot for experiment 6, 7, Soxhlet method and Bligh and Dyer method. 85
Figure 68 - Calibration plot for experiment 8. 85
Figure 69 - Calibration plot for monoglycerides. 86
Figure 70 - Calibration plot for diglycerides. 86

Figure 71 - Calibration plot for triglycerides. 86

List of Equations

Equation 1 - Relationship between mono-, di-, and triglycerides concentration and peak area. 43
Equation 2 - Calculation of yield of oil extracted (%). 52
Equation 3 - General mass balance to the fluid phase. 62
Equation 4 - Axial dispersion coefficient. 62
Equation 5 - Binary diffusion coefficient calculation. 63
Equation 6 - Determination of correlation values. 63
Equation 7 - Interstitial fluid velocity 64
Equation 8 - Solute mass flux from solid to fluid phase. 64
Equation 9 - Mass transfer coefficient 64
Equation 10 - Schmidt number. 64
Equation 11 - Solute partition coefficient. 65
Equation 12 - Particle specific surface area. 65
Equation 13 - Boundary condition for the fluid phase at z=0. 65
Equation 14 - Boundary condition for the fluid phase at z=L. 65
Equation 15 - Initial condition for mass balance to the fluid phase. 65
Equation 16 - General particle mass balance. 65
Equation 17 - Boundary condition for the particle phase at r=0. 66
Equation 18 - Boundary condition for particle phase at r=R. 66
Equation 19 - Initial condition for particle phase. 66
Equation 20 - Biot number calculation. 67
Equation 21 - Peclet number calculation. 68

1. Introduction

1.1. Motivation

1.1.1. Agro-Food Industry – Environmental Safety and Residue Production Management

Nowadays, there is a major interest to reach a sustainable energy balance for the whole world as soon as possible, to both avoid negative effects of global warming as well as to avoid significant economic problems. [1] The massive wide scale use of organic solvents by a diverse range of global industries represents a serious threat to the environment.

Currently, by-products of agro-food processing represent a major disposal problem for the industry concerned, due to cost of drying, storage and shipment. Also, these materials are prone to microbial spoilage, thus limiting further exploitation. So, it is necessary to diminish these economically limiting factors, with efficient, inexpensive and environmentally sound utilization of these added-value residues.

The development of food processing technologies has been influenced by numerous factors, with consumer demands driving new trends in the manufacturing, preservation, and formulation of food.

There is increasing public awareness of the health, environment, and safety hazards associated with the use of organic solvents in food and ingredient production and possible solvent contamination of the final product. The high cost of organic solvents and the increasingly stringent environmental regulations, together with the requirements of the food industry for ultrapure and high-added-value products, have highlighted the need for the development of new and more environment friendly technologies for the processing of food products.[2] The traditional extraction methods used to obtain these types of products have several drawbacks: they are time consuming, laborious, have low selectivity and/or low extraction yields. Moreover, these traditional techniques employ large amounts of toxic solvents. In many industrial processes the use of hazardous (toxic, flammable, etc.) solvents is not the only concern, because their full recovery and recycling often are not easy, or economically viable. The pharmaceutical industry is a suitable example, since only 1% (w/v) product comes out the solvent used, with about 50% solvent recovery in the whole process. [3]

For instance, the use of artificial dyes is a common practice in the modern food industry, but there is growing concern about their actual or potential on human health. This concern has led to an increasing interest and utilization of natural products as alternative food colorants.[4]

In today's society, where great demand for appropriate nutritional standards, the rising costs and decreasing availability of raw materials together with much concern about environmental pollution, is bringing a great need to recovery, recycling and upgrading of wastes. For the food and food processing industries, this is particularly valid in which wastes, effluents, residues, and by-products can be recovered and can often upgrade to higher value and useful products.

Large volumes of wastes, both solids and liquids resulting from the production, preparation, and consumption of food, are produced by the food industry. These wastes create an increasing disposal and severe pollution problems, and represent a loss of valuable biomass and nutrients. Wastes produced have, for the most part, been dumped or used without treatment for animal feed or as fertilizers, but the increasing necessity to take into consideration aspects aimed at preventing pollution of the environment as well as for economic motives, and the need to conserve materials, some new methods and policies have been introduced in the recovery and utilization of valuable compounds from food processing wastes.

Strategies in the manufacturing of new products and compounds must focused on the development of cost effective technology, the optimization of processes including separation steps, alternative processes for the reduction of wastes, optimization of the use of resources and improvement in production efficiency. Hereupon, three options of industrial waste management techniques can be summarized – source reduction via in-plant modification, waste recovery/recycling or waste treatment by detoxifying, neutralizing or destroying the undesirable compounds. [5] Waste recover/recycling represent the most promising waste management strategies, because significant economic and environmental benefits can came from recovering or recycling these value components.

A global concept (Figure 1) for food and food related products is shown here, in order to connect different goals, such as highest product quality and safety, highest production efficiency and the integration of environmental aspects into product development and food production.

Development of clean production processes must be the aim of the upcoming and already established industries, with some goals to reach [5]:

- Short term goal – Waste reduction and recycling of valuable by-products and residues, which will result in emissions and risk reduction.
- Medium term goal – Adding value to by-products, which will bring higher environmental responsibility for the companies with competitive advantages.
- Long term goal – Development of “innovative” products, which will bring new market segments.

Considering the vegetable industry, the goals mentioned above can be reached by some usual approaches, like disposal, feeding (animals), fertilization/composting or conversion[1]. Some drawbacks are pointed out that hindered the possibilities for the utilization of these residues, such as transportation cost and sales problems due to low quality of the residual matter.

[1] Bio-refinery – Biomass conversion into fuels, energy, and high added-value chemical products.

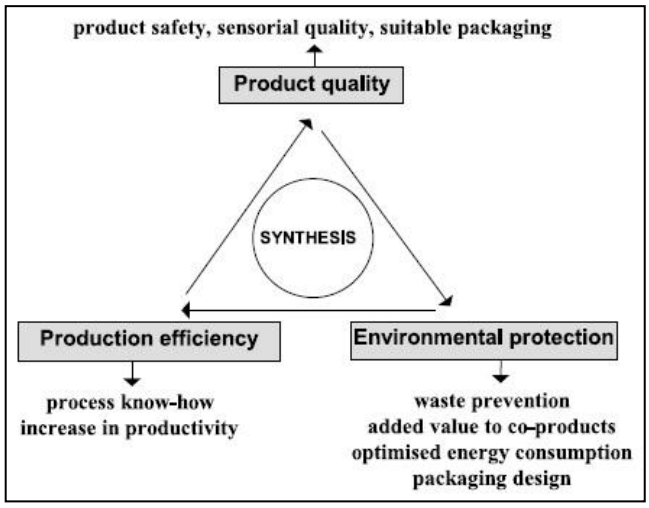

Figure 1 - The global concept of food and food related products production. [5]

The magnitude of the problem can be understood if we take a look at the residue production around the world, in 2007 (Figure 2). According to the Food and Agriculture Organization, approximately 33% of the edible parts of food produced for human consumption gets lost or wasted globally. [6]

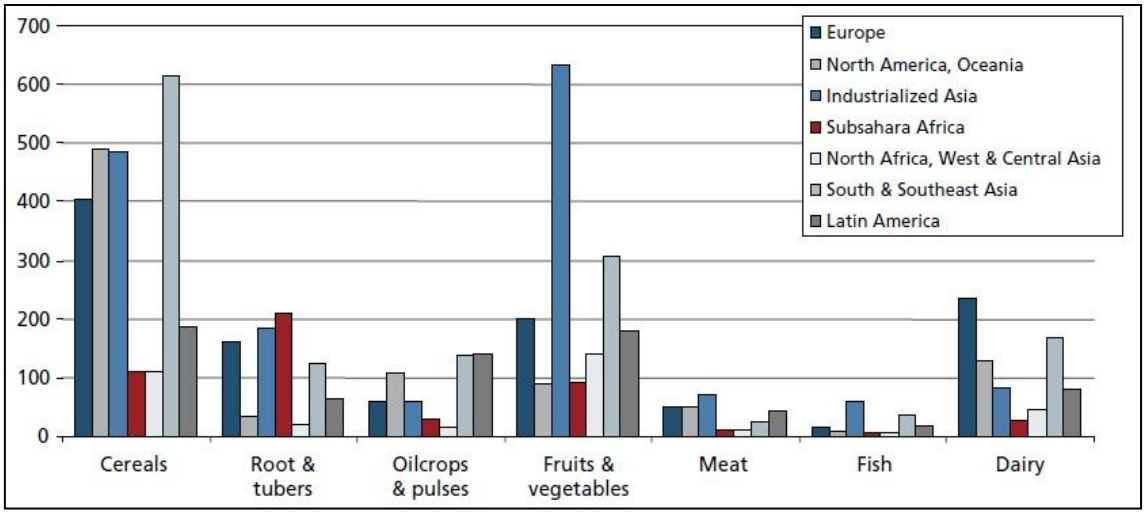

Figure 2 - Production volumes of each commodity group (million tons), in 2007. [6]

To better understand the whole process of residue/waste formation of the food industry, five system boundaries were distinguished in the food supply chain (FSC) [6]:

- Agriculture Production – losses due to mechanical damage and/or spillage during harvest operation.
- Postharvest Handling and Storage – includes losses due to spillage and degradation during handling, storage and transportation between farm and distribution.
- Processing – losses may occur when crops are sorted out if not suitable to process or during washing, peeling, slicing and boiling or during process interruptions and accidental spillage.

- Distribution – here are included losses and waste from wholesale markets, supermarkets, retailers.
- Consumption – including losses and wastes during consumption at the household level.

The food losses and waste, at consumption and pre-consumption stages, per capita is shown in Figure 3, and also the initial production lost or wasted, at different stages of the FSC for fruits and vegetables is shown in Figure 4.

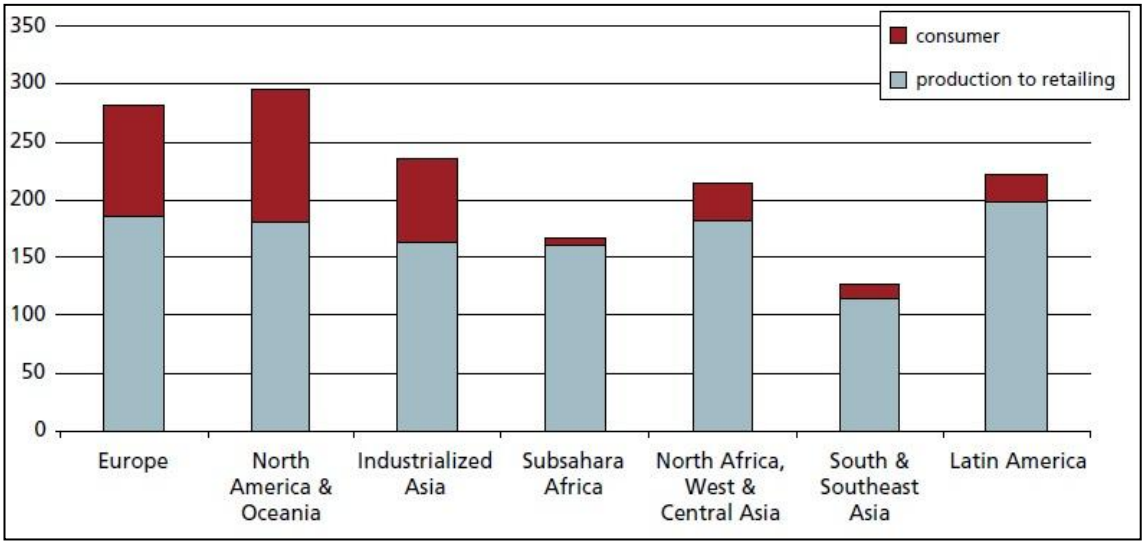

Figure 3 - Food losses and waste, at consumption and pre-consumption stages (kg), in 2007. [6]

Figure 3 shows that in Europe and North America, between 280 and 300 kg/year of food waste are produced, per capita, alone. From Figure 4 we can see that the major lost of edible material is in the agriculture production.

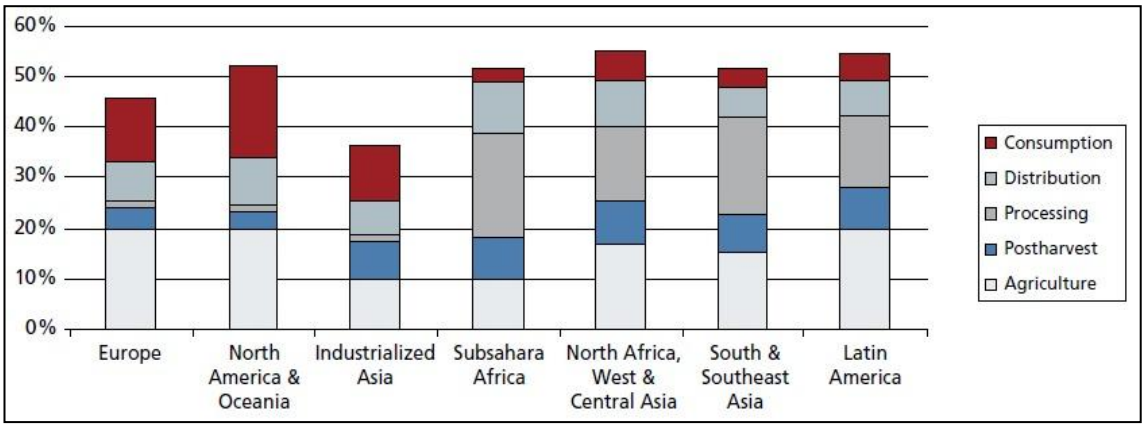

Figure 4 - Initial production lost or wasted at different stages of the FSC, for fruits and vegetables, in 2007. [6]

"Food wastes" are residues of high organic load that usually derive from the processing of raw materials into food products and result in a liquid or solid form. These substances are removed from the production process as undesirable materials, and classified as "wastes", in most European legislations (Commission Regulations 442/1975/EEC; 689/1991/EEC). They come from various different branches of the food industry, as shown in Figure 4.

Nevertheless, discharging of wastes does not account the possibility of re-utilizing them inside the food chain; even more the increase of disposal costs reinforces this idea.

Generally, fruits and vegetables processing wastes are the most widely investigated substrates for the extraction of several types of antioxidants and dietary fibers.

For the recovery of the high added-value compounds from these residues, some principles must be followed:

- Maximizing the yield of the target compound,
- Adjust to the industrial processing demands,
- Separate the added-value ingredients from impurities and toxic compounds,
- Avoid the deterioration and loss of functionality during processing,
- Ensure the food grade nature of the final product.

In this work, *Cucurbita moschata* butternut was used as the by-product for the extraction of high value-added compounds, excluding seeds. Pumpkin production in Portugal has grown since 2011, from 1900 to 2100 hectares, in 2012. In the year 2012, pumpkin production reached 46.500 tons in continental Portugal, showing an increase regarding the year before, with a production of 40.000 tons, approximately. [7] Since the food processing industry makes use of 70% of the fruit, and considers the rest to be agro-industrial residue (as mentioned above), it can be assumed that in 2012, 13.934 tons of pumpkin residues were produced.

1.1.2. *Cucurbita moschata* – Growth, Characteristics and Properties

Pumpkin is a gourd-like fruit of the genus *Cucurbita* and the family *Cucurbitaceae*, indigenous to western hemisphere, is comprised of five domesticated species. Three of these species, *Cucurbita pepo* L., *Cucurbita maxima* , and *Cucurbita moschata* represent economically important species cultivated all around the world [8], being the one used in the extraction processes, *Cucurbita moschata* butternut (Figure 5).

It is a seasonal crop that has been used as both human and animal feed. Since ancient times, it has been essential in the diet of rural communities and some urban areas of the Americas, and many other parts of the world. *C. moschata* is eaten as vegetable and cultivated for its shoots, fleshy, edible flowers and above all, for its fruits. Their seeds are eaten whole, roasted, toasted and ground into different stews.

Figure 5 - *Cucurbita moschata,* butternut species. [9]

In terms of morphology (Table 1), the squash of *C.* moschata is extremely variable, with a variety of fruits and seeds.

Table 1 - Morphologic characteristics of winter squash *C. moshcata*. [10]

Squash Fruits	(%)
Oval	23
Bule	20
Buchona	37
Herradura	20

The fruits have variable size and different forms that preserves the ovary (Table 2). They are also smooth or with rounded ribs, rarely viscose or granular.

The skin is also variable in thickness, but soft, smooth and durable. The skin color can be from light to dark green, light to dark orange, and the pulp can vary considerably from brown, to completely white, bright orange to greenish light. It can be sweet, smooth and usually non-fibrous, and the seeds can be numerous, ovate-elliptic, with a yellowish white surface.

Nutritional plants and herbal preparations have been traditionally used in developing countries and, a revival of its use in the United States and Europe can be observed. Winter squash is popular in various systems of traditional medicine for treatment of several ailments, such as antidiabetic, antihypertensive, antitumor, antibacterial, antihypercholesterolemia, intestinal antiparasitia, and antiinflammation. [11] Pumpkin contains biologically active components that include polysaccharides, para-aminobenzoic acid, fixed oils, sterol, proteins and peptides. [12,13,10,14]

Table 2 - Physical characteristics of *C. moschata*. [10]

Parameter	Value
Fruit	
Weight (Kg)	0,59-8,75
Length (cm)	13,2-92
Width (cm)	11,7-43
Thickness (cm)	1,8-6,95
Shell (%)	8,2-14
Pulp (%)	72-86
Seed (%)	2,7-6
Seed	
Individual Weight (g)	0,0,17-0,15
Length (mm)	7,9-21
Width (mm)	5-10,2
Thickness (mm)	2,75-3

This residue can be used for the production of added-value compounds. A variety of compounds, such as carotenoids, can be extracted from this residue, through the extraction of the oil that is contained in the pumpkin (Table 3).

Table 3 - Chemical composition of *C. moschata*. [10,]

Composition	Content
Pulp	
Moisture (%)	79-93
Protein (%)	0,97-1,4
Lipid (%)	0,07-0,16
Crude Fiber (%)	0,56-1,56
Ash (%)	0,57-0,89
Total Sugar (%)	1,9
Pectin (%)	0,7
Vitamin C (mg/100 g)	22,9
Vitamin A (mg/g)	20
β-carotene (ug/g)	0,006-2340
Lutein (ug/g)	0,03-20,6
α-carotene (ug/g)	6,1-47
Violaxantina (ug/g)	0,6
Total Phenolic Content (mg GAE[2]/100 g)	476,6
Soluble Solids (°Brix)	5,4-11
pH	5,4-6,4
Acidity (% citric acid)	0,06-0,1
Viscosity (Pa.s)	0,09-0,095
Shell	
Total Carotenes (ug/g)	171,9-461,9

[2] GAE = Gallic Acid Equivalents

1.2. Value-Added Compounds

Human nutrition science has greatly developed in the past decades, turning from consideration of food and food products as simply energy sources to the recognition of their role in maintaining health and in reducing the risk of diseases. The recent progresses in analytical methods allowed scientists to demonstrate the role of food and food products in human health, and not to simply hypothesize it.

Strong research is focused in the development of new technologies and new uses for these by-products, in order to reduce their environmental impact. [15]

There has been a growing interest in so-called functional foods because, for their physiological, nutritional and energetic benefits, such as antioxidant properties. A functional food can be defined as a food that provides some sort of beneficial effect in human physiological functions, increasing the wellbeing and/or decreasing the risk of suffering a particular disease. [16] Usually, a functional food is obtained from traditional food, but is enriched with human health promoting ingredients. On the other hand, over the past few years, some old terms are being employed more frequently, impacting today's food, health food, cosmetics and pharmaceutical industries – nutraceuticals [17], cosmeceuticals [18] and nutricosmetics [19]. The term "nutraceutical" was coined, in 1989 by the Foundation for Innovation in Medicine, to provide a name for the rapidly growing area of biomedical research, although in 1992, DeFelice define nutraceutical as any nontoxic substance that may be considered a food or part of a food and provides medical or health benefits including the prevention and treatment of a disease. The nutraceuticals may range from isolated nutrients, dietary supplements and diets to genetically engineered "designer" foods, herbal products and processed products such as cereals, soups and beverages. On the other hand, cosmeceuticals products are the result of the fusion between cosmetic and pharmaceutical industries, and in 1984, the termed was marked by Albert Kligman [18], at the National Scientific Meeting of the Society of Cosmetic Chemist. It refers to applied products that are capable of making changes in the skin status, decorating it, and are not considered drugs, or cosmetics. [20] Finally, nutricosmetic products are a new concept in the cosmetic field, and it can be described as the consumption of food or oral supplements to produce an appearance benefit. These products can also be called "beauty pills", "beauty from within" and even "oral cosmetics". [19]

The pumpkin oil is a complex mixture of lipid components, being the main component triglycerides. However, the oil also contains mono- and diglycerides, free fatty acids, phospholipids, glycolipids, sterols, and other fat-soluble components including tocopherols, tocotrienols, carotenoids and squalene. Each component has different physical, chemical and physiological properties, being used extensively not only in the food industry, but also in the cosmetic, pharmaceutical and other industries, like functional food, nutraceutical, cosmeceuticals and nutricosmetic industries. Target compounds, like carotenoids (β-carotene), ω-3 and ω-6 fatty acid families are the some of the major bioactive compounds used in these industries, for their health benefits. [21]

One key group of components contained in pumpkin oil are carotenoids, and are one of the major compounds used in this growing market [22], for its properties and availability. In this market, β-carotene has the largest share, expecting to be worth USD 285 million by 2015. [23]

1.1.1. Carotenoids

Carotenoids are currently the most widespread pigments used in the food industry as functional food ingredients or colorants. [24] They are efficient singlet oxygen quenchers and function as chain-breaking antioxidants, protecting cells and other body components from free radical attack. Oxidative damage resulting from free radical attack has been linked to the onset of premature aging, cancer, atherosclerosis, cataracts, age-related macular degeneration and an array of other degenerative diseases.[25] For example, lutein together with zeaxanthin, imparts color to the macula lutea, the spot in the human retina that allows the appreciation of the fine details. [26] Epidemiological studies have shown that people with high carotenoid intake and high plasma levels of carotenoids have a significantly reduced risk of cancer, cardiovascular diseases, cataracts, and heart disease.[27]

Carotenoids belong to a large and diverse family of natural occurring compounds, terpenoids, which are widespread in plants and lower invertebrates. They are involved in the defense, wound sealing, and thermotolerance of the plants as well in the pollination of seed crops, the fragrance of lowers, and the flavor of fruits, determining the quality of agricultural products. The term terpenoids is used for a group of compounds that have a basic C_5 isoprene unit, and which can be classified according to the number of units (1 to 8): hemiterpenoids, monoterpenoids (C_{10} – limonene, carvone, carveol), sesquiterpenoids (C_{15}), diterpenes (C_{20} – retinoids), sesterterpenoids (C_{25}), tri- (C_{30}), and tetraterpenoids (C_{40} - carotenoids).[28]

The main function of carotenoids in nature is related to the photosynthetic process in plants as photo protectors of the photosynthetic apparatus and as antioxidants. In plants, the functionality of carotenoids determines whether they are primary or secondary carotenoids. A primary carotenoid is necessary in the photosynthetic process like β-carotene, lutein or neoxanthin, while a secondary carotenoid is not directly involved in the survival of the plant like α-carotene, capsanthin or lycopene.[29]

There are more than 600 different carotenoids in nature, distributed among higher plants, bacteria, fungi and some animals. Most of them can be found in higher plants, especially in their leaves, flower and fruits.[30]

1.1.1.1. Structure, Classification and Properties of Carotenoids

Carotenoids are compounds constituted by eight isoprene units (Figure 6), joined in a head to tail pattern.[29]

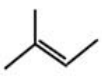

Figure 6 - Isoprene group [29].

Most of them have 40 carbon atoms and present a chemical structure similar to the one presented in Figure 7.

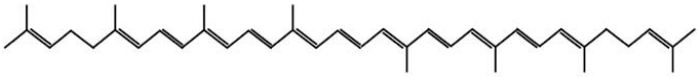

Figure 7 - Lycopene, carotenoid typical chemical structure.[29]

By far the most stable form of the conjugated polyene chain is a linear, extended conformation, and there are two major factors responsible for this. The first one is that a conjugated system is greatly stabilized when the double bonds are coplanar, and second, the steric hindrance is smallest when each C-C single bond is in the s-trans conformation, which is identical to a *trans* double-bound configuration [25], represented in Figure 8.

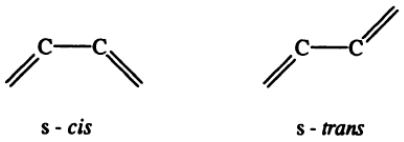

Figure 8 - The s-*cis* and s-*trans* conformations of single bonds in the polyene chain. [31]

This skeleton can be modified by cyclization at one end or both ends of the molecule, to give the seven different end groups (Figure 9), by changes in hydrogenation level, and by addition of oxygen-containing functional groups.

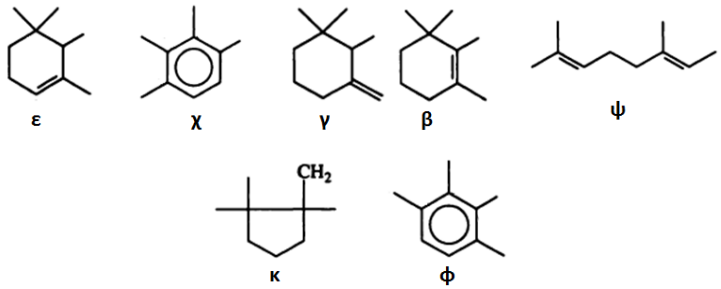

Figure 9 - The seven different end groups found in natural carotenoids (adapted from [31]).

In essence, all specific names are based on the stem name “carotene”, preceded by a Greek-letter prefixes that designate the two end groups. To avoid confusion, the use of both end-group prefixes for a carotene is recommended, as the example of, “β-carotene”, which is correctly referred as β,β-carotene (Figure 10). The same happens with α-carotene, which really is β,ε-carotene, along with others.

Carotenoids can be classified by two different ways, by their chemical structure or by their functionality. They can be classified by their structure as carotenes, if their only elements are carbon and hydrogen, like β-carotene or lycopene.[29]

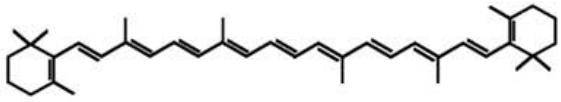

Figure 10 – Structure of β-carotene. [29]

And they can be considered as xanthophylls, if they also have oxygen in their structure as for example, lutein (Figure 11) or zeaxanthin (Figure 12).[29]

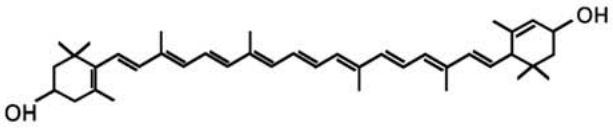

Figure 11 – Structure of Lutein. [29]

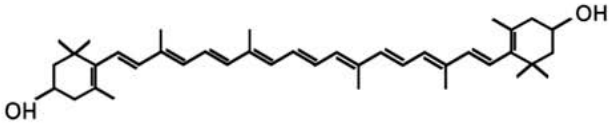

Figure 12 - Structure of Zeaxanthin. [29]

The most striking feature of the carotenoid structure is the long system of alternating double and single bonds that form the central part of the molecule. This conjugated polyene chromophore[3] determines not only the light absorption properties, and hence color, but also the photochemical properties of the molecule and consequent light-harvesting and photoprotective action.

Due to the isomerism around C=C double bounds, different configurations are possible and, each of these double bounds in the polyene chain can exist in two forms (configurations), designated *trans* or *cis,* depending on the disposition of substituent groups. The presence of *cis* double bound creates greater steric hindrance between nearby hydrogen atoms and/or methyl groups, so that *cis* isomers are generally less stable thermodynamically than the *trans* form. For these reason, most carotenoids occur in nature predominantly or entirely in the all-*trans* form. [31]

The carotenoids as a group are extremely hydrophobic molecules with little or no solubility in water, thus being expected to be restricted to hydrophobic regions in the cell, like the inner core membranes. When associated with proteins, these molecules can be found in an aqueous environment.[31] All colored carotenoids in the all-*trans* configuration have an extended conjugated double-bond system and are linear, rigid molecules. The *cis*-isomers, however, are no longer simple linear molecules, with a different overall shape of the all-*trans* form, altering greatly their ability to fit into subcelular structures.

The absorption of light energy, in carotenoids, holds to the fact that a relevant transition has to occur, a $\pi \rightarrow \pi^*$ transition. In this transition one of the bonding π-electrons of the conjugated double-bond system is promoted to a previously unoccupied π* antibonding orbital.[31] The π electrons are highly delocalized and the excited state is of comparatively low energy, so the energy required to bring about the transition is relatively small and corresponds to light in the visible region in the wavelength range of 400-500 nm. Carotenoids are therefore intensively colored yellow, orange and red.[32]

There are several distinct mechanisms whereby carotenoids function as antioxidants, being the first the ability to quench the highly reactive form of oxygen, known as singlet oxygen, $^1O_2$. [33] The singlet oxygen is usually formed through photochemical reaction which involves the absorption of light by a sensitizer molecule (S), such as porphyrins, chlorophylls and riboflavin, in the biological system. [24] This sensitizer molecule is converted into a triplet state sensitizer (^3S), which reacts with a ground state oxygen that exists in a triplet

[3] Chromophore – Is the part responsible for the color, in molecules, when hit by light.

configuration, ($^3O_2$). This reaction occurs with the transfer of energy, thus forming the ground state sensitizer (S), and the singlet oxygen. The reactions mentioned are shown below.

$$S + light \rightarrow {}^1S \rightarrow {}^3S$$
$$^3S + {}^3O_2 \rightarrow S + {}^1O_2$$

Reaction 1 – Biological synthesis of a singlet oxygen molecule.

This highly reactive molecule ($^1O_2$) is capable of oxidizing nucleic acids, various amino acids in proteins, and unsaturated fatty acids. The roll of carotenoids to avoid this degradation process is very important, being the most effective quenchers of singlet oxygen molecules found in nature.

$$^1O_2 + CAR \rightarrow {}^3O_2 + {}^3CAR$$
$$^3CAR \rightarrow CAR + heat$$

Reaction 2 – Quenching reaction of a singlet oxygen molecule. (adapted from [24])

The excess energy accumulated in the excited state of carotenoid (^{3}CAR), can be released via vibrational and rotational interactions of the conjugated polyene chain, with the solvent system. Thus the carotenoid returns to the ground state (CAR), ready to begin another cycle of $^1O_2$ quenching.

The number of conjugated double bonds in the polyene chain affects the ability of the carotenoid molecule to quench singlet oxygen radicals. As the number of this double bonds increase, the ability to quenching increases too; k_q (quenching coefficient) is higher. [33]

Along with the ability to quench singlet oxygen molecules, carotenoids can also react with free radicals (HO^* and ROO^*). Nevertheless, unlike the quenching of singlet oxygen which mainly leads to energy dissipation as heat, the reactions that occur between a carotenoid (or any antioxidant) with a free radical leads to electron transfer or even other side reactions. The 'odd' electron which characterizes a free radical is not lost, and reacts with the carotenoid. The carotenoid radical can then react with another peroxy radical to form a nonradical product, accordingly to the next reactions. [32]

$$ROO^\bullet + CAR \rightarrow ROO - CAR^\bullet$$
$$ROO - CAR^\bullet + ROO^\bullet \rightarrow ROO - CAR - OOR$$

Reaction 3 – Reaction between a free radical and a carotenoid. (adapted from [31])

At relatively low oxygen concentrations, this process would consume peroxy radicals and the carotenoid acts as a chain-breaking antioxidant.

Technological requirements for food antioxidants include - low volatility and stability in order to avoid losses during processing and storage, the ability to protect from oxidation at low concentrations, solubility and compatibility with other components of the oxidizable substrate, possess a nontoxic and nonirritant character at the effective concentration. [28]

1.1.1.2. β-carotene – Market Interest to Industrial Applications

Approximately 10% of all carotenoids are called – Provitamin A – which indicates that they posses at least one unsubstituted β-ionone ring that can be converted into vitamin A. [28] Vitamins are essential, organic compounds which are not synthesized in the human and animal organism or formed only in insufficient amount. Therefore, they must be regularly consumed with the diet either as such or as a precursor (provitamin) that can be converted to vitamin in the body. β-carotene (Table 4) is a typical representative of the provitamins, which is split in two molecules of vitamin A in the organism. Vitamins are classified not chemically but by their activity. The distinction between fat- and water-soluble vitamins holds to the behavior of vitamins in the organism: resorption, transport, excretory pathways and storage.

Table 4 - Chemical name, molecular formula and molecular weight of β-carotene. [34]

Chemical Name	**(all-E)-1,1'-(3,7,12,16-tetramethyl-1,3,5,7,9,11,13,15,17-octadecanonaene-1,18-diyl)bis[2,6,6-trimethylcyclohexene]**
Molecular Formula	$C_{40}H_{56}$
Molecular Weight	536,88 $g.mol^{-1}$

In the animal organism, vitamin A compounds occur as metabolites of the provitamins A, especially of β-carotene, which is resorbed from plant food in the small intestine. In intestine cells, part of the β-carotene is homolytically cleaved in two molecules of retinal (the aldehyde of vitamin A_1 – Figure 13), by the enzyme carotene dioxygenase. Retinol (vitamin A_1 – Figure 13) is then produced by a reduction reaction of retinal, by the retinal reductase. [32] The term "vitamin A" should be used to all compounds which present the biological activity of retinol.

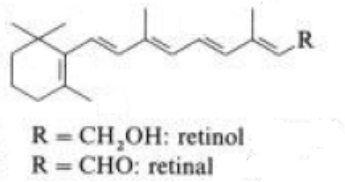

Figure 13 - Chemical structure of retinol and retinal (adapted from [32]).

The vitamin A_1 plays an important role as a cofactor in the eyesight process, binding with opsin (a retina protein), to give rhodopsin, a visual pigment.

It is estimated that the worldwide market of carotenoids will grow 2,3% per year, being responsible for about USD 766 million in 2007, and will reach USD 920 million in 2015. The β-carotene commercialization accounts for 32% of this market (Figure 14). [23] Nowadays, some private companies old the international trade of this compounds, such as Roche, BASF, Merck and DSM. [35]

Although carotenoids are widely present in nature, the worldwide bulk production is dominated by synthetic methods. Nowadays only eight of the nearly 600 carotenoids in nature

are industrially produced by synthesis. These are lycopene, β,β-carotene, (3R,3'R)-zeaxanthin, canthaxanthin, astaxanthin, β-apo-8'-carotenal, ethyl β-apo-8'-carotenoate and citranaxanthin.[32]

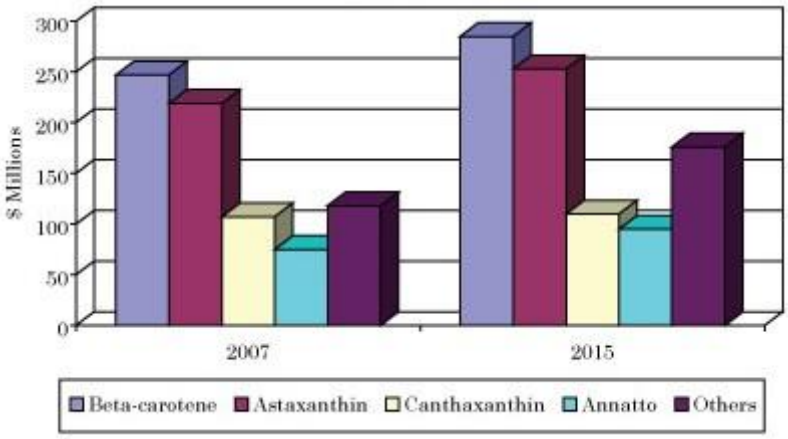

Figure 14 - Market value of the major carotenoids.

The industrial synthesis of β-carotene is described here through the Roche process, and the BASF process. Each company uses a different method for its production, but the both use the same precursor, β-ionone, which is produced from acetone and butadiene. The Roche method follows the $C_{19} + C_2 + C_{19}$ synthesis principle, where β-carotene is produced enol-ether condensation, allowing a gradual and specific lengthening of conjugated aldehyde by two carbon atoms each time. [34] This process presents a yield of 60% and it is shown in Figure 15.

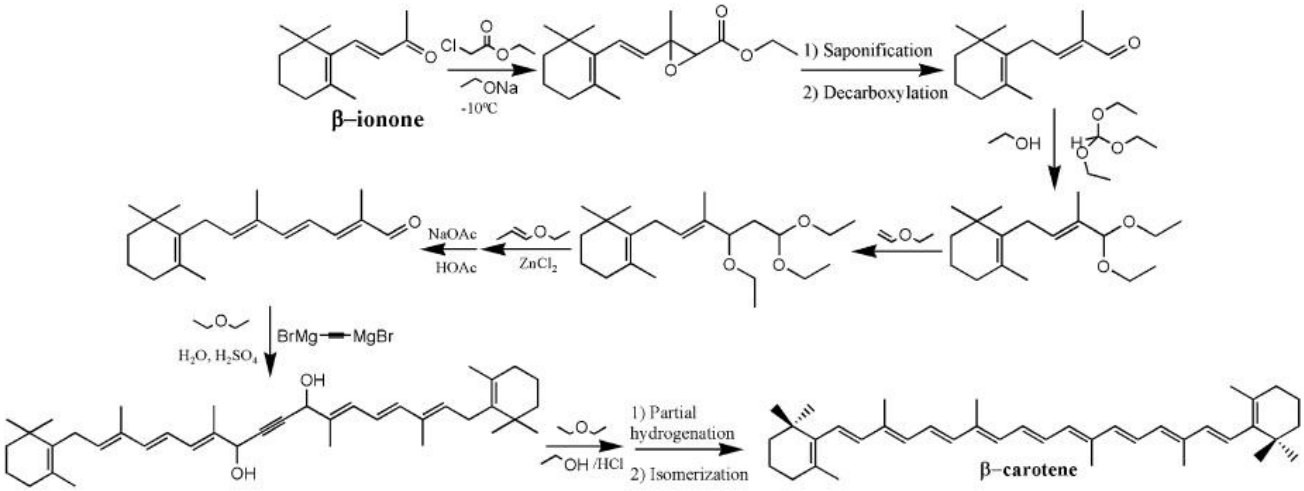

Figure 15 - β-carotene synthesis by the Roche method. [36]

Meanwhile, the BASF process (Figure 16), which presents 85% yield of β-carotene, uses the Wittig condensation. Phosphonium salts, previously derivatized with triphenylphosphine, react with an aldehyde, generating a double bound and enlarging the polyenic chain. The reaction that occurs between retinal and retinyltriphenylphosphonium salt, requires recycling of triphenylphosphine oxide, due to its low biodegradability. This recovery process comprehends three phases, being the first one distillation, followed by chlorination with phosgene and finally dehalogenation with aluminum. [34]

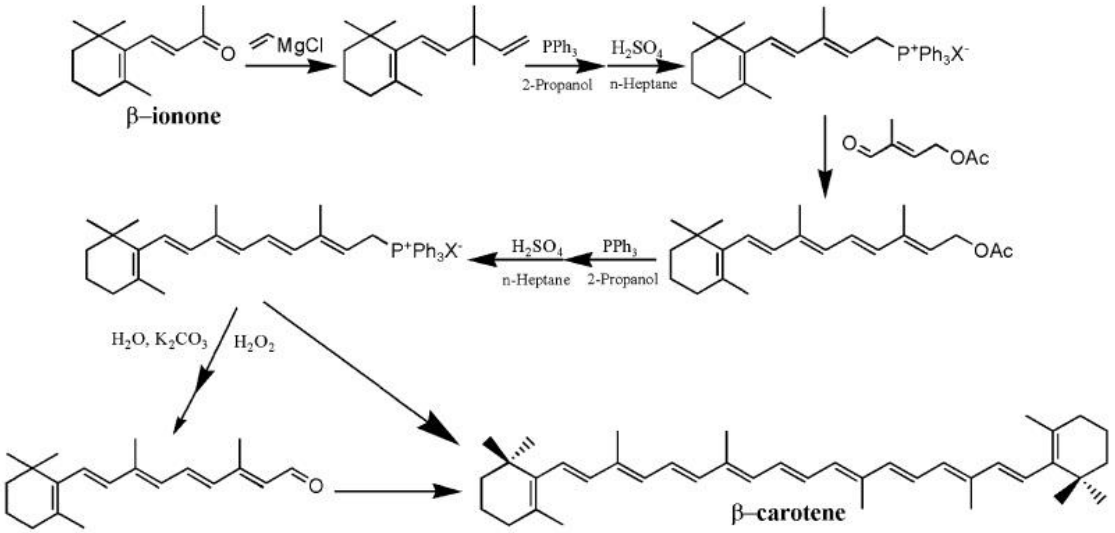

Figure 16 - β-carotene synthesis by the BASF Company. [36]

A different option to produce carotenoids is by means of biological processes: algae, fungi, and bacteria. Some species of the genus *Dunaliella*, like *bardawil* and *salina*, are one of the most reported microalgae for the production of β-carotene, being able to accumulate between 100 to 400 $mg.m^{-2}.day^{-1}$ (m^2 = growing area). The major filamentous fungi that produce β-carotene are *Blakeslea trispora* and *Phycomyces blakesleeanus*. *B. trispora* was able to produce 596 $mg.L^{-1}$, in 5 days of fermentation. Among bacteria, there are some species that can produce β-carotene as their main carotenoid. The production by *Flavobacterium multivorum* was 2.9 $mg.g^{-1}$ of dry biomass, after 2 days of fermentation. [36]

For industrial applications β-carotene has a great impact in the food, food supplement, pharmaceutical and cosmetic industries. In the food industry is used as natural colorant with the E name, E 160a (i) and E160a (ii) [37], being the first one mixed with other carotenoids, and the second just β-carotene. It is used as natural colorant because of the double conjugated bounds present in their chemical structure that absorbs light within the visible range, providing the substances with an intense yellow to red-orange color. [29] Food colorants has always been target of complains of the food industry consumers, mainly because of the bad fame of the initial synthetic pigments that only have a cosmetic value and were associated with health damage. Nowadays the food market demands functional foods, and healthy products, while the use of chemical products is considered as bad and natural additives provide the final product with a healthy value. [29] It can also be sold as a food supplement, in pills (Newton-Everett Biotech®, BioEva [38]).

In the pharmaceutical and cosmetic industry, β-carotene is used and commercialized in a variety of products, such as *Murad®*, a "beauty pill" [39] (nutricosmetic industry) (Figure 17), as creams, *Amazing Grace®* [40], skin lotion, *Pevonia®* [41], among many others.

Figure 17 - *Murad*®, "beauty pill". [39]

1.1.2. Fatty Acids and Triglycerides

Lipids are biomoleculas, soluble in organic non-polar solvents such as supercritical carbon dioxide, and insoluble in water. They can be classified into two major groups; fatty acids (saturated and unsaturated – Figure 18) and glycerides (triglycerides and phosphoglycerides). Glycerides and waxes form a group of compounds which have an ester as the major functional group, and in this group are included waxes, triglycerides and phospholipids. On the other hand, steroids, fatty acids, soaps, sphingolipids and prostaglandins form another group without an ester functional group.

Fatty acids are carboxylic acids (hydrophilic) with long hydrocarbon chains (hydrophobic) which are either saturated or unsaturated, being produced as the end product of fat digestion. The hydrocarbon chain may vary from 8 to 30 carbons, and is an important counter balance to the polar acid group. In the case of acids with only a few carbons, the acid functional group dominates and gives the whole molecule a polar character. When the carboxylate end of the fatty acid molecule is bonded to an uncharged head group, like glycerol, a neutral lipid molecule is formed – triglyceride. On the other hand, the association of a fatty acid molecule to a charged head group like glycerol and phosphate complex, a polar lipid molecule is formed – phospholipid (Figure 21).

Fatty acids can be divided in two functional groups, based on the ability of the human body to synthesize them.

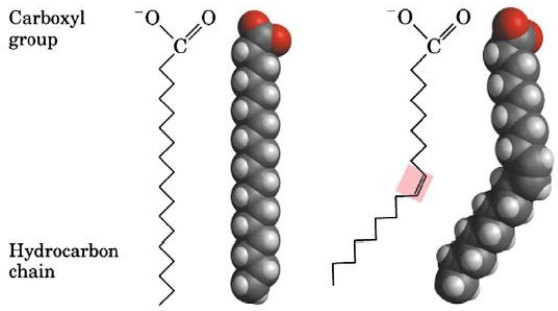

Figure 18 - On the left: Saturated fatty acid (C18:0 or stearic acid). On the right: unsaturated fatty acid (C18:1 or oleic acid). [42]

Essential fatty acids [43], like *cis*-linoleic acid, arachidonic acid (AA), and linolenic acid must be supplied externally from the diet. Non-essential fatty acids [43], like oleic acid (Figure 18, right side), can be synthesized in the body. A conventional shorthand notation for fatty acids identifies the chain length followed by a colon and the number of double bonds in the chain, e.g., oleic acid is 18:1. [44] There are two types of essential unsaturated fatty acids, which are designated by the position of the terminal double bound, being ω-6 and ω-3. [42] The ω indicates the position of the first double bound that starts either 6th (ω-6) or 3rd (ω-3) carbon atom from the methyl end, respectively.

Figure 19 - Chemical structure of linoleic acid, ω-6 family. [45]

Polyunsaturated fatty acids (PUFA) are those which contain more than two double bounds. The ω-6 and ω-3 families are PUFA, and are necessary for the growth and development of the central nervous system and retina, and proper functioning of the cardiovascular system. [44] Some of exemplas of the ω-6 and ω-3 fatty acids families are represented in Figure 19 and Figure 20, respectively.

Figure 20 - Chemical structure of heneicosapentaenoic acid, ω-3 family. [45]

Some researchers have shown that ω-3s can reduce the risk of heart disease and high blood pressure, prevent blood clots, protect against cancer and even alleviate depression. [45]

Naturally occurring oils contain about 97% triglycerides, i.e., triesters of glycerol with fatty acids (Figure 21 – left side); up to 3% diglycerides, and up to 1% monoglycerides.

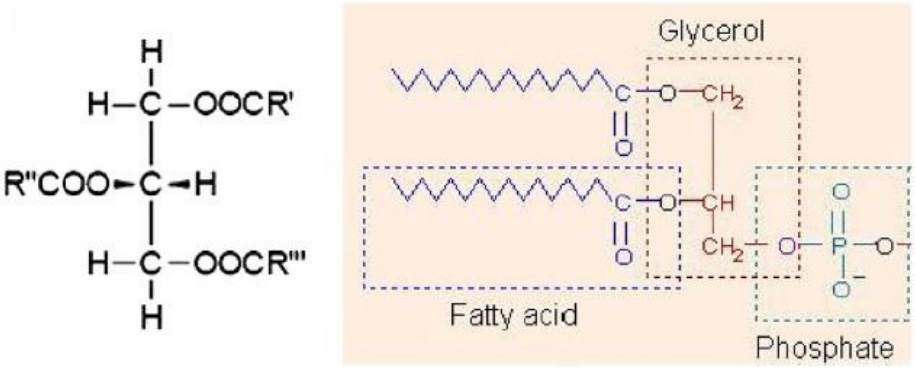

Figure 21- On the left: Triglyceride (neutral lipid). R', R'' and R''' represent fatty acid chains. On the right: Phospholipid (polar molecule). [42]

Tri-, di, and monoglycerides consist of 1 mol of glycerol esterified with 3 mol, 2 mol, or 1 mol of fatty acid, respectively. [44] The triglycerides of natural oils contain at least two different fatty acid groups, and the chemical, physical and physiological properties of the oil are determined by the type of the fatty acid groups and their distribution over the triglycerides molecules. The melting point of these molecules, generally increases with the increasing of the long chain fatty acid or decreases with the shortening of the chain or with unsaturated fatty acids. [44] Vegetable oils are liquid at ambient temperature because of their high proportion of unsaturated fatty acids.

1.1.2.1. Biodiesel Production from Fats and Oils

From oil, biodiesel can be produced, with an end product as fatty acid methyl ester (FAME). Several methods have been employed to transform the oils and fats into biodiesel such as pyrolysis, microemulsion and transesterification (alcoholysis). [43,46] It is important to refer that are also some types of neutral lipids that do not contain fatty acids, such as hydrocarbons, sterols, ketones, and pigments, such as carotenes and chlorophylls. Even though these lipids fractions are soluble in organic solvents, they are not convertible to biodiesel. [42] As shown is Reaction 4, the transesterification reaction is the process of

exchanging the alkoxy group of an ester compound with another alcohol. In order to achieve high yields, a catalyst is necessary, and it can be a basic or an acid catalyst, or even an enzymatic catalyst. [42] Excess amount of alcohol is used in this reversible reaction to assure total conversion of glycerides. [46] Methanol is widely used as the alcohol for producing biodiesel because it is the least expensive alcohol, and also for its advantages, like (*i*) its high reactivity, (*ii*) the fact that it does not absorb water which interferes with transesterification reaction, (*iii*) prevention of soap formation and (*iv*) easy recovery/recycling. [46]

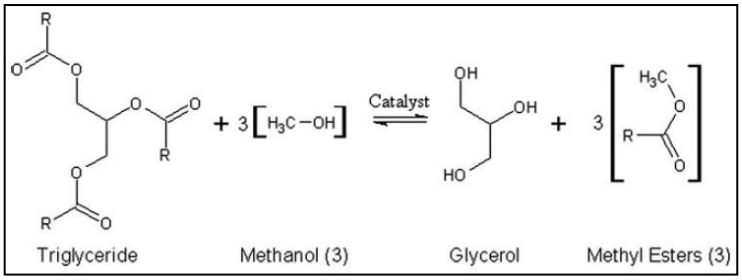

Reaction 4 - Transesterification reaction of triglycerides with methanol to FAME. [46]

1.2. Extraction Processes to Obtain Pumpkin Oil

1.2.1. Mechanical, Organic Solvent, and Other Extraction Processes

Nowadays, the industrial production of pumpkin oil is achieved by hydraulic cold pressing, using mainly its seeds. The process begins with the addition of water and table salt to ground kernels, which have been dried to a residual water content of 5–7%. The soft pulp formed is then roasted for up to 60 min, at around 100°C. This roasting process is responsible for the generation of the typical aroma of the end product. Afterwards, a pressing process is performed under isothermal conditions, at pressure ranging from 300 to 600 bar. As the end product of this pressing process, a dark green oil results. The major drawback of this process is the residual oil left in the seeds is high, varying from 5 to 15%. [47]

In most laboratory practices, such as Soxhlet Extraction (2.2.1 - Soxhlet Extraction) and the *Bligh and Dyer* method (2.2.2 - *Bligh and Dyer* Method), both non-polar and polar organic solvents are used, to determinate the content of lipids.

The principles underlying these extraction methods are built on the basic chemistry concept of 'like dissolving like'. Due to the interactions between their long hydrophobic fatty acid chains, neutral lipids participate in weak van der Waals attractions between one another, forming globules in the cytoplasm. So, when a vegetable cell is exposed to a non-polar organic solvent, such as hexane or chloroform, the solvent penetrates through the cell membrane in to the cytoplasm, and interacts with the neutral lipids using van der Waals forces to form a solvent-lipids complex. This organic solvent-lipids complex diffuses through the cell membrane and the static organic solvent film surrounding the cell, driven by a concentration gradient, into the bulk organic solvent. As a result, the neutral lipids are extracted out of the cells and remain dissolved in the apolar organic solvent. [42]

In some cases, neutral lipids are found in the cytoplasm as a complex with polar lipids. This complex is linked with higher strength, due to hydrogen bounding to cell membrane proteins. The aforementioned van der Waals interactions formed between the apolar solvent and the neutral lipids of the complex are not sufficient to disrupt the associations of the membrane-based lipid-protein. However, polar organic solvents, such as methanol or isopropanol are able to disrupt these lipid-protein associations by forming hydrogen bounds with the polar lipids in the complex. The organic solvent mixture (polar and non-polar) passes through the cell membrane and interacts with the lipid complex. In this interaction, the polar fraction of the solvent mixture is going to surround the lipid complex and form van der Waals associations with the neutral lipids in the complex, while the polar fraction, of the solvent mixture, will also surround the complex, forming hydrogen bounds with the polar lipids in the complex. This last association is strong enough to detach the lipid complex from the membrane proteins. Once again, the solvent-lipids complex formed diffuses through the cell membrane, into the bulk organic solvent. [42] The mixture of a polar solvent and a non-polar solvent facilitates the extraction of lipids from the vegetable cells, increasing the yield of oil extracted.

Some other processes used for recovering pumpkin bioactive materials, besides oil, are summarized in Figure 22.

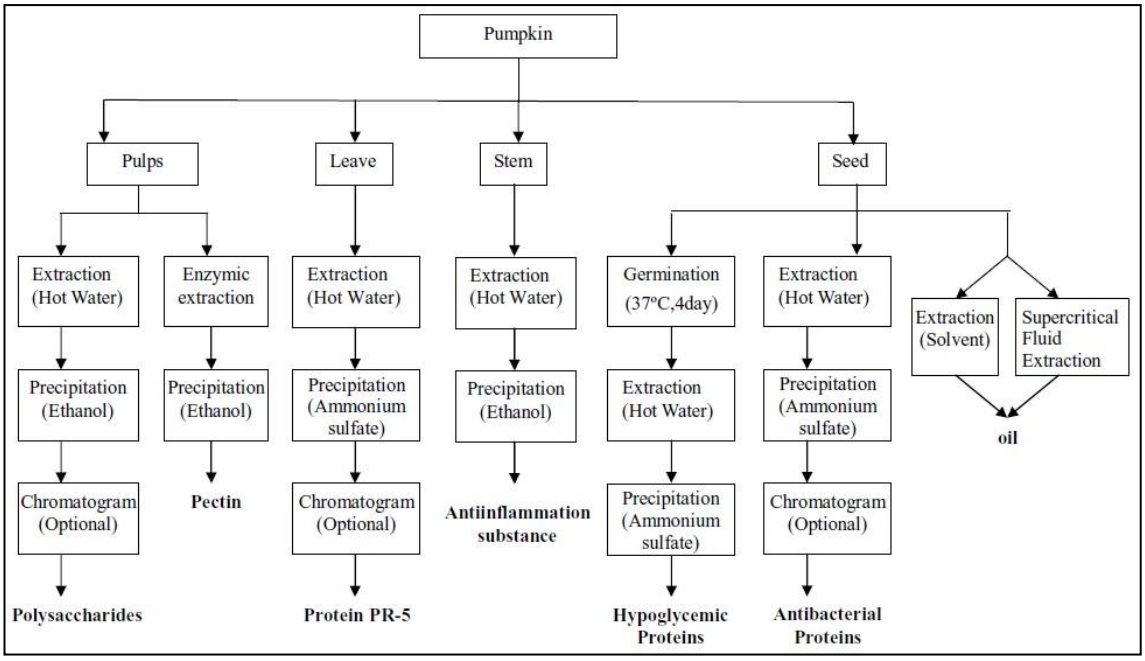

Figure 22 - Recovery processes for pumpkin bioactive materials. [11]

As mentioned above, organic solvents are usually used in food processing, but this method is under great scrutiny due to increasing governmental restrictions and consumer concerns regarding safety to the use of these so mentioned organic solvents.

Consequently, supercritical carbon dioxide ($scCO_2$) has become a viable alternative to replace *n*-hexane, among other organic solvents, and meet the growing consumer demand for natural products.

1.2.2. Supercritical Fluids

When a fluid is subjected to conditions that exceed supercritical temperature and pressure, it is referred to as a supercritical fluid (SCF – Figure 23). When the fluid enters this region, it adopts an array of gas and liquid properties, with low viscosity, high diffusibility, and almost no surface tension. The critical temperature and critical pressure are characterized by the point in which phase transition is no longer possible, regardless of changes in pressure.[48]

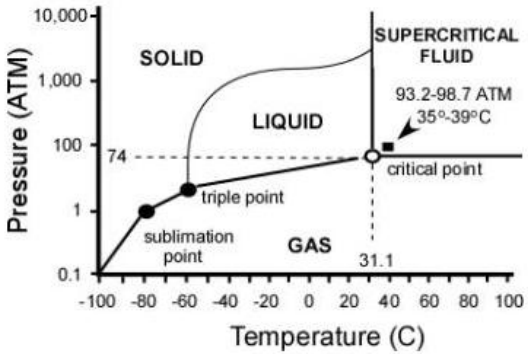

Figure 23 - Supercritical pressure-temperature diagram for carbon dioxide.[49]

These fluids display two major properties of having liquid-like density as well as high compressibility (offering large variability of solvency by small changes in temperature and pressure). Physical characteristics, including diffusivity, viscosity, and surface tension attribute to the increased solvent capacity of the fluid, which may be exploited for extraction applications.[50]

The solvation power (dissolving capacity) of a supercritical fluid is sensitive to the temperature and pressure changes in the supercritical region. [49] In this region, there is only one phase, which possesses properties of both gas and liquid, making the solvation power higher due to high, liquid-like, density. The mass transfer rates also increase because of a high, gas-like diffusion coefficients and low viscosity values. [51] These are the main characteristics of supercritical fluids that make them an attractive agent. [49] As a result, supercritical fluids are ideal alternatives to organic solvents, and with these properties, mixing of compounds can be improved, resulting in a better heat and mass transfer.

In order to choose a supercritical fluid as solvent, a number of aspects must be considered, such as (*i*) solubility of the solute in the supercritical fluid, (*ii*) viscosity of the fluid in the supercritical region, (*iii*) diffusivity of the supercritical fluid, (*iv*) heat and mass transfer parameters of the solvent and (*v*) all the conditions that are necessary to achieve the supercritical point of the fluid, regarding economical and safety aspects.

In this work, it was used carbon dioxide as the supercritical fluid, despite of any pure compound present a supercritical point (Table 5). The choice of this particularly solvent was based on the many advantages it presents. It is an inexpensive, nontoxic compound, it is easy to obtain with high purity, is nonflammable (unlike conventional liquid organic solvents), has a low critical temperature, and it is easily separable. In addition it is a key by-product in several industrial processes, and it's recycling reduces GHG (Green House Gases) emission to the atmosphere.[52,53]

Carbon dioxide (Table 6) always behaves as a non-polar solvent and reaches the supercritical point at 304,25K and 7,43 MPa [49]. Being a non-polar solvent it has high affinity to non-polar compounds, such as hydrocarbons, like lipids.

Table 5 - Critical point for some pure components [49].

Component	T_c (°K)	P_c (MP_a)
Methane	190,70	4,60
Ethane	305,40	4,88
Oxygen	156,60	5,04
Hydrogen	33,00	1,29
Ethylene	282,40	5,04
Methanol	512,60	8,09
Ethanol	513,90	6,14
Carbon Dioxide	304,15	7,38
Water	647,30	22,12

Table 6 - Carbon dioxide properties as a liquid, supercritical fluid and vapour. [54]

Properties	Liquid	Supercritical (at 260 bar, 323,15K)	Vapour
Density ($Kg.m^{-3}$)	1170	844,87	1,87
Viscosity ($N.m^{-2}.s$)	$2,5x10^{-4}$	$7,95x10^{-5}$	$1,4x10^{-5}$
Thermal Conductivity ($W.m^{-1}.K^{-1}$)	0,1798	0,6556	0,0146

1.2.2.1. Supercritical Fluid Extraction

The supercritical fluid extraction process have emerged over the last years as highly promising environmentally benign technology for the production of natural extracts with high potency of active ingredients, such as flavors, fragrances, spice oils, and oleoresins, natural colors, nutraceuticals or herbal medicines, for the food, cosmetics and pharmaceutical industries. [15]

To better understand what is a supercritical fluid extraction process, first it must be clarified what consists this type of process. A schematic diagram of this process is represented in Figure 24. The carbon dioxide leaving the vessel is sub cooled before it reaches the pump, which assures a liquid phase, avoiding cavitations problems. Once the pressurized solvent is pumped, it passes through a heater, where it will be heated from its critical temperature to the extraction temperature. The extraction vessel, which is filled with the feed material, is electrically or water heated to the extraction temperature. The supercritical solvent flows through the fixed bed and the soluble compounds are extracted from the feed material. Once the supercritical solvent with solutes leaves the extraction vessel through the top, it passes in a pressure reduction valve. The solvent power decreases with pressure reduction, and the solutes precipitate. To assure that all compounds precipitate, the supercritical fluid is heated,

in the separation vessel, above the saturation temperature to reach the gas phase. The material is then collected from the separator vessel, and the gas phase solvent, leaves the separator vessel from the top, and can be recirculated back to the extraction vessel.

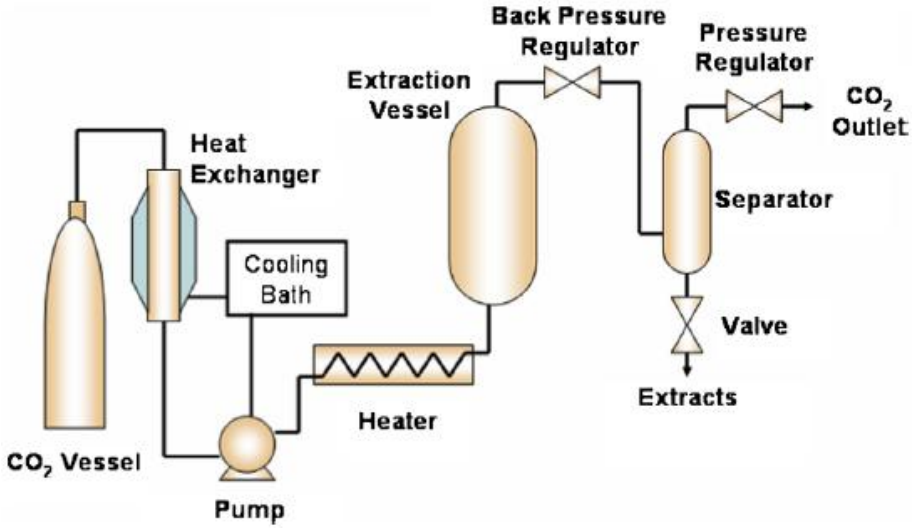

Figure 24 - Schematic diagram of a typical supercritical fluid extractor with a single separator. [55]

Accordingly to objective of the extraction, two different scenarios can be considered:

1) *Carrier material separation* – where the final product is the feed material, without the initial solutes that were undesirable. Fine exemplum of this type of extraction process is the decaffeination of coffee. [28]
2) *Extract material separation* – the compounds extracted from the raw/feed material are the final product, like the extraction of essential oils and antioxidant compounds. [28]

In the present work, the extraction process was the same mentioned in (2), with the extraction of oil from pumpkin. The extracted oil contains an antioxidant compound, β-carotene which was the initial target of this project; to extract a high added-value compound with antioxidant capacity *via* a green and environmental friendly process.

For the separation of the soluble compound from the supercritical fluid, it is necessary to modify the thermodynamic properties of the solvent, either by manipulating the operating pressure and temperature, thus changing the solvation power of carbon dioxide, or by adding an external agent, an adsorbent. If the first method is used, it is possible to decrease the operating pressure by an isenthalpic expansion, which causes the lowering of fluid density and consequently the reduction of solvent power. On the other hand, if the temperature is manipulated, two situations may occur, depending only on the solubility of the dissolved compounds. If the solubility of the compounds increases with temperature at constant pressure, then a decrease in temperature will lower the compound solubility, thus allowing the separation of those compounds from the supercritical CO_2. Then again, if solubility decreases with the increase of temperature, at a constant pressure, an increase in temperature will separate the solutes from the solvent. For the second method, where an auxiliary agent is used, no significant changes in pressure occur. This type of process implies lower operating costs; though, the recovery of the extract from the adsorbent matrix is usually very difficult.

The extract dissolved in the supercritical fluid is absorbed by a wash fluid in a countercurrent flow using a packed column or spray tower under pressure. [28]

Besides pressure and temperature, solvent flow rate, solvent-to-feed ratio, particle size, residue moisture content, modifier/co-solvent type and concentration must be taken into account. [49] High solvent flow rates results in shorter contact time between the solvent and solute, resulting in a loading of the solvent much lower than the saturation concentration, and also imply high operating and capital costs. On the other hand, a low solvent flow rate or a high residence time implies a long batch. This parameter must be optimized to fulfill the need of the extraction process. The solvent-to-feed ratio depends on many factors, such as concentration of the solute in the feed material, solubility in the supercritical CO_2, type of feed material, and distribution of the solute in the raw material. [49] The size and morphology of the solid material have a direct effect on the mass transfer rate. Generally, increasing the surface area will increase the extraction rate, thus smaller particle size or geometry, usually favors higher mass transfer, which decreases the batch time and the diffusion controlled process. However, very small particles induce a channeling effect, which decreases the extraction rate. Also, high moisture content is not desirable because moisture acts as a mass transfer barrier, but in some cases, moisture can expand the cell structure, facilitating the mass transfer of the solvent and the solute through the solid matrix, e.g., in seeds and beans.

In order to enhance the solvent strength capacity, a common method is used; the addition of a polar co-solvent. Frequently polar cosolvents include methanol, ethanol, acetonitrile, acetone, water, ethyl ether, and dichloromethane. Of these, ethanol may be a better choice in $scCO_2$ extraction of bioactive compounds from fruit and vegetable, because of its lower toxicity compared to other cosolvents, which may present problems in industrial-scale operations because of their cost, flammability, and disposal requirements. [56] Sunflower oil was also used as a co-solvent; however in this case, the purpose was to enrich the sunflower oil with an added-value compound – β-carotene.

The extraction enhancement resulting from the addition of a cosolvent may be related to several phenomena, including (*i*) change in polarity, density, or viscosity of the extraction fluid; (*ii*) miscibility of the modifier and solvent solubility; (*iii*) interaction between $scCO_2$ and the matrix; (*iv*) interaction between the solute and co-solvent; and (*v*) disruption of the bonding between solutes and the solid matrix.[56] The addition of cosolvents such as ethanol also changes solubility, transport properties, and intraparticle resistance in the matrix. Co-solvents may also aid in increasing the extraction yields and/or rates, depending on the pressure and temperature used.

In the present project, the separation of the oil from the supercritical CO_2 (carbon dioxide) was achieved by reducing the pressure. In order to study the extraction process of the pumpkin oil, the solvent flow rate, and co-solvent type were varied. In addition, the pumpkin residue used was previously grinded and dried in all the extraction, except for one, where it was wet.

The extraction process, as a whole, must be considered as a semi-batch process given that carbon dioxide is only fed to the system according to its losses, and also because, no new material is fed during the extraction process. This carbon dioxide feed process is made automatically, according to pressure drop created between the CO_2 vessel and the system, by a check valve. The carbon dioxide is continuous recycled through the system in order to extract

the maximum yield of the target compound. So, one key aspect of the extraction process is recycling the supercritical carbon dioxide, which allows the reduction of operating and capital costs. Recycling of the solvent depends on the separating conditions of the solute from the extraction fluid, because it can either be in the liquid phase or in the vapour phase. Also, and as mentioned before, the supercritical solvent flow rate affects the economical balance of the process, because either a liquid pump or a compressor can be utilized to increase the pressure in an extraction process. To better understand these aspects, two pressure-enthalpy diagrams (P-H diagram) were used; one illustrating the pump liquid scenario, and another the compressor. In Figure 25 and 26 is demonstrated the solvent cycle of an extraction process, where a compressor and a liquid pump are used, respectively.

In both cases, the separation of the soluble compound from the solvent is achieved by isenthalpic throttling (D-E), leading to a fast decrease in pressure value, from 260 bar to 65 bar. Afterwards the carbon dioxide is heated (E-F), and at F, the temperature is 304,15K (31°C), approximately, and the solvent is in a gas state, so the solvent power is negligible. Then, the solvent is recycled (F-A) and equals the temperature of the CO_2 vessel, 293,15K (20°C). In the next step, the carbon dioxide is cooled (A-B) and compressed or pumped. When a compressor is used, the solvent is cooled down to 273,15K (0°C), just to prevent overheat of the output current of the compressor and to maximize the compressor efficiency. However, when the liquid pump is used, the solvent must be in the liquid phase so it passes through a chiller, which will bring it to 263,15K (-10°C), to guarantee that even with heat losses from the pipes and valves, the liquid phase is maintained.

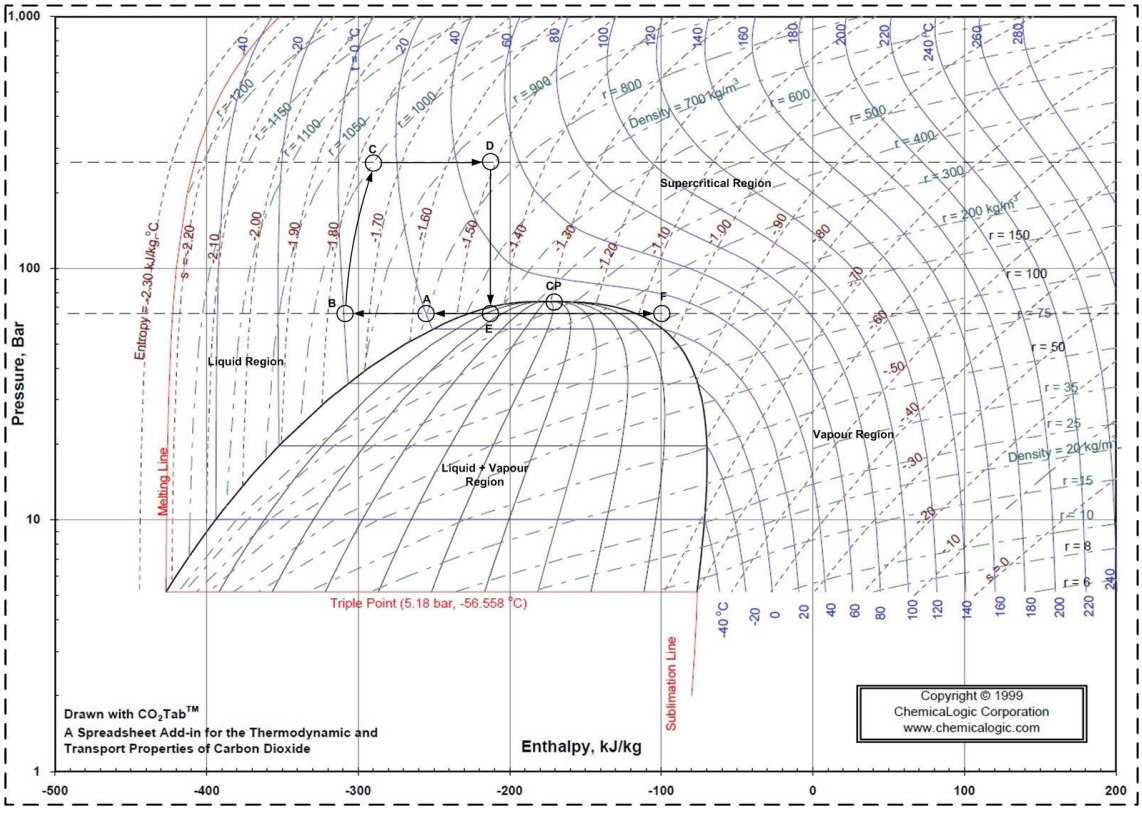

Figure 25 - Solvent cycle P-H diagram for the compressor. (adapted from [57])

Once the solvent starts to be compressed, the pressure begins to rise and so the temperature (B-C). Afterwards, the extraction temperature is reached (C-D), along the static mixer, and throughout the extractor.

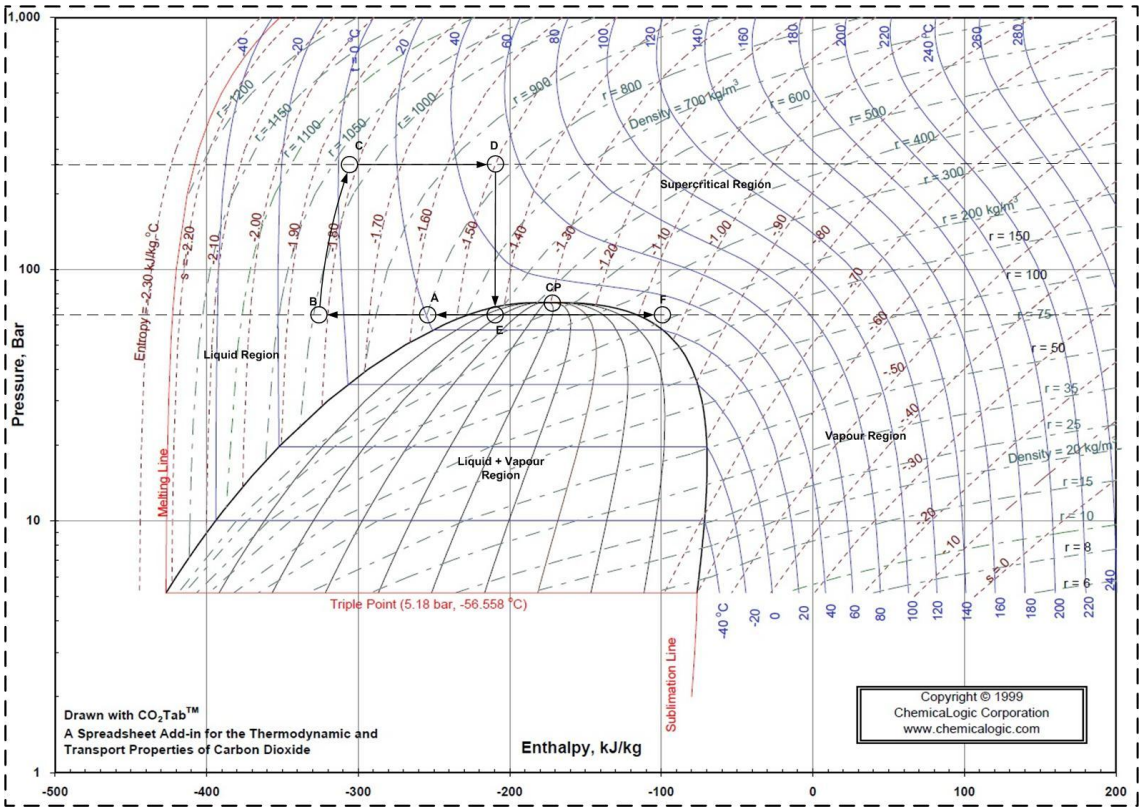

Figure 26 - Solvent cycle P-H diagram for the liquid pump.(adapted from [57])

An additional factor that must be considered to reduce operating costs is to minimize solvent losses, which take place from the extraction vessel during the depressurization for unloading the spent material, as well as in the separator when withdrawing the extract. Although, most of the CO_2 losses occur in the depressurization process, so, a storage vessel was used.

1.2.2.2. Applications and Today's Industry

The principal interest in exploring the use of SCFs in the chemical industry arises from a desire to replace volatile organic chemicals (VOCs) with SCFs. Among the many reactions that have been study, some are noteworthy, like polymerization, oxidation, metathesis, alkylation, hydrogenation, hydroformylation, among others (Figure 27). Some of these examples are described in this chapter.

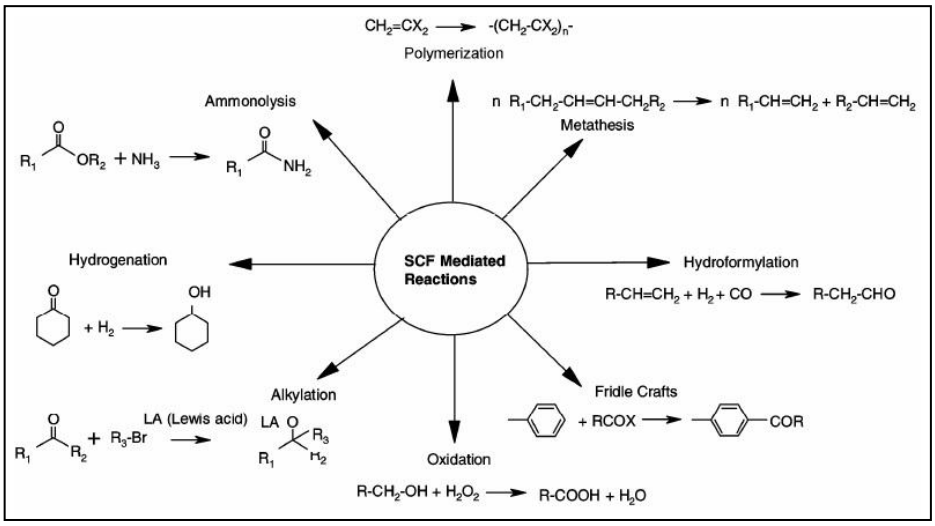

Figure 27 - Some industrial reactions carried out with SFCs. [58]

The implementation of SCFs technology has already been done for some industrial processes (Figure 28), while the scientific viabilities are being actively explored for others.

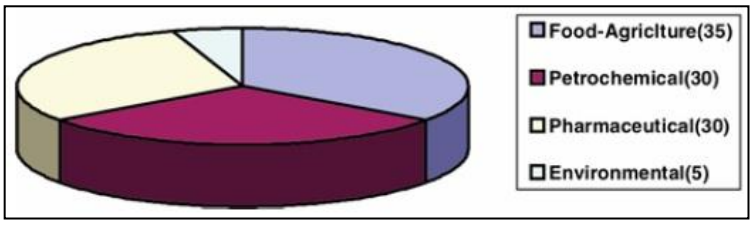

Figure 28 - SFC technology distribution in key industries sectors. [58]

The Roche company used $scNH_3$, scN_2O, and $scCO_2$, for the production of some pharmaceutical products and intermediates, such as D,L-α-tocopherol, with scN_2O (Figure 29).

An important recent development was the hydrogenation of a specialty chemical, cyclohexylamine[4], from aniline in continuous rather than batch process. This technology took a 7 year period to expand from the bench scale (5mL reactor) to a plant with a capacity of 1000 tons/year. [59]

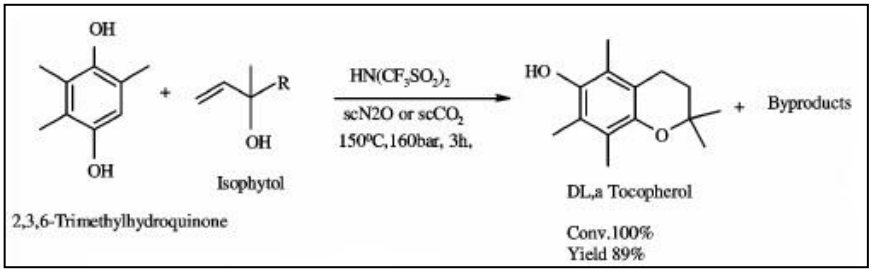

Figure 29 - D,L-α-tocopherol synthesis with scN_2O. [58]

Terephthalic acid has great commercial importance, because it is one of the monomers for the production of polyesters. The production of this monomer can be carried out in a $scCO_2$

[4] Cyclohexylamine – It is a building block for pharmaceuticals, such as mucolytics, analgesics, and bronchodilators.

environment, with the carboxylation of toluene to give *p*-toluic acid, rather than using *p*-xylene as the raw material. The oxidation reaction of toluic acid to terephthalic acid is well understood, since the conversion of *p*-xylene to terephthalic acid involves the formation of toluic acid as an intermediate. The reaction is shown in Figure 30.

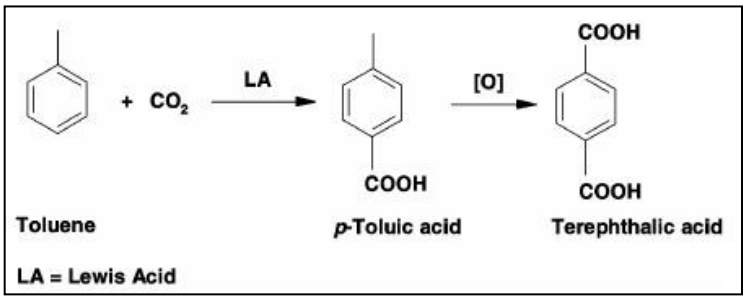

Figure 30 - Terephthalic acid formation using $scCO_2$. [58]

Olefin metathesis[5] is a heterogeneous catalytic reaction, which has been employed in the chemical industry for many years. The synthesis of epilachnene[6] is carried out with $scCO_2$, using a ruthenium-catalyzed RCM (Ring Closing Metathesis).

Another significant achievement was the completion of a plant with a production capacity of 50.000 tons/year of polycarbonate, from alkene oxide and $scCO_2$, by Asahi Kasei Corp. (AKC). This is an environment-friendly manufacturing process which not only avoids the use of high hazardous phosgene, but also reduces carbon dioxide emissions. [60]

The decaffeination of coffee beans and tea leaves are another example of the use of SCFs for extraction processes. This technology is already carried out industrially. The CO_2 is regenerated by washing with water or by adsorption in activated carbon. [61]

1.2.2.3. Mathematical Model for SCF Extraction

From an engineering point of view, the scale-up of supercritical fluid extraction process requires both knowledge of the relevant process parameters such as equilibrium and mass transfer kinetics, and also the optimum operating conditions. All of these parameters may be obtained by using an accurate mathematical description of the extraction process and experimental laboratory data.

The mathematical modeling of SCF extraction of value-added compounds from plant matrixes such as herbs, seeds, leafs or bark is difficult due to the existence of different structures in the material, nevertheless, this research has been the basis of most present-day SFE processes. Before the extraction, the raw material is usually grinded, in order to increase the surface area in contact with the supercritical solvent and also to increase the accessibility of the solute inside the cell structures, which will increase mass transfer kinetics. This enables the description of the resulting particles using the basic geometries of slab, cylinder or sphere.

[5] Metathesis – Is an organic reaction in which occurs the redistribution of fragments of alkenes (olefins) by the scission and regeneration of C-C double bounds.

[6] Epilachnene – It is an alkaloid with antiinsectan activity.

In order to reduce the complexity of the model used, it is necessary to make simplified assumptions about how the solute is distributed inside the solid – adsorbed in the pore network, entailed inside cell structures or homogeneously distributed inside particles – and about the mechanisms involved in the mass transfer kinetics – internal mass transfer resistance, external mass transfer resistance or a combination of various resistances. The understanding of these parameters can be used to economically evaluate the extraction process from laboratory to pilot and industrial scale. Through fitting experimental data, mathematical models are used not only to provide a quantitative interpretation of the experimental data, and discover the true values of the parameters that are physically important, but also to give information at points where measurement cannot be carried out.

From these regards, the most valuable models are those developed from differential mass balance equations for the packed bed of solid substances, which when integrated, time-dependent concentration profiles in both solvent and solid phase can be obtained. [62] Figure 31 demonstrates a diagram of a fixed bed extractor showing a finite volume element, bed and particle characteristics, and the concentration profiles of solute within the particles and surrounding solvent [55].

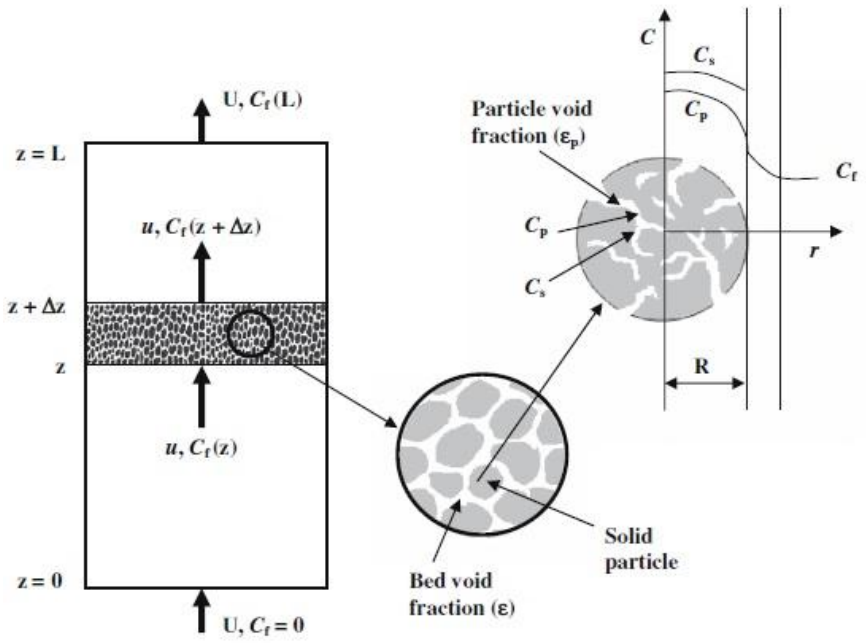

Figure 31 - Diagram of a general fixed bed extractor, particle characteristics and concentration profile.[55]

There are several models employed to describe the SCF extraction of oils or other compounds from plant material [63,62]:

- Diffusion layer theory (DLT) model – By this model it is assumed that the mass transfer flux is proportional to difference between an average solute concentration in the porous particle and the solute concentration in equilibrium with the fluid phase.
- Shrinking core model – The shrinking core model is based on the assumption that as the extraction proceeds, a sharp boundary between the extracted and non-

extracted parts of the particle, recedes until it reaches the center of the particle, and all solute is exhausted.

- Broken plus intact cells (BIC) model – In this model, broken and intact cells are considered, and extraction kinetics from broken cells is faster than that from intact cells, since cell walls introduce an additional mass transfer resistance.
- BIC plus shrinking core model – This model combines the features of both shrinking core and BIC models, where the cells can either be intact or broken. Broken cells are assumed to be in the out layer of the particle, and during extraction process each layer is depleted in sequence, from the out layer to the center of the particle, like the shrinking core model.

Other models can be applied to the aforementioned processes.

For this project a more simplified model was used, where the mass transfer within a fixed-bed, inside a cylindrical extractor, may be described by a set of partial differential equations [55]. The extraction vessel is divided into finite difference volume elements of height Δz, according to Figure 31. To solve this mathematical model, assumptions were made: isothermal operation, negligible pressure drop across the extractor, and constant bed porosity and solid density along extraction. Also, it was assumed that the solute loading in the SCF is low and, therefore, fluid density, axial dispersion, and fluid velocity remain approximately constant. [61,62] These assumptions reduce the number of equations necessary to describe the extraction process to mass balances, equilibrium relations, and kinetics laws.

2. Materials and Methods

2.1. Materials

2.1.1. Raw Materials, Chemicals and Compounds

Pumpkin was purchase at the supermarket and used. Trans-β-carotene (95% type I, Sigma-Aldrich) was purchased and used.

Carbon dioxide (CO_2, MW = 44,01 g/mol), with purity higher than 95%, and Nitrogen (N_2, MW = 28,01 g/mol) were used. These two compounds were supplied by Air Liquid (Portugal).

n-Hexane for chromatography and extraction experiments (Soxhlet method) ($CH_3(CH_2)_4CH_3$, MW = 86,18 g/mol, Carlo Erba Reagents), *n*-heptane ($CH_3(CH_2)_5CH_3$, MW = 100,20 g/mol, Carlo Erba Reagents), ethylene glycol ($C_2H_6O_2$, MW = 62,07 g/mol, purity NA, Merck), acetone (C_3H_6O, MW = 58,08 g/mol, Carlo Erba Reagents), Sodium sulphate anhydrous (Na_2SO_4, MW = 142,04 g/mol, Panreac), methanol (CH_3OH, MW = 33,04 g/mol, PA grade, Sigma-Aldrich), acetyl chloride (CH_3COCl, MW = 78,49 g/mol, PA grade, Flucka), heptadecanoic acid ($CH_3(CH_2)_{15}COOH$, MW = 270,45 g/mol, purity higher than 98%, Sigma-Aldrich), tricaprin ($C_{33}H_{62}O_6$, MW = 554,84 g/mol, ≥ 98% pure, TCl), pyridine (C_5H_5N, MW = 79,10 g/mol, ≥ 99% pure, Carlo Erba), N-methyl-N-(trimethylsilyl)trifluoroacetamide (MSTFA) ($C_6H_{12}F_3NOSi$, MW = 119,25 g/mol, 97% pure, Alfa Aesar), chloroform ($CHCl_3$, MW = 119,38 g/mol, ≥ 99% pure, Carlo Erba Reagents) were purchased and used.

2.2. Methods

2.2.1. Soxhlet Extraction

Soxhlet extraction is a standard technique and the main reference for evaluating the performance of other solid-liquid extraction methods. It is a general and well-based technique, which exceeds in performance over conventional extraction techniques, except in the extraction of thermolabile compounds. The Soxhlet extraction is a conventional method that uses organic solvents, such as *n*-hexane. This apparatus is constituted by three compartments: a continuously heat round-bottom flask, the Soxhlet extractor, and a cooled reflux condenser (Figure 32).

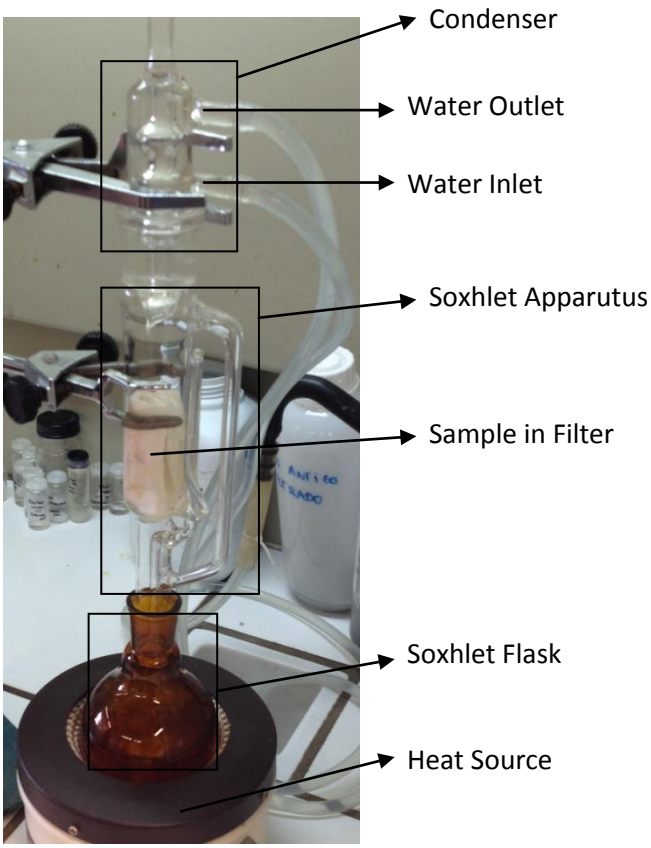

Figure 32 - Soxhlet apparatus.

The raw material is placed in a thimble-holder, and is filled with condensed fresh solvent from the distillation flask. Once the liquid reaches the overflow level, a siphon aspirated the solution and unloads it back into the heat round-bottom flask, carrying extracted solutes into the bulk liquid. The solute is separated from the solvent by distillation, and goes back to the Soxhlet extractor where the plant solid bed is. This operation is repeated until complete extraction of the solutes is achieved, usually 6 hours. The main disadvantage of this method is high energy requirement. [64]

2.2.2. *Bligh and Dyer* Method

The *Bligh and Dyer* method (1959) was used to perform lipid extraction from pumpkin residue.

Firstly, 2g of residue is added to 200ml of methanol:chloroform:water (10:5:4) solution, and submitted to a magnetic stirring, for 5 hours. Subsequently, the solvent mixture with lipids is submitted to centrifugation for 10min, and then, the liquid phase is removed. This liquid phase corresponds to the chloroform phase containing total lipids – fatty acids and sterols. The chloroform phase is removed and placed into a separatory funnel. This step is repeated until the liquid phase has no color. Afterward, the volume is corrected: per 200ml MeOH:$CHCl_3$:H_2O (10:5:4) is added 120ml of MeOH:$CHCl_3$ (1:1). Then, the separatory funnel is shake gently and let for at least 3 hours, or until two phases are completely formed. Finally, the lower phase (containing the chloroform and lipids) is collected and filtered to a Soxhlet flask and, subsequently, the organic solvent is evaporated in a rotavapor.

With the results from this extraction method it was possible to determine the maximum yield of extraction, when both polar and non-polar organic solvents are used.

2.2.3. Supercritical Fluid Extraction

For the oil extraction process, the installation represented in the schematic diagram of Figure 35 (see chapter 2.3.1 – High-Pressure Installation for Oil Extraction), was used. First of all, it is necessary to fill the extraction vessel (height = 55 cm, inner diameter = 2,48 cm) with the raw material, forming a packed bed of ,e.g., ±24 g of grind pumpkin, between an amount of cotton and a porous plate to avoid undesired entrainment effects.

The carbon dioxide vessel (293,15K and 65 bar) valve is open, and the CO_2 (gaseous) flows through CV-1, and SDV-1 until it reaches a chiller (263,15K) (Mina Frio, Refrigeração e Ar Condicionado, Lda), where a phase change to a liquid state occurs. PI-1 (WIKA) shows the pressure in the segment between the carbon dioxide vessel and the CV-1, and RV-1 can be used, if it is necessary to reduce the pressure in this segment.

The installation is able to work with high (150 g/min) and low (10 g/min) CO_2 flow rates, because either a liquid pump (KNAUER® 1800) or a compressor (KISSILING & Co®) is used. When the LP-1 is used, the supercritical solvent passes through the SDV-2, and enters the pump, then it passes the CV-3, and SDV-3 until it reaches a flow meter (MassFlo®, Compact IP67), where the flow rate can be measured. If the compressor is used, the carbon dioxide passes through SDV-4 until it reaches the flow meter. PI-2 (VDO) indicates the outlet pressure of the compressor (260 bar), and RV-2 can utilized for the same purpose of RV-1.

Once the carbon dioxide passes the flow meter and SDV-5, it reaches the static mixer (323,15K). Some experiments require the use of a co-solvent, which is pumped by the liquid pump 2 (Minipump®, LDC Analytical), passing through CV-3 and SDV-6, until it reaches the static mixer. PI-3 indicates the outlet pressure of the LP-2.

Once the carbon dioxide passes the static mixer it arrives to the extraction vessel, at 325,15K and 260 bar. After the extractor, the CO_2 pressure can be measured by the PI-5 (BOURDON HENNI). RV-3 can be used for the same purpose as RV-2 and RV-1.

BPR-1 (Back Pressure Valve) regulates the pressure drop of the installation, from 260 bar to the operating pressure of the CO_2 storage vessel, 65 bar. After the BPR-1 the carbon dioxide passes through SDV-8 (Parker), and PI-6 (VDO) into the separation vessel, which is at 65 bar and 304,15K (31°C). When is necessary to take a sample, V-2 (Valve) opens and a sample is collected to a vial. The carbon dioxide leaves the separation vessel (gaseous), passes through SDV-9, and SDV-10 and is recycled back to system. PI-7 (WIKA) is used for the same purpose as the others PI's.

All the high pressure tubing, valves, and fittings are from HIP®, SWAGELOK®, and Tescom Europe®.

2.2.4. Mathematical Model – Gproms® Software

The mathematical modeling of the extraction process was performed using the *Process System Enterprise Gproms*® Software, version 3.7.1. The implementation of this mathematical model allowed predicting the effective diffusion coefficient (D_e), given the extraction yields obtained in 7 experiments.

The code used in the mathematical model is shown in Annex A.

2.3. Experimental Set-Up

2.3.1. High-Pressure Installation for Oil Extraction

Figures 33 and Figure 34 are photography's of the high-pressure installation, used in the extraction of pumpkin oil, described in this work.

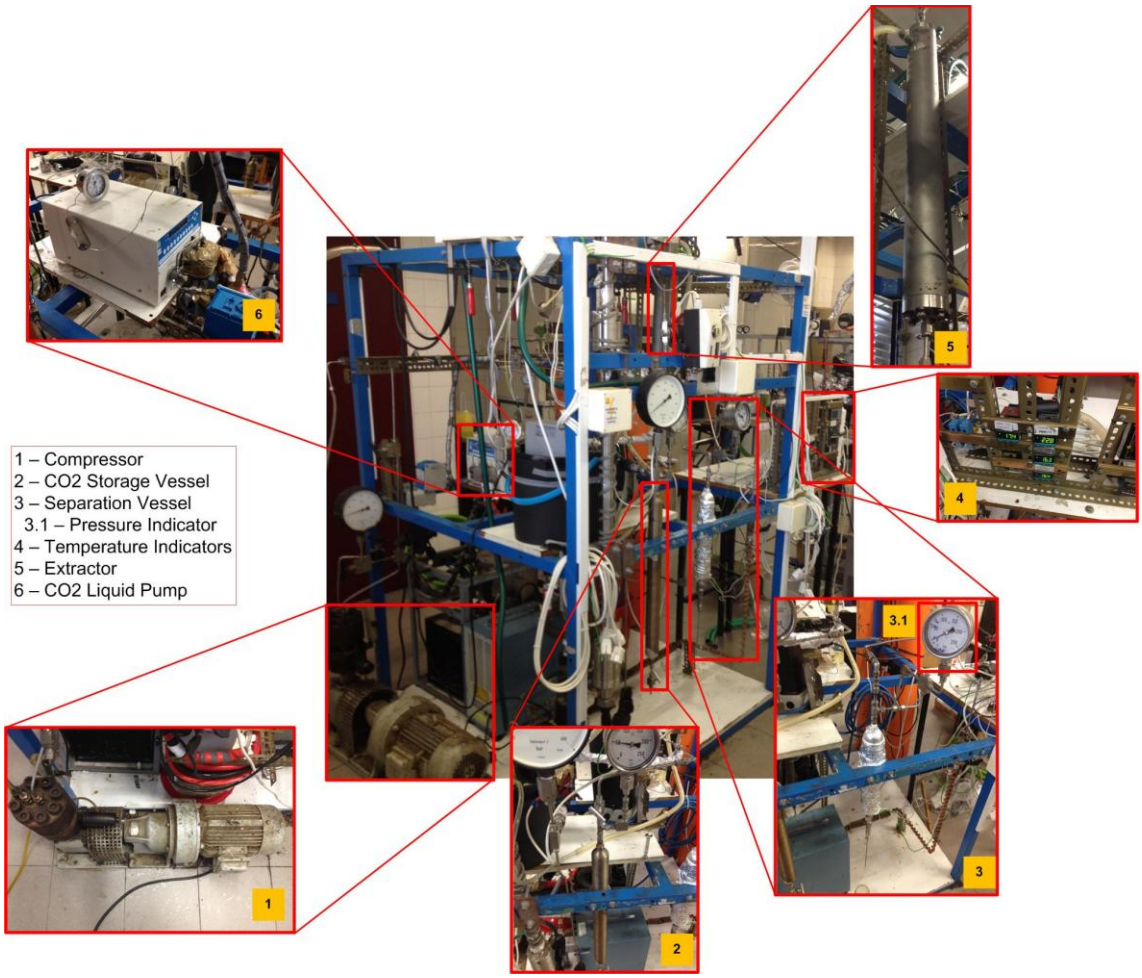

Figure 33 - High-pressure installation used for pumpkin oil extraction.

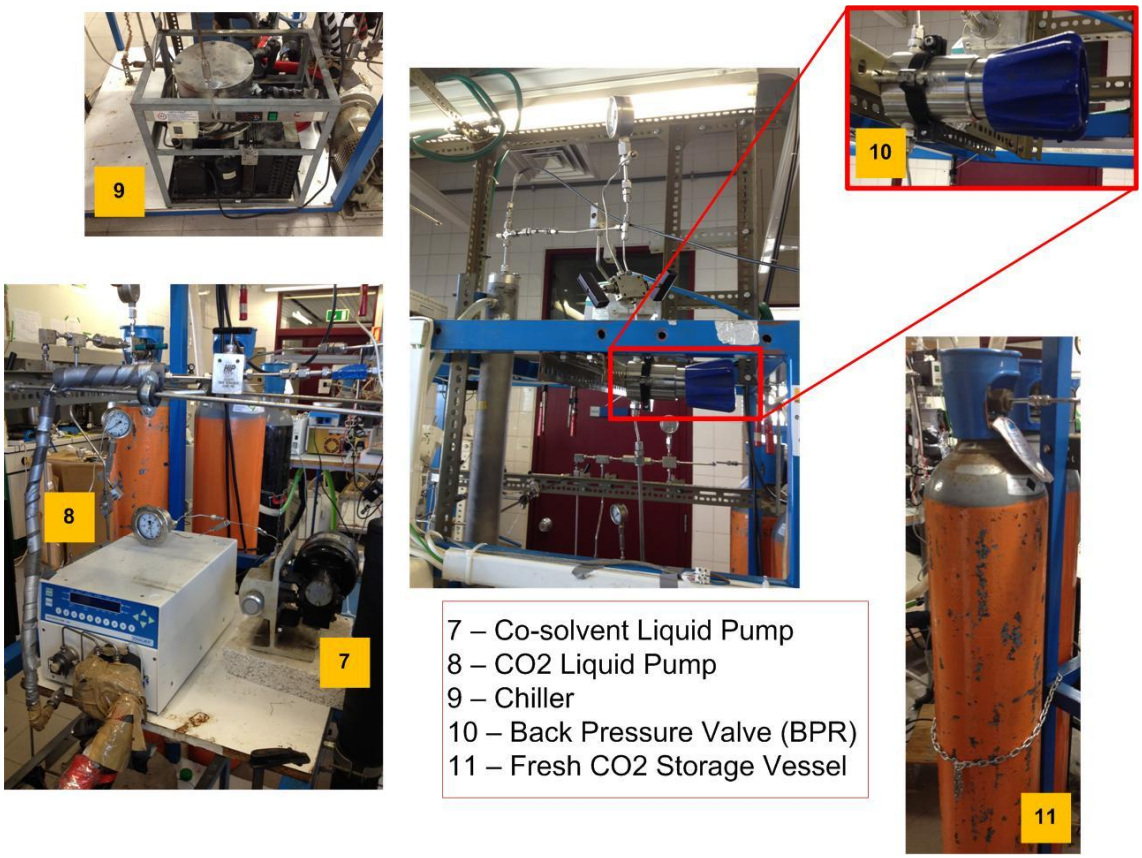

Figure 34 - High-pressure installation for pumpkin oil extraction (cont.)

The flow sheet of the installation is illustrated in Figure 35.

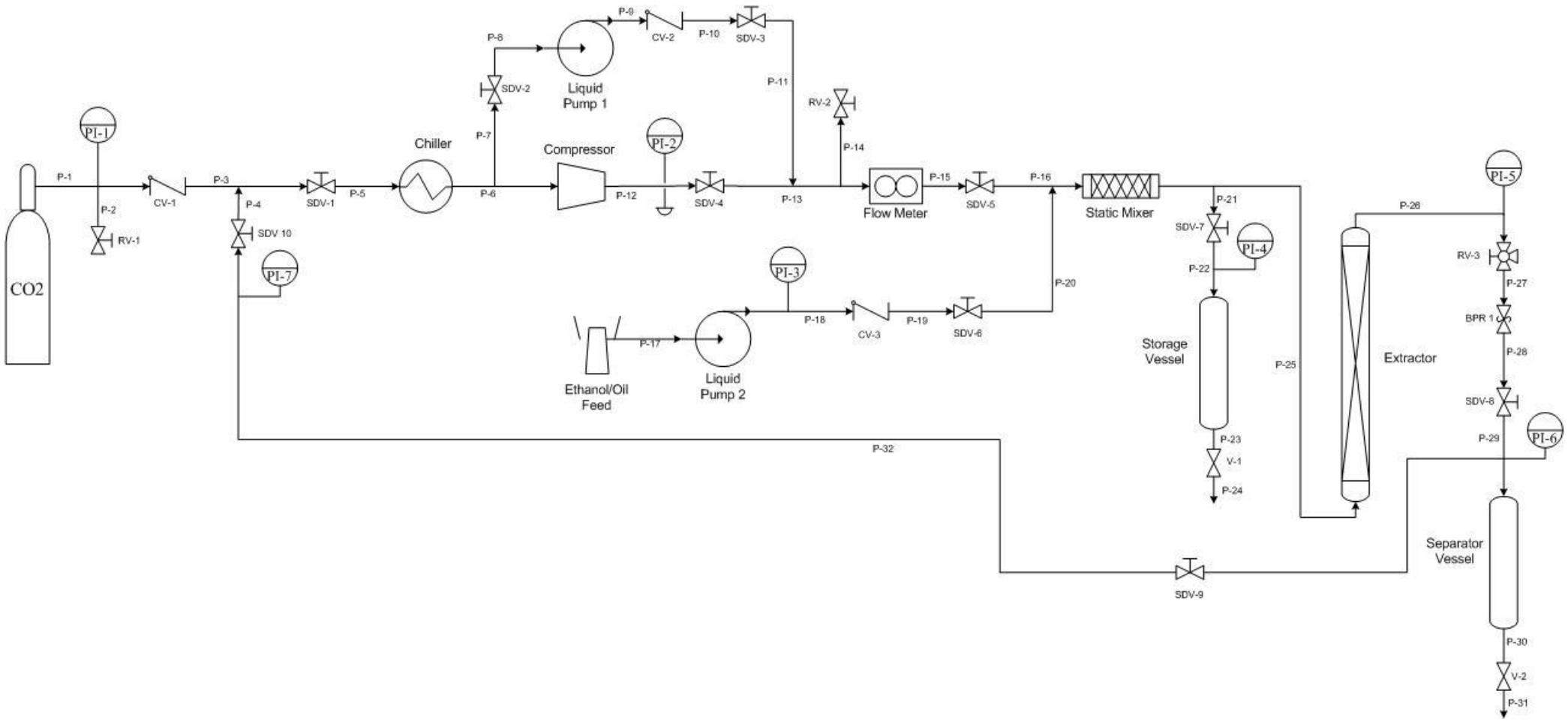

Figure 35 - Extraction process installation diagram.

2.4. Sample Analysis

Before analysis of samples, when ethanol (co-solvent) was used, a drying process was performed. The drying process was carried out with gaseous nitrogen (N_2) to avoid oxygen exposure.

2.4.1. Direct Transesterification – Lepage & Roy Method

To analyze the fatty acid profile in the extracted pumpkin oil, direct transesterification was used, based on the method derived by *Lepage* and *Roy* (1984). From the direct transesterification fatty acid methyl esters (FAME) are formed.

The method consists of adding 2 mL of methanol:acetyl chloride (95:5 v/v), and 0,2 mL of heptadecanoic acid in *n*-hexane (5 mg/mL), as the internal standard, to 10-25 mg of oil extract. Subsequently, the mixture is well sealed, and heated at 353,15K (80°C) for 1 hour. After, the vial is cooled at room temperature, and is diluted with 2 mL of *n*-heptane and 2 mL of water, to improve phase separation. Then, the heptadecanoic phase (upper phase) is separated by transferring it to a cotton filter bed with anhydrous sodium sulphate and filtered, to a vial.

2.4.2. Gas Chromatography

Triglycerides, diglycerides, and monoglycerides were determined by gas chromatography (GC) with on-Column injection – Thermo Scientific Trace GC Ultra Series (Figure 36 – Right side). The fatty acid profile of the extracted oil was determined by gas chromatograph (LC) (Figure 36 – Left side).

Figure 36 - Gas chromatograph on-column Thermo Scientific Trace GC Ultra.

Gas chromatography is an analytical technique used for the separation and analysis of compounds. These compounds pass through a capillary column aided by the flow of an inert gas, which consists in the mobile phase. The inert gas can be Helium (He), Argon (Ar), Nitrogen (N_2), etc. The column also contains a stationary liquid phase absorbed to the surface in an inert solid, where the sample to analyze is retained. The compounds can be separated according to their affinity (polarity) with the stationary phase or by their boiling point. With the on-Column injection, the sample injection is made directly in the injector of the column, placing the syringe inside the column without depressurize it. On this work, all compounds (TG, DG, MG) are separated according to their boiling points and unsaturated compounds are eluted before the corresponding saturated acids of the same chain length.

On-column gas chromatograph is equipped with a flame ionization detector (FID), with a ZB-5HT INFERNO column – 10 x 0.32 mm, 0.10 µm film thickness. The method used was the EN 14105 modified, which is exhibited on Table 7.

LC gas chromatograph is equipped with a flame ionization detector (FID), with a 30 m TERMO TR-BIODIESEL (F) 10 capillary column (0,25 mm of internal diameter and 0,25 µm of film thickness). The method used was the EN 14103 (2003), which is exhibited on Table 8.

In order to determine the molar concentration of glycerides (mono-, di-, and triglycerides) in the pumpkin oil extracted with $scCO_2$, calibration curves were previously done. Two internal standards were required: 1,2,4-butanetriol (IS1), and tricaprin (IS2) for mono-, di-, and triglycerides. Also, reference compounds were necessary – monolein, diolein, and triolein. The method used requires derivatization with MSTFA (N-methyl-N-

(trimethylsilyl)trifluoroacetamide) in pyridine, which transforms these compounds into more volatile silylated derivatives. Therefore, for each 100 mg of homogenized sample, 80 µl of IS1 (1 mg/ml), 100 µl of IS2 (8 mg/ml), and 100 µl of MSTFA were added to a 10 ml vial, which was hermetically sealed and shaken vigorously. After 15 min, 8 ml of *n*-heptane were added.

Table 7 - Selected instrument and modified EN 14105 method for the Trace Ultra GC and TriPlus AS (Glycerides).

Trace GC Ultra	
Injector	True cold on-column
Carrier Gas	Helium, 1 ml.dm^{-1}
FID	653,15 K
Oven Program	353,15 K (1 min) to 453,15 K at 288,15 K.min^{-1}, then to 503,15 K at 280 K.min^{-1}, then to 638,15 K (4min) at 283,15 K.min^{-1}
TriPlus AutoSampler	
Syringe Size	10 µl with 80 mm needle
Injected Volume	1 µl

Table 8 - Selected instrument and EN 14103 method for the Trace Ultra GC and TriPlus AS (Fatty acid).

Trace GC Ultra	
Injector	
Carrier Gas	Hydrogen, 1 ml.dm^{-1}
FID	553,15 K
Oven Program	393,15 K (0,5 min) to 493,15 K (1 min) at 303,15 K.min^{-1}, then to 523,15 K (5 min) at 283,15 K.min^{-1}
TriPlus AutoSampler	
Syringe Size	10 µl with 80 mm needle
Injected Volume	1 µl

Peak identification was carried out using known standards and the Chrom-Card software.

To determine the concentration of mono-, di-, and triglycerides in the extracted oil, a relationship between concentrations and peak area was used. This relationship is shown in Equation 1, where A is the peak area and IS2 is the internal standard 2 – tricaprin. The angular and linear coefficient for each compound is shown in Table 9.

$$\frac{A_{TG,DG,or\ MG}}{A_{IS2}} = a\frac{[TG, DG, or\ MG]}{[IS2]} + b$$

Equation 1 - Relationship between mono-, di-, and triglycerides concentration and peak area.

Table 9 - Linearization parameters of calibration curves to correlate concentrations and GC peaks areas of methyl esters.

Compound	Angular Coefficient (a)	Linear Coefficient (b)
Monolein	1,383	-0,0154
Diolein	1,1002	-0,0145
Triolein	0,4048	-0,0249

To analyze the fatty acid content in the extracted oil, the Lepage & Roy method was performed as explained above (2.4.1 Direct Transesterification – Lepage & Roy Method). The fatty acid profile of the extracted oil was determinate with their corresponding peak areas and the internal standard peak area (Annex B).

2.4.3. High Performance Liquid Chromatography

A conventional technique for the qualitative and quantitative quantification of carotenoids is high performance liquid chromatography (HPLC). The analysis of β-carotene content in the extracted oil was conducted with Thermo Scientific (Finnigan Surveyor AutoSampler Plus) HPLC, with a reverse-phase analytical 5-µ particle diameter, polymeric C_{18} column equipped with a UV diode array detector (Accela Uv/Vis Detector). The mobile phase consisted of (methanol and 0,2% H_2O)/acetonitrile (75:25 v/v). Total run time was 30 min, with an injection volume of 10 µl. β-carotene was monitored at 450 nm at a flow rate of 1 mL/min, and was quantified using a calibration curve (Annex C) of the corresponding standard compound (trans-β-carotene – 95% type I, Sigma) at the specific absorption maximum.

2.4.4. UV Spectrophotometry

UV Spectrophotometry (DU® 800 Spectrophotometer, Beckman Coulter) analysis was used to determine β-carotene content in the samples acquired from experiment 8 (see chapter 3.2.5 – β-carotene – Sunflower Oil Natural Additive), through the Beer-Lambert law. Spectra was run between 250 and 700 nm, and the concentration was determine at $\lambda_{[max]}$ = 450 nm, according to the specific optical coefficient of β-carotene.

3. Results and Discussion

3.1. Pumpkin Oil Analysis

Pumpkin oil extraction was performed by three different methods, in which organic solvents were used – Soxhlet method and Bligh and Dyer method – and a third extraction process where supercritical carbon dioxide was used.

3.1.1. Oil Extraction with Soxhlet Apparatus

The Soxhlet extraction method allows determining the quantity of extractable oil in the pumpkin residue that could be extracted by a non-polar solvent (*n*-hexane). This method was used to compare the results from the extraction process by $scCO_2$, where a non-polar solvent is used as well. Table 10 gathers all the studied parameters obtained by the Soxhlet extraction, and we can see that the yield of extraction is 13,5 $mg_{Oil}/g_{Pumpkin}$. It is assumed that the maximum extractable oil, when performing an extraction process with $scCO_2$, will not surpass the aforementioned value.

Table 10 - Experimental parameters for the Soxhlet extraction method.

Parameters	Time (min)	Pumpkin Mass (g)	Oil Extracted (mg)	Extraction Rate (mg_{Oil}/min)	Yield ($mg_{Oil}/g_{Pumpkin}$)
Value	420	2,0103	27,1	0,06	13,5

HPLC analysis was carried out to determine the content of β-carotene in the extracted oil by the Soxhlet method, to compare the results with the $scCO_2$ extraction. In order to do so, different standard β-carotene concentrations were plotted against their peak areas (Annex C), given the relationship necessary to calculate the β-carotene concentration of the extracted oil. The results are presented in Table 11.

Table 11 - Soxhlet extraction results from HPLC analysis.

Parameter	Yield ($mg_{\beta\text{-carotene}}/g_{Oil}$)	Yield ($\mu g_{\beta\text{-carotene}}/g_{Pumpkin}$)
Value	2,4	32

3.1.2. Oil Extraction by *Bligh and Dyer* Method

Similarly to the Soxhlet extraction method, the Bligh and Dyer (BD) method can be used to determine the quantity of extractable oil, when a polar and a non-polar organic solvent are used. This method was performed in order to compare the results from the $scCO_2$ extraction for the cases when the co-solvent, ethanol (polar solvent) was used. However, in the BD method, three different solvents are used (as mentioned above): water, methanol and chloroform, so, many other compounds are extracted besides β-carotene, like sugars. In order to determine the content of non-polar and polar organic solvent soluble compounds in the extracted oil, hexane, acetone and ethanol were added to the extracted oil mixture. From this, resulted an extraction yield of 35,1 $mg_{Oil}/g_{Pumpkin}$ (Table 12) was achieved.

Table 12 - Experimental parameters for the Bligh and Dyer extraction method.

Parameters	Time (min)	Pumpkin Mass (g)	Oil Extracted (mg)	Extraction Rate (mg_{Oil}/min)	Yield ($mg_{Oil}/g_{Pumpkin}$)
Value	600	2,0041	70,35	0,117	35,1

HPLC analysis was carried out to determine the content of β-carotene in the extracted oil by the BD method, to compare the results with the $scCO_2$ extraction. The results are presented in Table 13 and calibration plot is shown in Annex C.

Table 13 - BD extraction method results from HPLC analysis.

Parameter	Yield ($mg_{β\text{-carotene}}/g_{Oil}$)	Yield ($\mu g_{β\text{-carotene}}/g_{Pumpkin}$)
Value	2,7	94

3.1.3. Oil Extraction with SC-CO_2

The main objective of this work is the study of $scCO_2$ extraction of pumpkin oil, being the β-carotene the key component of interest. So, 7 experiments were done varying certain parameters in order to understand the behavior of the extraction process, regarding this compound. In this set of experiments three parameters were varied:

- Pumpkin Residue – Extractions were made with wet and dry pumpkin residue;
- CO_2 Mass Flow – The carbon dioxide mass flow was change, ranging from 150 $g.m^{-1}$ to 30 $g.m^{-1}$;
- Co-solvent – Ethanol was used as co-solvent.

The oil extraction conditions are shown in Table 14. Temperature and pressure were maintained constant in all experiments, at 323,15K and 260 bar, respectively.

Table 14 - Experimental conditions used in the $scCO_2$ extraction process.

	Experiments						
Conditions	1	2	3	4	5	6	7
Time (min)	180	180	180	180	210	180	240
Pumpkin Mass (g)	24	139,76	24	24	24	24	24
Pumpkin Residue	Dry	Wet	Dry	Dry	Dry	Dry	Dry
CO_2 Flow Rate (g/min)	100	100	150	30	10	30	30
EtOH Flow Rate (g/min)	-	-	-	-	-	3	3

3.1.3.1. Fatty Acid Profile and Glycerides Content

A total of 8 fatty acids were identified with the $scCO_2$ (Table 15), with a higher proportion of unsaturated fats than saturated. In general, the extracted oil is mainly constitute by Palmitic acid (C16:0), oleic acid (C18:1), linoleic acid (C18:2), and linolenic acid (C18:3). The chromatogram obtained is shown in Figure 37.

Table 15 - Fatty acid profile for scCO2 oil extraction.

Fatty Acid	%
Saturated	
C14:0	1,08
C16:0	24,15
C18:0	7,30
C20:0	0,18
Unsaturated	
C16:1	0,23
C18:1	24,24
C18:2	20,42
C18:3	22,40

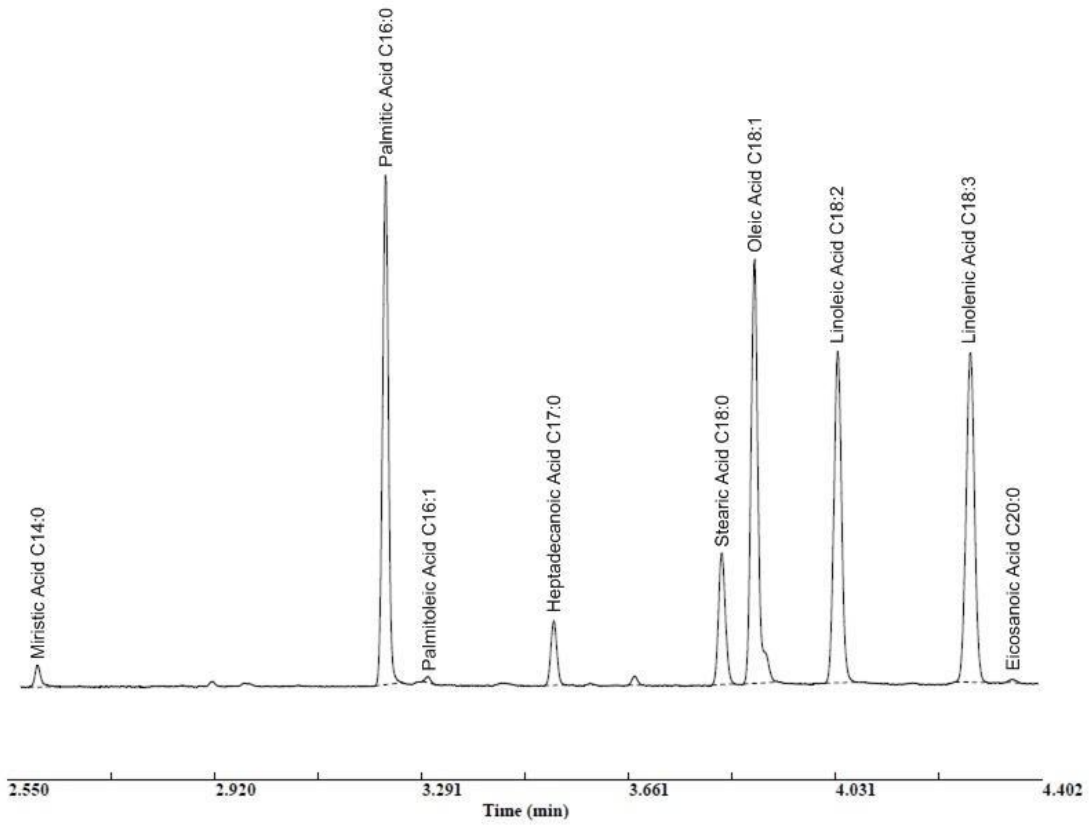

Figure 37 - Chromatogram obtained by GC for fatty acid content in $scCO_2$ pumpkin oil extraction.

The content of glycerides (mono-, di-, and triglycerides) in the extracted oil was determined by Equation 1 (2.4.2 – Gas Chromatography) and the corresponding calibration plots (Annex C). A typical chromatogram is shown in Figure 38.

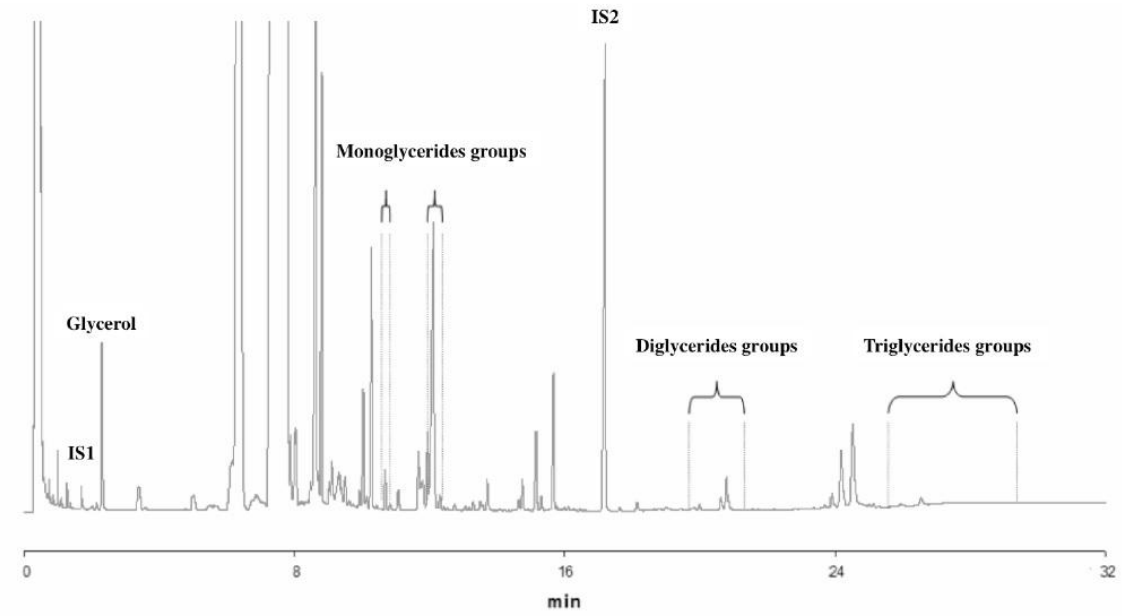

Figure 38 - Typical GC chromatogram obtained for glycerides analysis.

This analysis was performed to three experiments (1, 2, and 7) in order to study the importance of pumpkin humidity and co-solvent presence in the extracted oil composition. Results are shown in Table 16.

Table 16 – Mono-, di-, and triglycerides content in $scCO_2$ extracted oil according to experimental conditions.

	Experiments		
Yield ($mg_{Glycerides}/ml_{Oil}$)	1	2	7
Triglycerides	4,41	1,97	1,42
Diglycerides	0,46	0,12	0,17
Monoglycerides	0,11	0,05	0,01
Total	4,98	2,14	1,60

Glycerides content tends to increase when carbon dioxide is used as a solvent and decrease when a polar co-solvent (ethanol) is added to the process, 4,98 $mg_{Glycerides}/ml_{Oil}$ compared to 1,6 $mg_{Glycerides}/ml_{Oil}$. Water presence also influences glycerides content in the final extracted oil, being this decrease less marked, 2,14 $mg_{Glycerides}/ml_{Oil}$.

3.2. Pumpkin Oil Extraction with SC-CO_2

As mentioned before pumpkin oil residue offers a promising feedstock for β-carotene extraction. Pumpkin has always been integrated in the human diet, not just because of the favorable price/quality ratio, but also due to the awareness of healthy eating.

For the set of experiments, the configuration of the installation used is represented in Figure 35 (2.3 – Experimental Set-Up). The extraction took place in the packed-bed extractor, operating at different conditions of carbon dioxide flow, pumpkin humidity and co-solvent presence (Table 14, see chapter 3.1.3 – Oil Extraction with SC-CO_2). The experimental results are shown in Table 17.

Table 17 - Experimental results for oil extraction, with scCO_2 (325,15K and 260 bar).

	Experiments						
Parameters	1	2	3	4	5	6	7
Accumulated Oil Extracted (mg)	40,5	147,3	44,6	98,7	199,7	1285	1552,1
Extraction Rate (mg_{Oil}/min)	0,23	0,82	0,25	0,55	0,95	7,14	6,47
Accumulated Yield ($mg_{Oil}/g_{Pumpkin}$)	1,02	1,05	1,62	2,59	8,28	54,63	62,23

High performance liquid chromatography analysis was made to determine the β-carotene content in the extracted oil from the above mentioned set of experiments. The obtained results are shown in Table 18.

Table 18 - β-carotene content regarding oil extraction and pumpkin mass.

	Experiments						
Parameters	1	2	3	4	5	6	7
Accumulated Yield ($mg_{β\text{-carotene}}/g_{Oil}$)	45	240	111	131	132	156	135
Accumulated Yield ($\mu g_{β\text{-carotene}}/g_{Pumpkin}$)	2	21	17	38	67	591	533

The yield of extracted oil, in %, can be calculated from the Soxhlet method and BD method values, and the accumulated yield ($g_{Oil}/g_{Pumpkin}$) of extracted oil for each experiment.

$$Yield\ Oil\ Extracted\ (\%) = \frac{Yield_{g_{Oil}/g_{Pumpkin}}}{Yield_{g_{Oil}/g_{Pumpkin}(Soxhlet/BD)}} \times 100$$

Equation 2 - Calculation of yield of oil extracted (%).

Regarding β-carotene, the same parameter can be calculated, following the same line of thought, just by changing the yield ($g_{β\text{-carotene}}/g_{Pumpkin}$). However, and for practical use, the yield of extraction for oil and β-carotene will be shown in $mg_{Oil}/g_{Pumpkin}$ and $\mu g_{β\text{-carotene}}/g_{Pumpkin}$, respectively.

3.2.1. Influence of Pumpkin Humidity in $scCO_2$ Oil and β-carotene Extraction

3.2.1.1. Oil Extraction

Oil extraction from PR, using $scCO_2$ as an extracting agent, was performed when wet and dry PR was used. In Figure 39, is shown the extraction yield obtained for oil extraction from PR, in the aforementioned condition. Temperature, pressure and carbon dioxide flow rate were maintained constant during the extraction processes.

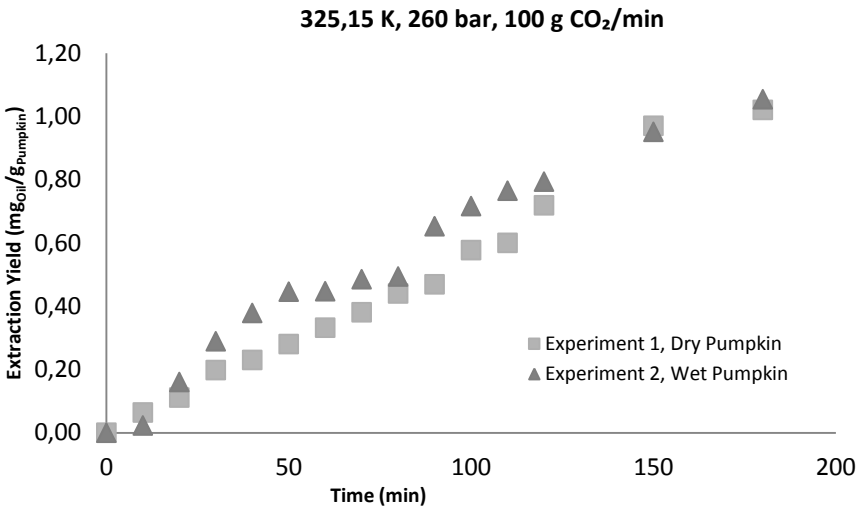

Figure 39 – Yield of extraction ($mg_{Oil}/g_{Pumpkin}$) of oil for dry and wet pumpkin (325,15K and 260 bar).

Both extraction yield values are practically the same, dry pumpkin – 1,02 $mg_{Oil}/g_{Pumpkin}$ and, wet pumpkin – 1,05 $mg_{Oil}/g_{Pumpkin}$ (Figure 39). However, this result correspond to a global yield of the process, since in experiment 2 (wet pumpkin) the total mass used (water + pumpkin) is higher than experiment 1 (dry pumpkin). Considering Table 2 (see chapter 1.1.2 – *Cucurbita moschata* – Growth, Characteristics and Properties) approximately 90% of pumpkin mass is water, which means that of 139,7 g (used in experiment 2) 13,98 g are dry pumpkin, giving an extraction yield of 10,53 $mg_{Oil}/g_{Pumpkin}$. On the other hand, the yield of extraction for experiment 1 (dry pumpkin) is 1,02 $mg_{Oil}/g_{Pumpkin}$. As mentioned before (see chapter 1.2.2.1 – Supercritical Fluid Extraction) high moisture content can hindered mass transfer because water acts as a barrier for non-polar solutes [65], but water can also act as a entrainer, in some cases, facilitating solute diffusion between the solid particle and the $scCO_2$.

3.2.1.2. β-carotene Extraction

In Figure 40 is demonstrated the yield of extraction of β-carotene, when wet pumpkin is used, 21 $\mu g_{\beta\text{-carotene}}/g_{Pumpkin}$. This value is much higher than the value when dry pumpkin is used, 2,3 $\mu g_{\beta\text{-carotene}}/g_{Pumpkin}$. Once again, regarding the wet pumpkin case if we considered the same dry mass (13,98 g), β-carotene yield of extraction is much higher than the case of the dry

pumpkin, 210 $\mu g_{\beta\text{-carotene}}/g_{Pumpkin}$ comparing to 2,3 $\mu g_{\beta\text{-carotene}}/g_{Pumpkin}$, respectively. As mentioned above, water may have a benign effect when extracting β-carotene from PR.

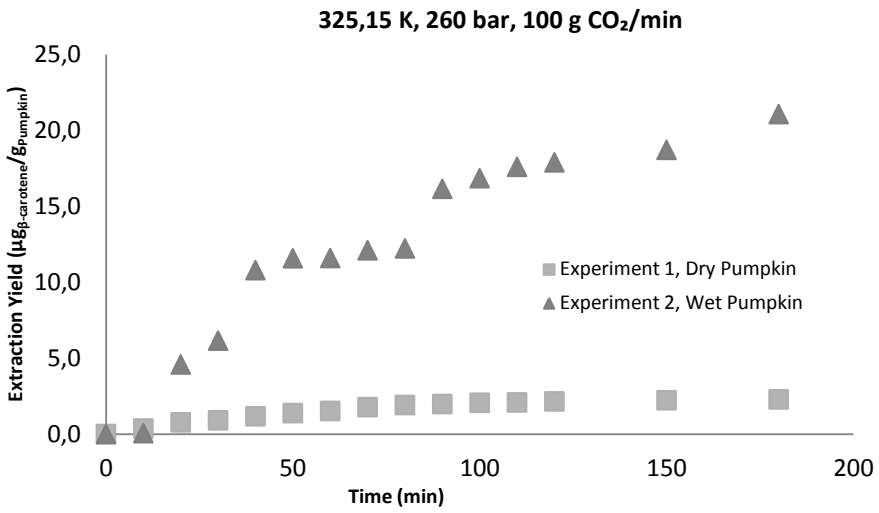

Figure 40 - SC-CO_2 extraction yield ($\mu g_{\beta\text{-carotene}}/g_{Pumpkin}$) for β-carotene with wet and dry PR (325,15K and 260 bar).

3.2.2. SC-CO_2 Flow Rate Influence in Pumpkin Oil and β-carotene Extraction

3.2.2.1. Oil Extraction

Carbon dioxide flow rate was also studied. To maximize the extraction of oil from PR, the solvent flow rate must be in a region where the solute's diffusion and solubility in the solvent are optimal. In Figure 41 it is represented an extraction curve, for a constant operating temperature and pressure, changing the carbon dioxide flow rate – 10, 30, 100, and 150 g_{CO2}/min. It is possible to observe that for higher flows, the extraction yield decreases. Although at 150 g_{CO2}/min, the yield of extraction is higher than 100 g_{CO2}/min. For lower flow rates (10 and 30 g_{CO2}/min), the extraction yield improves greatly, since the solvent residence time is higher, resulting in an oil loading substantially greater, and so, a higher slope.

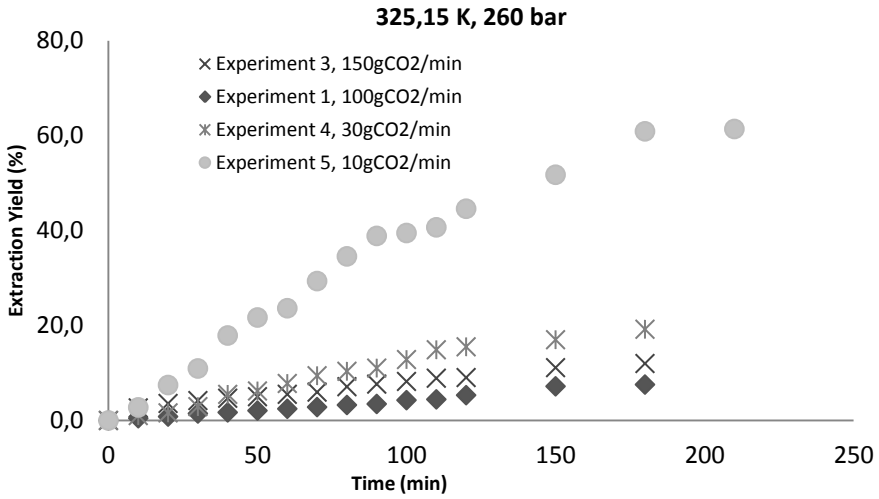

Figure 41 - Extraction yield (%) at different CO2 flow rates for oil extraction (325,15K and 260 bar).

According to Table 19 and Figure 42, the amount of CO_2 needed for each experiment can be studied. Table 19 gives the oil extraction 180 min (180') – and corresponding S/F ($g_{solvent,CO2}/g_{Pumpkin}$) value parameter. When operating at the lowest solvent flow rate, 10 g_{CO2}/min, it was possible to extract up to 200 mg of oil comparing to 98,7 mg, when a higher flow rate was used (30 g_{CO2}/min). Although it must noted that the extraction time was longer when 10 g_{CO2}/min were used. So, looking at Table 19 it is possible to understand that even if experiment 5 (10 g_{CO2}/min) was to be performed until 180', the amount of extracted oil would be higher than experiment 4 (30 g_{CO2}/min). Moreover, the amount of solvent used is higher too.

According to experiment 1, 4 and, 5, in experiment 3 an experimental error must have occurred, since the values of the yield of extraction tend to increase with increasing of solvent flow rate. Looking at the solid particle level, the resistance to external mass transfer decreases when the solvent flow rate decreases (see chapter 3.2.4 – Understanding Experimental Data with a Mathematical Model), so, for an elevated solvent flow rates the yield of extraction should decrease, as it does for experiment 4 and 5 (30 and 10 g_{CO2}/min, respectively).

Table 19 - Influence of solvent flow rate on oil extraction from PR according to S/F (325,15K and 260 bar).

Q (g_{CO2}/min)	Oil Extracted$_{mg}$ (180')	S/F (180')
150	44,6	1125
100	40,5	750
30	98,7	225
10	198,1	75

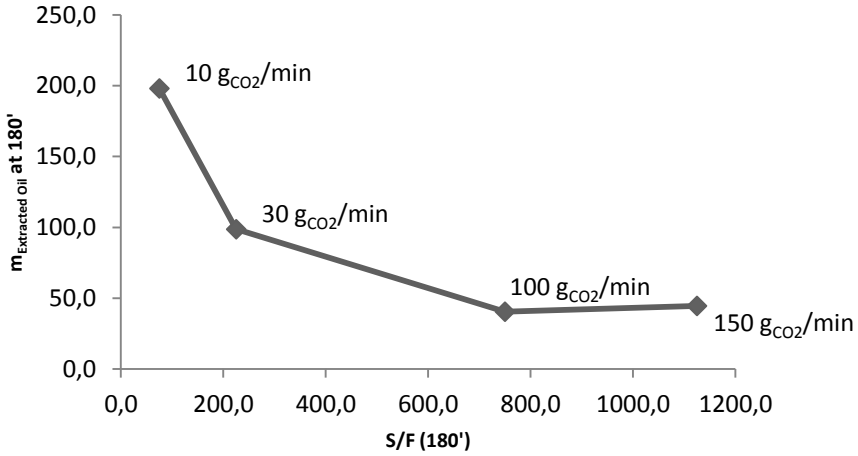

Figure 42 - Amount of extracted oil, at 180 minutes, according to the S/F parameter.

The energy demand for the extraction process must be taken into account, and as shown in Table 19, for a lower extraction yield of oil at 150 g_{CO2}/min, a higher amount of solvent is used. Among the obtained results, 10 g_{CO2}/min is the best option, considering yield of oil extracted, and solvent consumption (lower S/F), for the same operating time. Another way to look at this situation is by observing Figure 43. This extraction curve shows that with less solvent consumption (2 kg_{CO2}), a much higher extraction yield is achieved (8,28 $mg_{Oil}/g_{Pumpkin}$), and can be compared to maximum extractable oil when performing the Soxhlet extraction method of 13,5 $mg_{Oil}/g_{Pumpkin}$.

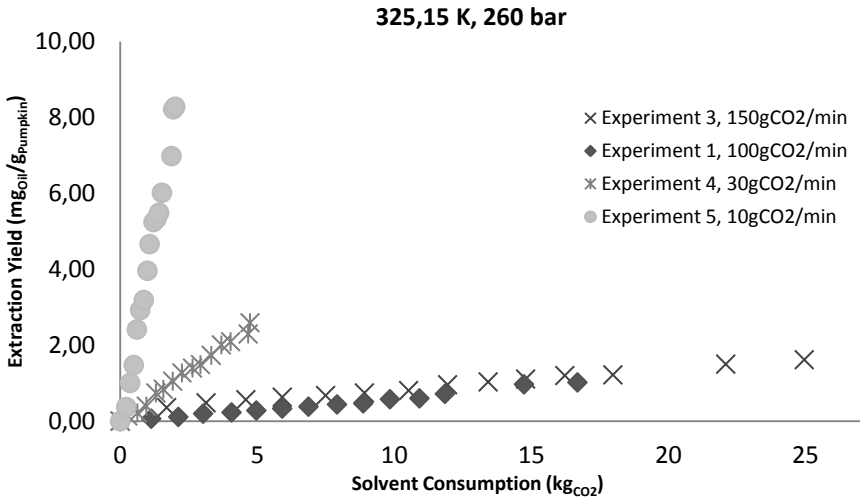

Figure 43 - Extraction yield ($mg_{Oil}/g_{Pumpkin}$) vs. solvent consumption (kg_{CO2}), for oil extraction (325,15K and 260 bar).

3.2.2.2. β-carotene Extraction

The CO_2 flow rate was also studied for β-carotene extraction at different solvent flow rates. Figure 44 shows the extraction yield ($\mu g_{\beta\text{-carotene}}/g_{Pumpkin}$) for β-carotene. Higher yield of extraction is achieved for the lowest flow rate of 10 g_{CO2}/min, while the lowest yield of extraction is registered at 100 g_{CO2}/min, and as explained before, this result is considered to be an experimental error. Solvent flow rate of 10 and 30 g_{CO2}/min achieved the highest extraction yields with 38 and 67 $\mu g_{\beta\text{-carotene}}/g_{Pumpkin}$, respectively (Table 18).

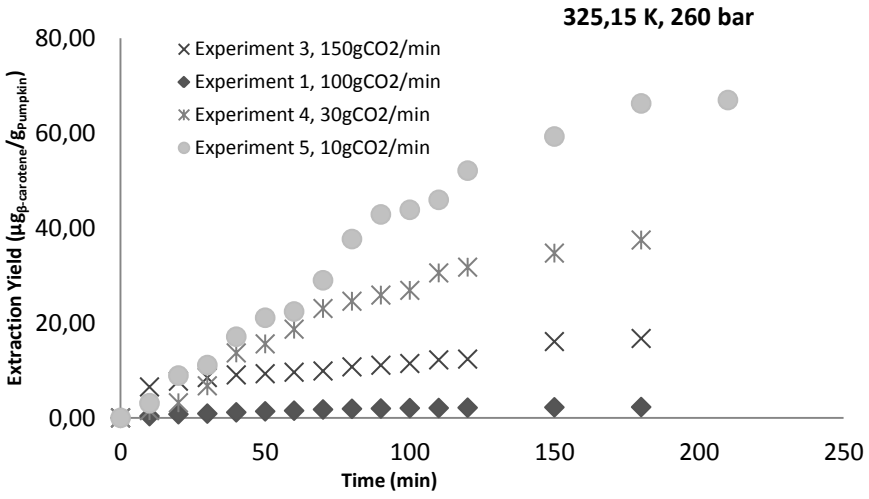

Figure 44 – Extraction yield ($\mu g_{\beta\text{-carotene}}/g_{Pumpkin}$) at different CO_2 flow rates for β-carotene extraction (325,15K and 260 bar).

The $scCO_2$ at the aforementioned pressure and temperature conditions (325,15K and 260 bar) may be more suitable for β-carotene extraction, when 10 g_{CO2}/min are used. According to Table 20 it is possible to see that, at 10 g_{CO2}/min, the extraction yield for β-carotene is 2 times higher than the value obtained for the Soxhlet method. In this work, it was assumed that the maximum extractable oil that could be obtained in a $scCO_2$ oil extraction of PR, was the Soxhlet method, but for the β-carotene extraction this value was surpassed.

Table 20 - Extraction yield of β-carotene ($\mu g_{\beta\text{-carotene}}/g_{Pumpkin}$), for different solvent flow rates at extraction time = 180 min (325,15K and 260 bar).

	Experiments			
Parameters	1	3	4	5
Q (g_{CO2}/min)	100	150	30	10
Yield ($\mu g_{\beta\text{-carotene}}/g_{Pumpkin}$)	2	17	38	66
	Soxhlet Method			
Yield ($\mu g_{\beta\text{-carotene}}/g_{Pumpkin}$)	32,4			

As mentioned above (see chapter 1.2.2 – Supercritical Fluids), when CO_2 enters the supercritical region, it possesses properties of both gas and liquid, thus increasing solvation power, due to high, liquid-like, density, and the mass transfer rates also increase because of a high, gas-like diffusion coefficients and low viscosity values. These factors contribute for an effective extraction process of non-polar compounds, when compared to the operating conditions of the Soxhlet method, which relays on the organic solvent and solute properties of diffusion to enhance the yield of extraction.

3.2.3. Influence of Co-solvent Presence in $scCO_2$ Oil and β-carotene Extraction

3.2.3.1. Oil Extraction

The influence of a co-solvent (ethanol) in the extraction of oil from PR was studied. Through the addition of a co-solvent, polar compounds or less non-polar compounds can be more easily extracted. To compare the behavior of the extraction process between these two different situations – non-polar solvent vs. non-polar solvent + polar co-solvent – at the same solvent flow rate (30 g_{CO2}/min), the yield of extraction was plotted against time (Figure 45).

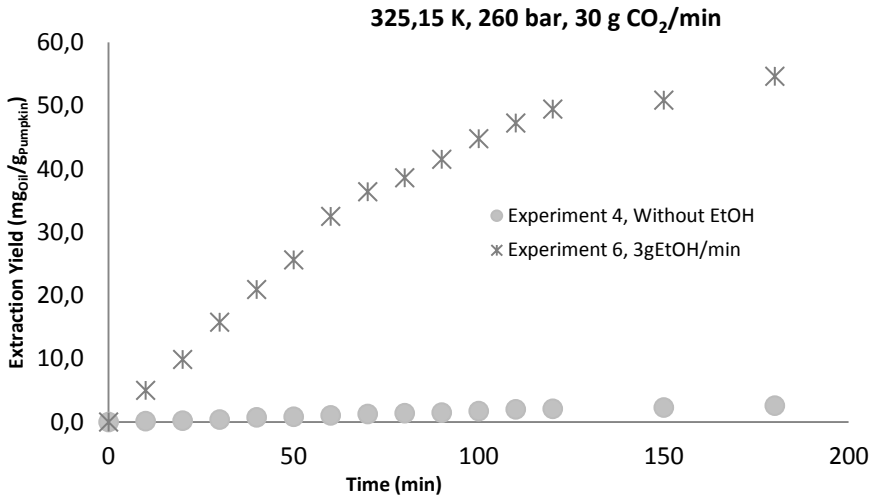

Figure 45 - Oil extraction ($mg_{Oil}/g_{Pumpkin}$) with and without co-solvent presence.

Ethanol presence influences greatly the oil extraction process, since not only non-polar lipids are extracted but also polar lipids (see chapter 1.2.1 – Mechanical, Organic Solvent, and Other Extraction Processes). The extraction yield ($mg_{Oil}/g_{Pumpkin}$) for the free co-solvent experiment was 8,28 $mg_{Oil}/g_{Pumpkin}$, while adding ethanol increased almost 7 times the yield of extraction, up to 54,6 $mg_{Oil}/g_{Pumpkin}$ (experiment 6).

Experiment 7 was carried out in the same conditions as experiment 6, but with a longer extraction time. This increase in the time of extraction was to try to understand if a baseline in the extraction curve would be achieved; however, as shown in Figure 46 it was not possible. The yield of extraction in experiment 7 is higher than experiment 6, 62,23 $mg_{Oil}/g_{Pumpkin}$ comparing to 54,63 $mg_{Oil}/g_{Pumpkin}$, respectively. Either value surpassed the yield of extraction of the BD method, 35,1 $mg_{Oil}/g_{Pumpkin}$.

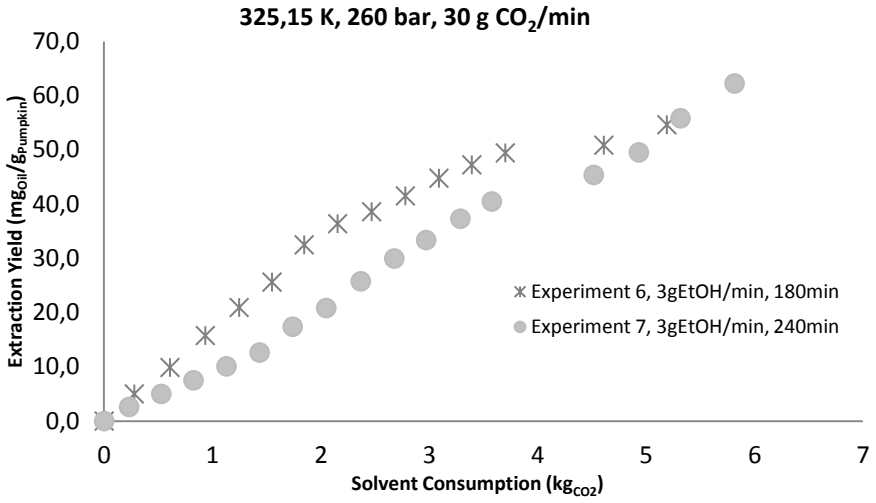

Figure 46 - Extraction yield ($mg_{Oil}/g_{Pumpkin}$) for experiment 6 and 7 (325,15K and 260 bar).

3.2.3.2. *β-carotene Extraction*

The extraction of β-carotene was analyzed when ethanol was used as a co-solvent. β-carotene content was higher for experiment 6, with 591 $\mu g_{\beta\text{-carotene}}/g_{Pumpkin}$ comparing to 38 $\mu g_{\beta\text{-carotene}}/g_{Pumpkin}$ in experiment 4 (Figure 47).

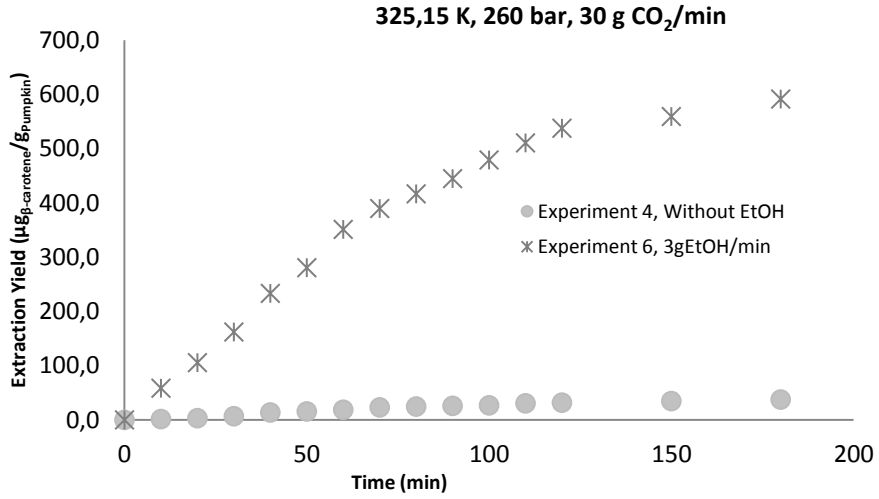

Figure 47 - Extraction yield ($\mu g_{\beta\text{-carotene}}/g_{Pumpkin}$) with and without co-solvent (325,15K and 260 bar).

The extraction of polar and less non-polar compounds may have increased β-carotene extraction yield, aiding carry it through the solid particle to the bulk solvent-co-solvent phase.

The yield of extraction in experiment 6 is higher than experiment 7, 591 $\mu g_{\beta\text{-carotene}}/g_{Pumpkin}$ comparing to 533 $\mu g_{\beta\text{-carotene}}/g_{Pumpkin}$, respectively. Either value surpassed the yield of extraction of the BD method, 94 $\mu g_{\beta\text{-carotene}}/g_{Pumpkin}$.

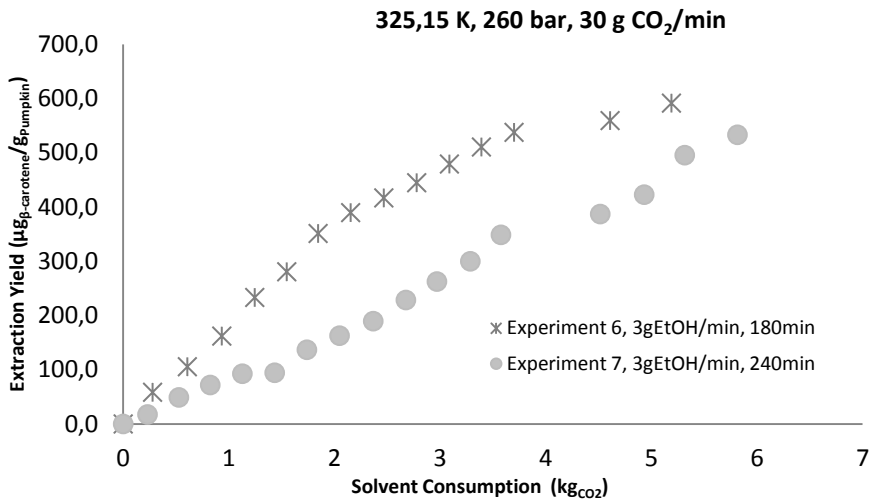

Figure 48 - Extraction yield ($\mu g_{\beta\text{-carotene}}/g_{Pumpkin}$) for experiment 6 and 7 (325,15K and 260 bar).

3.2.4. Understanding Experimental Data with a Mathematical Model

3.2.4.1. Mathematical Model Description

In this work, the behavior of oil extraction, from PR, was studied using a general mathematical model for the mass balance in a fixed-bed extractor. In order to do so, some assumptions were taken into account:

- The extract is a single component, a pseudo-solute (triolein, MW = 885,47 mol.g^{-1});
- The addition of a co-solvent was not took into account, considering always the CO_2 as solvent/co-solvent;
- Constant solute concentrations in the solid matrix (initial solute content, C_{s0}) and the SCF phase (saturation concentration or operational solubility, C_{f0}) all along the bed initially;
- Continuity in the solute flux leaving the solid particle and entering the SCF film surrounding it;
- A linear solute partition relationship for the solute between the two phases.

The general mass balance to the fluid phase of a SFE column is given by:

$$\frac{dC_f}{dt} = D_{ax}\frac{d^2C_f}{dz^2} - u_G\frac{dC_f}{dz} + a_p\left(\frac{1-\varepsilon_{bed}}{\varepsilon_{bed}}\right)j_f$$

Equation 3 - General mass balance to the fluid phase.

Where:

- C_f – Concentration of the solute in the supercritical fluid phase (g.g^{-1});
- D_{ax} – Axial dispersion coefficient of the solute (m^2.s^{-1});
- u_G – Interstitial fluid velocity (m.s^{-1});
- a_p – Particle surface area (m^2);
- ε_{bed} – Bed porosity;
- j_f – Solute mass flux from the solid to the fluid phase (g.g^{-1}.s^{-1}).

The axial dispersion coefficient (D_{ax}) was calculated through the binary diffusion coefficient (D_{12}) and it describes the solute dispersion along the extractor. On the other hand, the binary diffusion coefficient can be defined as the transfer or movement of molecules (solute) through a fluid (scCO_2) by means of random movements of the molecules. D_{ax} can be estimated according to the following correlation [66]:

$$D_{ax} = D_{12}\left(\frac{157.7Re^2 + 0.284Re + 0.199}{Re + 0.7}\right)$$

Equation 4 - Axial dispersion coefficient.

Where:

- D_{12} – Binary diffusion coefficient (m^2.s^{-1});
- Re – Reynolds number.

The Reynolds number can be defined as the ratio of inertial forces to viscous forces and consequently quantifies the relative importance of these two types of forces for given flow conditions. This number is also used to characterize different flow regimes within a similar fluid, such as laminar or turbulent flow, which occurs at low Reynolds numbers, where viscous forces are dominant, and is characterized by smooth, constant flow motion, or turbulent flows, which occur at high Reynolds number and is dominated by the inertial forces, which tend to produce vortices and other flow instabilities. [67] The Reynolds number was estimated through the next equation:

$$Re = \frac{2R_p u_G \rho_{sc}}{\mu}$$

Where:

- R_p – Particle radius (m);
- u_G – Interstitial fluid velocity (m.s^{-1});
- ρ_{sc} – Supercritical carbon dioxide density (kg.m^{-3});
- μ – Supercritical carbon dioxide dynamic viscosity (Pa.s^{-1} or kg.m^{-1}.s^{-1}).

The binary diffusion coefficient was estimated according to the *Catchpole and King* correlations [61]:

$$D_{12} = 5.152 D_c \frac{T}{T_{c,sc}} \left[\left(\frac{\rho_{sc}}{\rho_{c,sc}} \right)^{-2/3} - 0.4510 \right] \frac{S}{X}$$

Equation 5 - Binary diffusion coefficient calculation.

Where:

- D_c – Critical carbon dioxide diffusion coefficient (m^2.s^{-1});
- T – Extraction operating temperature (K°);
- $T_{c,sc}$ – Carbon dioxide temperature at critical point (K°);
- $\rho_{c,sc}$ – Carbon dioxide density at critical point (kg.m^{-3});

The S and X are correlation parameters[68], and are given by the following equations:

$$X = \left[1 + \left(\frac{V_{c,solute}}{V_{c,sc}} \right)^{1/3} \right]^2 \Bigg/ \left(1 + \frac{M_{w,sc}}{M_{w,solute}} \right)^{1/2}$$

$$S = \begin{cases} 1.0 \pm 0.1, & X < 2 \\ 0.664 X^{0.17} \pm 0.1, & 2 < X < 10 \end{cases}$$

Equation 6 - Determination of correlation values.

Where:

- $V_{c,solute}$ – Critical molar volume of the solute ($cm^3.mol^{-1}$);
- $V_{c,sc}$ – Critical molar volume of the fluid ($cm^3.mol^{-1}$);
- $M_{w,sc}$ – Molar weight of carbon dioxide ($mol.g^{-1}$);
- $M_{w,solute}$ – Molar weight of solute ($mol.g^{-1}$);

The interstitial velocity (u_G) it's the fluid (CO_2) velocity between solid particles and the solute mass flux (j_f) is the driving force. These two parameters are given by:

$$u_G = \frac{Q_m}{\rho_{sc} A \varepsilon_{bed}}$$

Equation 7 - Interstitial fluid velocity.

$$j_f = k_f \left(\frac{C_s}{k} - C_f \right)$$

Equation 8 - Solute mass flux from solid to fluid phase.

Where:

- Q_m – Fluid flow rate ($kg.s^{-1}$);
- ρ_{sc} – Supercritical carbon dioxide density ($kg.m^{-3}$);
- A – Extractor column base area (m^2);
- k_f – External mass transfer coefficient ($m^2.s^{-1}$);
- C_s – Solid phase concentration (particle phase) ($g.g^{-1}$);
- k – Partition coefficient.

The external mass transfer coefficient (k_f) gives the resistance to external mass transfer, varying with the solvent flow rate. This parameter was estimated through the *Wakao and Funazkri* correlations [61]:

$$k_f = \frac{D_{12} \left(2.0 + 1.1 Re^{0.6} Sc^{1/3} \right)}{2R_p}$$

Equation 9 - Mass transfer coefficient.

Where:

- Sc – Schmidt number.

The Schmidt number represents the ratio of the rates of diffusion of momentum and mass in the fluid, and it can be calculated by the following equation:

$$Sc = \frac{\mu / \rho_{sc}}{D_{12}}$$

Equation 10 - Schmidt number.

The solute partition coefficient (k) gives the ratio of the solute content in the solid matrix (Cs_0), and the operational solubility (Cf_0), by the following equation:

$$k = \frac{C_{s0}}{C_{f0}}$$

Equation 11 - Solute partition coefficient.

The values of Cs_0 and Cf_0 were estimated from the horizontal asymptote and initial slope, respectively, of cumulative extraction plots of oil yield (g solute/g raw material) versus solvent mass (g CO_2/g raw material). [69].

The particle area is given by:

$$a_p = \frac{6}{2R_p}$$

Equation 12 - Particle specific surface area.

To solve Equation 3, boundary conditions were applied. The boundary conditions are:

$$D_{ax}\frac{dC_f}{dz} - u_G C_f = 0, \qquad at\ z = 0, for\ all\ t$$

Equation 13 - Boundary condition for the fluid phase at z=0.

$$\frac{dC_f}{dz} = 0, \qquad at\ z = L, for\ all\ t$$

Equation 14 - Boundary condition for the fluid phase at z=L.

$$C_f = 0, \qquad at\ t = 0, for\ all\ z$$

Equation 15 - Initial condition for mass balance to the fluid phase.

Fluid transport of the solute within or out of the particle is assumed to take place by diffusion [55], and so, the particle mass balance is given by the next equation:

$$\frac{dC_s}{dt} = \frac{D_e}{r^2}\frac{d}{dr}\left(r^2\frac{dC_s}{dr}\right)$$

Equation 16 - General particle mass balance.

Where:

- C_s – Solute concentration in solid phase ($g.kg^{-1}$);
- D_e – Effective diffusion dispersion coefficient of the solid phase ($m^2.s^{-1}$).

The effective diffusion or internal mass transfer coefficient describes the solute diffusion through the solid matrix.

In order to solve equation 16, boundary and initial conditions were given:

$$\frac{dC_s}{dr} = 0, \qquad at\ r = 0, for\ all\ z\ and\ t$$

Equation 17 - Boundary condition for the particle phase at r=0.

$$k_f\left(\frac{C_s}{k} - C_f\right) = -D_e\frac{dC_s}{dr}, \qquad at\ r = R, for\ all\ z\ and\ t$$

Equation 18 - Boundary condition for particle phase at r=R.

$$C_s = C_{s0}, \qquad at\ t = 0, for\ all\ z\ and\ t$$

Equation 19 - Initial condition for particle phase.

3.2.4.2. Parameter Estimation with Experimental Data

In Figure 49, a typical extraction curve ($g_{Oil}/g_{Pumpkin}$ vs. $g_{CO2}/g_{Dry\ Residue}$) for vegetables (pulp or seeds) is shown. It is noticeable that after some time, an extraction baseline is achieved. However, in the extraction curves seen so far (Figures 39, 40, and 43 – 48) this behavior is not noticeable. The baseline indicates the point where no further extraction will occur due to the limitation of solute in the solid particle.

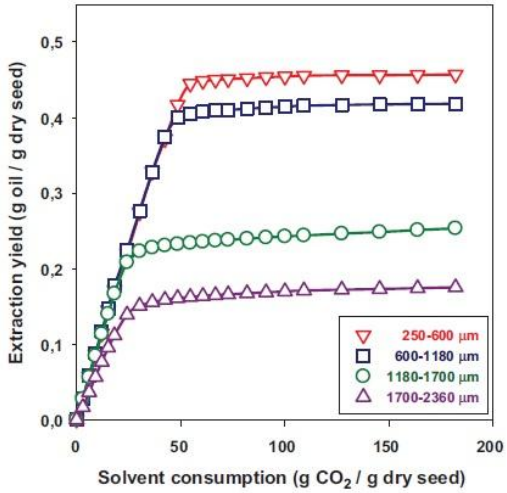

Figure 49 - Typical extraction curve for pumpkin oil extraction. [13]

From the slop of the extraction curve, the operating solubility (C_{f0} – see Equation 11) parameter can be calculated. This parameter indicates the maximum possible load of solute in the solvent, for certain extraction conditions, and it only varies when temperature, pressure or co-solvent concentration change. C_{f0} can be compared to the maximum extractable oil (C_{s0} – Equation 11) in the PR, by the partition coefficient (k – see Equation 11). In Table 21 the C_{f0} values are shown.

Table 21 - Operating solubility for different solvent flow rates (325,15K and 260 bar). (Max. EO = Maximum Extractable Oil)

	Experiments						
Parameter	1	2	3	4	5	6	7
C_{f0} ($\mu g_{Oil}/g_{CO2}$)	1,49	8,74	1,6	20,2	102	257	266
Method	Soxhlet Method			Bligh and Dyer method			
Max. EO ($mg_{Oil}/g_{Pumpkin}$)	13,5			35,1			

As demonstrated in Table 21, the C_{f0} values for each experiment are considerable low comparing to the C_{s0} values, confirming the baseline absence in the extraction curves seen so far. Only by changing the operating parameters, such pressure, temperature or co-solvent concentration, would the extraction curve eventually reach a baseline. [69,65,70,71]

Through the partition coefficient value the extraction yield behavior can be predict. The increase or decrease of the yield of extraction will occur, accordingly to the decreasing or increasing of the partition coefficient, respectively. This change occurs due to the increasing or decreasing of the driving force (j_f – see Equation 8), since the external mass transfer (k_f – see Equation 8) is achieved by solute diffusion through a thin film, from the more concentrated (solid particle) to the less concentrated phase (solvent). The solvent flow rate has an important role in this step, because as the solvent flow rate increases, external mass transfer resistance increases too, due to the formation of a thin film. On the other hand, diffusion inside the particle must also occur, so that the solute reaches the solid particle surface, and once more, passes through the thin film into the bulk solvent. This intraparticle solute diffusion can be described by the effective diffusion (D_e – see Equation 16). This parameter depends mostly on the operating pressure and temperature, particle size, and co-solvent presence and concentration. Particle radius was determined using molecular sieves for an average value ($R_p = \frac{D_p}{2} = 3{,}5E^{-4}\ m$).

The main purpose of modeling the extraction process was to predict the effective diffusion coefficient value, and to understand how the solute concentration behaves in the particle and in the fluid phase during the extraction. The operating conditions used in the mathematical model are from experiments 2, 5 and 7, so that water and co-solvent presence influence could be studied, and, since these were the best results.

The rate of scCO$_2$ extraction strongly depends on mass transfer factors, which are characterized by the effective diffusion coefficient, solute axial dispersion (D_{ax} – see Equation 3), and external mass transfer coefficient in terms of two dimensionless numbers. One is the Biot number (B_i) which characterizes the relative importance of effective intraparticle diffusion as compared to convective solid-to-scCO$_2$ film mass transfer on the particle surface, by the following equation [65]:

$$B_i = \frac{2k_f R_p}{D_e k}$$

Equation 20 - Biot number calculation.

The other one is the Peclet number[65] (P_e) that relates the relative importance of solute axial dispersion and convective flow in the displacement of dissolved solute in the $scCO_2$ along the extractor bed.

$$P_e = \frac{Hu_G}{D_{ax}}$$

Equation 21 - Peclet number calculation.

Where:

- H – Extractor bed height (m).

In Table 22 are shown all the key parameters to understand and study the extraction process, determined through the *Gproms*® Software.

Table 22 - *Gproms*® software key estimated parameters.

	Experiments		
Parameters	2	5	7
Effective Diffusion Coefficient, D_e ($m^2.s^{-1}$)	1,11E-16	1,87E-16	3,73E-16
Axial Dispersion Coefficient, D_{ax} ($m^2.s^{-1}$)	2,79E-5	2,32E-6	8,75E-6
Binary Diffusion Coefficient, D_{12} ($m^2.s^{-1}$)	4,01E-9	4,01E-9	4,01E-9
External Mass Transfer Resistance Coefficient, k_f ($m^2.s^{-1}$)	1,52E-4	4,78E-5	8,44E-5
Partition Coefficient, K	1545,33	132,35	131,95
Peclet Number, Pe	127,58	153,35	133,43
Biot Number, Bi	6,2E5	1,35E6	2,13E6
Reynolds Number, Re	30	3	9

Analyzing Table 22 it is possible to understand that for all experiments the Biot number is very high, because of the very low value for the D_e parameter – in the order of 10E-16 – and, also because external mass transfer resistance is high, between 10E-4 and 10E-5. Thus, it is not possible to get the $scCO_2$ at the extractor outlet saturated with oil, since intraparticle diffusion is very slow and hindered, making the extraction process limited to the internal solute diffusion.

Solute dispersion along the extractor can be disregarded when values of P_e are large ($P_e \geq 100$), which is the case for all experiments, however, this is an important parameter that should be taken into account, and can be avoid by some methods: (*i*) increasing the interstitial fluid velocity, (*ii*) using extraction vessels of small diameter and large length-to-diameter ratio to diminish radial variations along the bed, among others. [65] The interstitial fluid velocity is low for experiment 5 and 7, and higher for experiment 2, which do not affect the Peclet number, keeping it above 100. The binary diffusion coefficient is maintained for the three experiments, since solute diffusion in the supercritical solvent does not change. This parameter is greatly affected by changes in the operating temperature and pressure, which are kept the same for all experiments (325,15K and 260 bar).

The effective diffusion coefficient was estimated (Table 22) by *Gproms*® Software. To do so, experimental data – extraction time and yield of extraction – where inserted in the program. In Table 23 is demonstrated the final value for the extraction yield compared to the actual data from the performed experiments.

Table 23 - Measured values vs. predicted values.

Experiments	Parameters	
	Measured Value ($mg_{Oil}/g_{Pumpkin}$)	Predicted Value ($mg_{Oil}/g_{Pumpkin}$)
2	1,1	1,1
5	8,3	11,6
7	62,2	69,7

In experiment 2, the experimental and predicted values are equal, 1,1 $mg_{Oil}/g_{Pumpkin}$. However, for experiment 5 and 7, the experimental and predicted values differ, 8,3 $mg_{Oil}/g_{Pumpkin}$ compared to 11,6 $mg_{Oil}/g_{Pumpkin}$, and 62,2 $mg_{Oil}/g_{Pumpkin}$ compared to 69,7 $mg_{Oil}/g_{Pumpkin}$, respectively.

Experimental and predicted data (*Gproms*® Software) are plotted in Figure 49 to Figure 51. (Blue squares – experimental data, red squares – predicted data; x axis – extraction time, y axis – extraction yield).

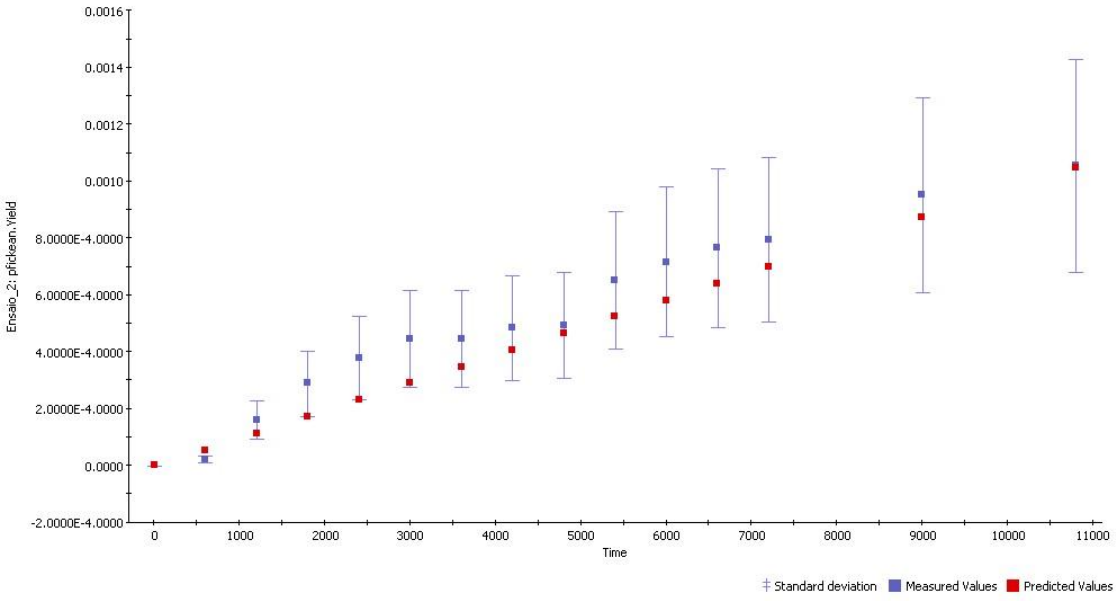

Figure 50 - Experimental vs. predicted data plot for experiment 2.

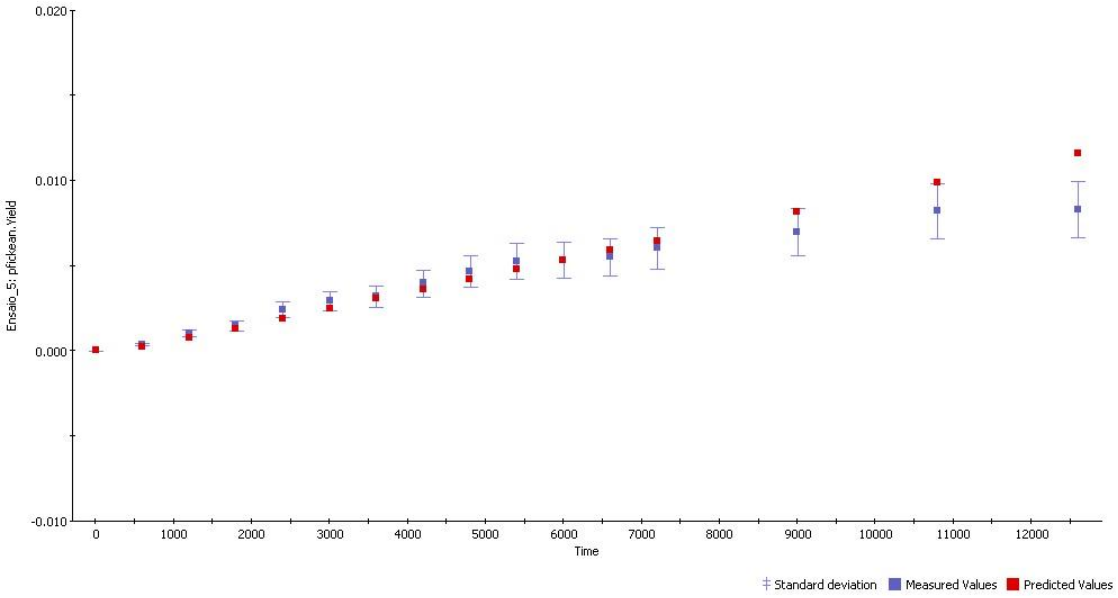

Figure 51 - Experimental vs. predicted data plot for experiment 5.

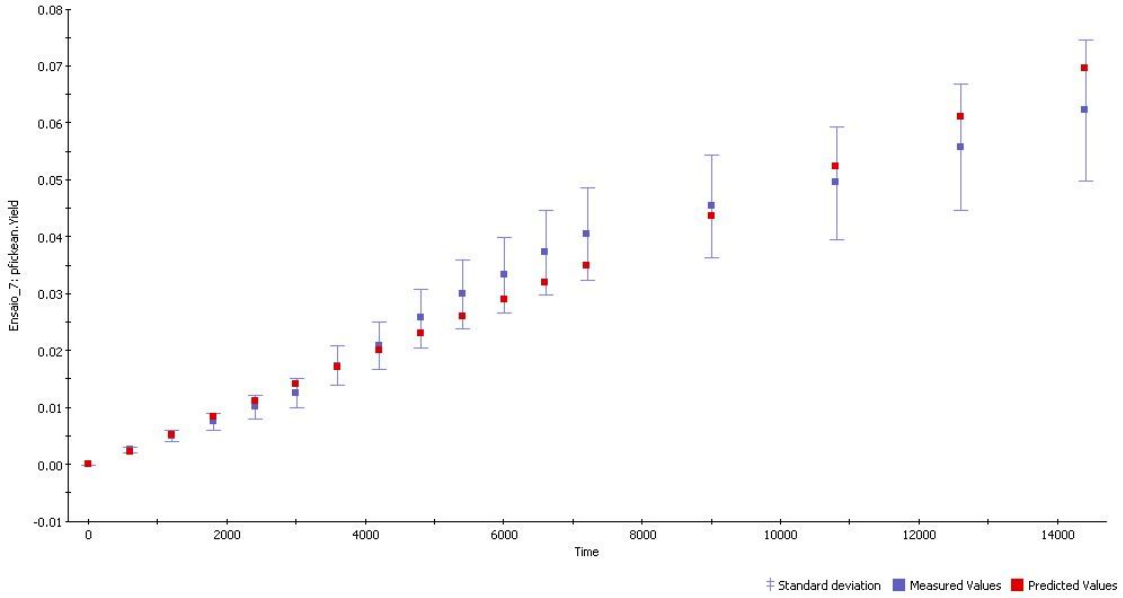

Figure 52 - Experimental vs. predicted data plot for experiment 7.

An ease way compare a theoretical value with an actually-measured value is with a parity plot. In a parity plot the experimental data is plotted against the predicted data, from the mathematical model. A y=x line is also plotted as a reference, and if the theoretical and experimental values agree, they should lie close to the y=x line and be randomly scattered around it. However, if they do not agree, then the data will be skewed away from the y=x. [28] The parity plots for each experiment are shown in Figures 52 – 54 (x axis – experimental data, y axis – predicted data).

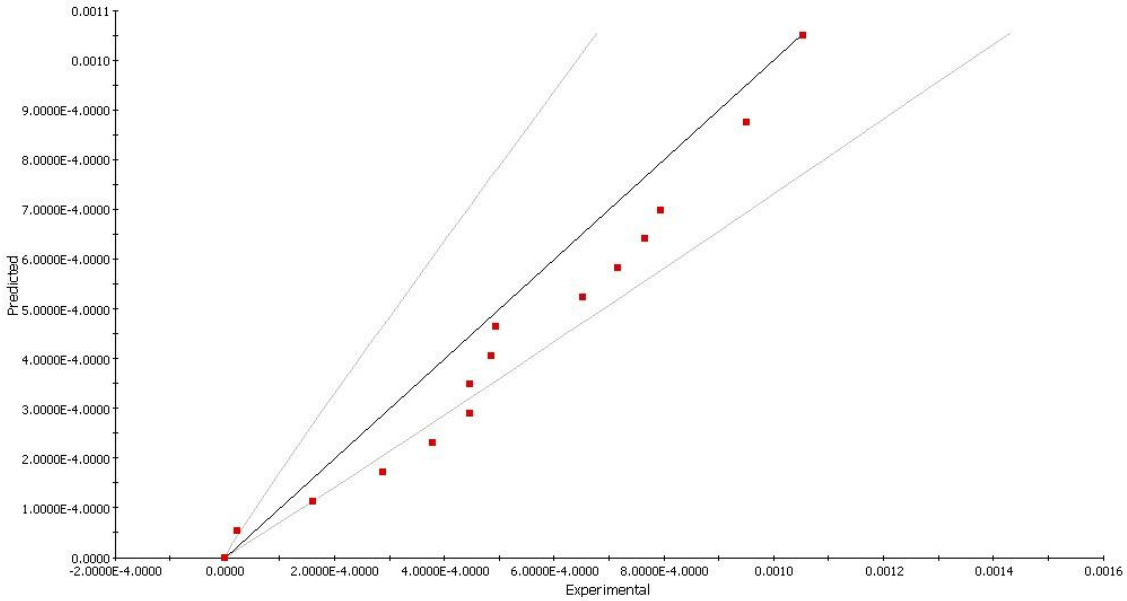

Figure 53 - Parity plot for experiment 2.

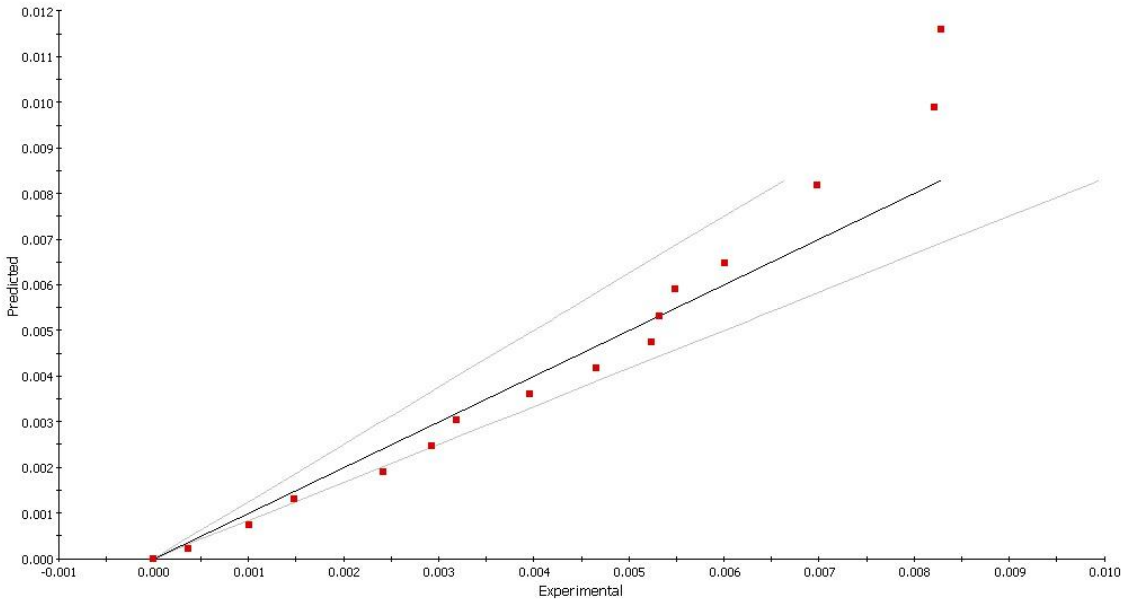

Figure 54 - Parity plot for experiment 5.

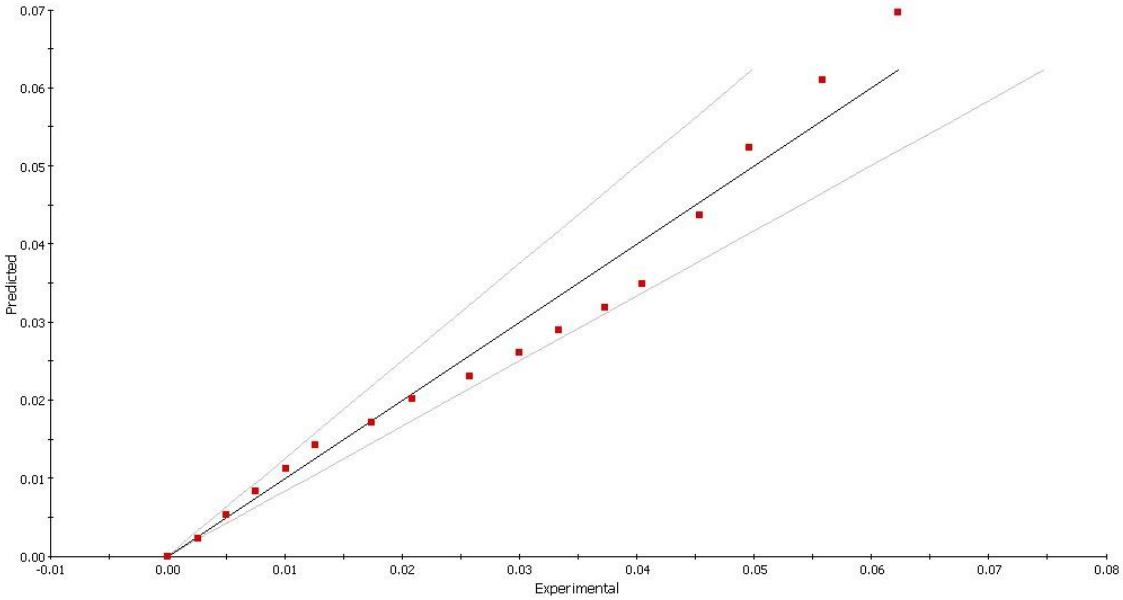

Figure 55 - Parity plot for experiment 7.

It is possible to see that in Figure 52 and 53 some points are skewed away from the y=x line, which means that measurement errors may have occur during the extraction process, at those acquiring sample times. However, it is possible to assert that the mathematical model describes better experiment 7, than 5 and 2, but once again, experimental errors may have occur during sample acquisition.

The behavior of solute concentration ($g_{Oil}/g_{Pumpkin}$) in the fluid phase, along the extractor bed, was also studied with *Gproms*® Software, and the results are shown in Figure 55 to Figure 57 (x axis – extraction time, y axis – solute concentration variation).

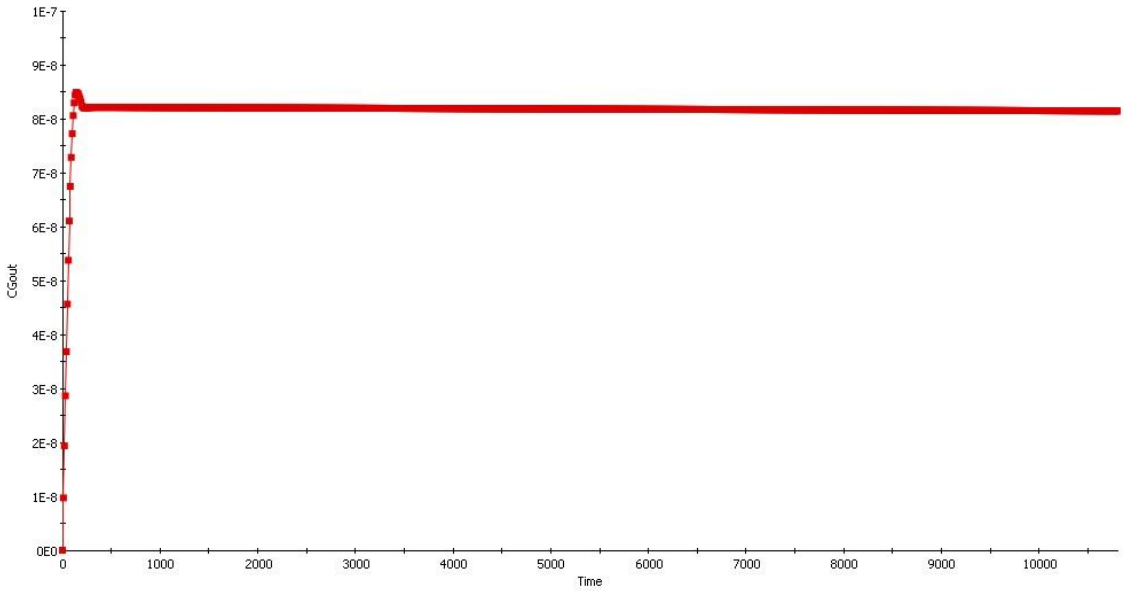

Figure 56 - Solute concentration variation, along the extractor bed, for experiment 2.

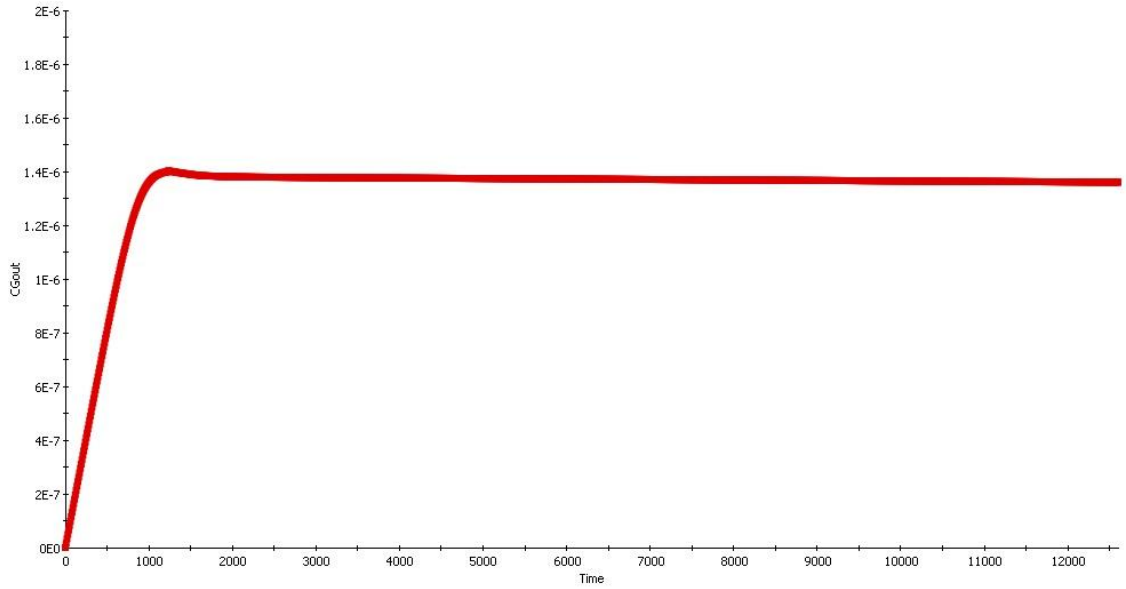

Figure 57 - Solute concentration variation, along the extractor bed, for experiment 5.

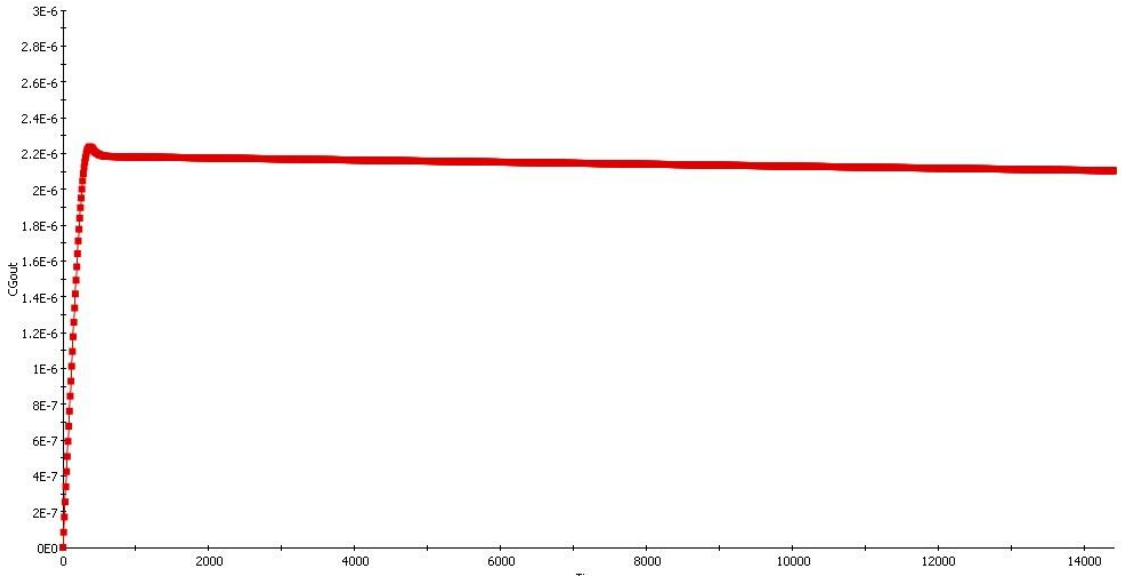

Figure 58 - Solute concentration variation, along the extractor bed, for experiment 7.

The solute concentration variation can be interpreted when looking at Figures 55 – 57. The presence of an entrainer (water) or a co-solvent (ethanol) gives higher slops to the presented curves in Figure 55 and 57. However, the higher values for the solute concentration in the fluid are for Figure 56 and 57, (experiment 5 and 7, respectively) due to the low solvent flow rate and the co-solvent presence. Even so, solute concentration in the fluid at the extractor's exit do not reach zero, which indicates that the fluid is leaving the extractor unsaturated and that the solid particle is not being completely depleted of solute.

3.2.5. β-carotene – Sunflower Oil Natural Additive

A different approach was tested in this work by using sunflower oil as a co-solvent. This study was carried out in order to determine β-carotene enrichment in the extracted oil. Sunflower oil can be used as a lipidic matrix for the cosmetic industry, e.g., in creams and lotion, so this additivation process can facilitate the transformation of this ordinary product, into a high added-value commodity. The extracted oil was compared with regular sunflower oil and in Table 24, the results are shown.

Table 24 - Sunflower oil enrichment parameters.
(SFO = Sunflower Oil, PRO = Pumpkin Residue Oil)

Parameters	
$[\beta\text{-carotene}]_{ppm}$ (SFO) [72]	24,65
$[\beta\text{-carotene}]_{ppm}$ (PRO + SFO)	499,06
Enrichment Factor	20
Extraction Time (min)	120
Accumulated CO_2 (g)	3661

According to Table 24, it is possible to see that sunflower oil enrichment was achieved, with a factor of 20. β-carotene yield of extraction varies when solvent flow rate changes, as seen so far (experiments 1 – 7), and on the other hand, sunflower oil enrichment depends on β-carotene concentration in the final extract. So, the amount of CO_2 used must be taken into account, or the final product (enriched sunflower oil) will be too diluted, and as consequence, the enrichment factor will not be maximized.

4. Conclusions and Future Work

The main objective of the present work is the β-carotene extraction from pumpkin residue, through a more environmental friendly extraction process with a supercritical fluid, carbon dioxide.

Primarily, the extraction process of oil was optimized, registering the highest extraction yield – 6,22 $mg_{Oil}/g_{Pumpkin}$ – at 325,15K, 260 bar, solvent flow rate at 30 g_{CO2}/min and co-solvent flow rate at 3 g_{EtOH}/min. For β-carotene, the highest yield of extraction was achieved at the same conditions, with a value of 533 $\mu g_{Oil}/g_{Pumpkin}$. The enrichment of sunflower oil was also achieved (325,15 K, 260 bar, 30 g_{CO2}/min and 3 $g_{Sunflower}$/min), being the resulting extracted oil (pumpkin oil and sunflower oil) enriched by a factor of 20 times, from 24 ppm (β-carotene concentration) to 499 ppm. The glycerides content varied when, water or ethanol were added, being higher when $scCO_2$ was used, 4,95 $mg_{Glycerides}/ml_{Oil}$. The extracted oil is mainly constitute by Palmitic acid (C16:0 – 24,15%), oleic acid (C18:1 – 24,24%), linoleic acid (C18:2 – 20,42%), and linolenic acid (C18:3 – 22,40%).

The second objective of this work was the estimation of the effective diffusion coefficient, through mathematical modeling of the extraction process. The modeling was done with *Gproms*® software, according to the best outcome of the set of experiments. D_e was determined accordingly to the measured data and the predict values given by the software. Experiment 7 register the highest value of D_e, 3,7330E-16 $m^2.s^{-1}$. The low value of this parameter, resumes the extraction process to a diffusion limitation of the solute inside the particle.

Regarding future work, it would be important to determine how, the oil extraction, and consequently, β-carotene extraction may be improved by changing key operating conditions that were maintained constant in this work: temperature and pressure. It is also important to understand why the presence of an entrainer (water) improves oil extraction. Ethanol concentration should be studied in order to understand how the extraction process behaves during different extraction times. On the other hand, it would be important to improve the mathematical model, so that β-carotene load in the oil, water presence and co-solvent presence would be taken into account when estimating thermodynamic parameters for the extraction process.

5. Bibliography

1. Dahlquist, E., Vassileva, I., Thorin, E. & Wallin, F. How to save energy to reach a balance between production and consumption of heat, electricity and fuels for vehicles. *Energy* **46,** 16–20 (2012).

2. Rawson, a. *et al.* Application of Supercritical Carbon Dioxide to Fruit and Vegetables: Extraction, Processing, and Preservation. *Food Rev. Int.* **28,** 253–276 (2012).

3. Constable, D. J. C., Curzons, A. D. & Cunningham, V. L. Metrics to green chemistry which are the best? *Green Chem.* **4,** 521–527 (2002).

4. Engineering, F. RECOVERY OF CAROTENOIDS FROM AGROINDUSTRIAL BY- PRODUCTS USING CLEAN EXTRACTION TECHNIQUES : SUPERCRITICAL FLUID EXTRACTION AND ULTRASOUND ASSISTED EXTRACTION. 1–7 (2013).

5. Laufenberg, G., Kunz, B. & Nystroem, M. Transformation of vegetable waste into value added products: (A) the upgrading concept; (B) practical implementations. *Bioresour. Technol.* **87,** 167–98 (2003).

6. Gustavsson, J., Cederbeg, C., Sonesson, U., Van Otterdijk, R. & Alexandre Meybeck. *Global Food Losses and Food Waste*. 1–38 (2011). at <http://www.fao.org/docrep/014/mb060e/mb060e00.pdf>

7. Instituto Nacional de Estatísitca. *Estatísticas Agrícolas 2012*. 1–180 (2012).

8. Staub, J. E. *et al. Cucurbit Genetics Cooperative*. 1–108 (2003).

9. Taylor, P. & Loy, J. B. Morpho-Physiological Aspects of Productivity and Quality in Squash and Pumpkins (Cucurbita spp .). 37–41 (2014). doi:10.1080/07352680490490733

10. Noelia, J., Roberto, M. M., Jesús, Z. J. De & Alberto, G. J. Physicochemical , technological properties , and health-bene fi ts of Cucurbita moschata Duchense vs . Cehualca A Review. *FRIN* **44,** 2587–2593 (2011).

11. Caili, F. U., Huan, S. H. I. & Quanhong, L. I. A Review on Pharmacological Activities and Utilization Technologies of Pumpkin. 73–80 (2006). doi:10.1007/s11130-006-0016-6

12. Nikolovski, B., Sovilj, M., Borota, O., Sad, N. & Serbia, R. Phytosterols in pumpkin seed oil extracted by organic solvents and supercritical CO 2. 1204–1211 (2012). doi:10.1002/ejlt.201200009

13. Salgın, U. & Korkmaz, H. A green separation process for recovery of healthy oil from pumpkin seed. *J. Supercrit. Fluids* **58,** 239–248 (2011).

14. Biesiada, A., Sokół-łe, A., Nawirska-olszan, A. & Kucharska, A. Z. Characteristics of organic acids in the fruit of different pumpkin species. **148,** 415–419 (2014).

15. Herrero, M., Mendiola, J. a, Cifuentes, A. & Ibáñez, E. Supercritical fluid extraction: Recent advances and applications. *J. Chromatogr. A* **1217,** 2495–511 (2010).

16. Herrero, M., Cifuentes, a & Ibanez, E. Sub- and supercritical fluid extraction of functional ingredients from different natural sources: Plants, food-by-products, algae and microalgaeA review. *Food Chem.* **98,** 136–148 (2006).

17. Defelice, S. The nutraceutical revolution : its impact on food industry R & D. (2000).

18. Kligman, A. The Future of Cosmeceuticals : An Interview with Albert Kligman , MD , PhD. (1938).

19. Draelos, Z. D. Nutrition and enhancing youthful-appearing skin. *Clin. Dermatol.* **28,** 400–8 (2010).

20. Anunciato, T. P. & Alves, P. Carotenoids and polyphenols in nutricosmetics , nutraceuticals , and cosmeceuticals. 51–54 (2012).

21. Temelli, F. Perspectives on supercritical fluid processing of fats and oils. *J. Supercrit. Fluids* **47,** 583–590 (2009).

22. Nicoletti, M. Nutraceuticals and botanicals: overview and perspectives. *Int. J. Food Sci. Nutr.* **63 Suppl 1,** 2–6 (2012).

23. bbc research. The Global Market for Carotenoids. 1 (2008). at <http://www.bccresearch.com/market-research/food-and-beverage/carotenoids-market-fod025c.html>

24. Krinsky, N. I. The Antioxidant and Biological Properties of the Carotenoids. **854,** 443–447 (2006).

25. Murkovic, M., Mülleder, U. & Neunteufl, H. Carotenoid Content in Different Varieties of Pumpkins. *J. Food Compos. Anal.* **15,** 633–638 (2002).

26. Wissgott, U. & Bortlik, K. I. ViewDoint Prospects for new natural food colorants. **71,** (1996).

27. Lidebjer, C., Leanderson, P., Ernerudh, J. & Jonasson, L. Low plasma levels of oxygenated carotenoids in patients with coronary artery disease. *Nutr. Metab. Cardiovasc. Dis.* **17,** 448–56 (2007).

28. Martínez, J. L. *Supercritical Fluid Extraction of Nutraceuticals and Bioactive Compounds*. 1–420 (CRC Press LLC, 2008).

29. Mattea, F., Martín, Á. & Cocero, M. J. Carotenoid processing with supercritical fluids. *J. Food Eng.* **93,** 255–265 (2009).

30. Granado, F., Olmedilla, B. & Blanco, I. ORIGINAL ARTICLE A Fast , Reliable and Low-cost Saponification Protocol for Analysis of Carotenoids in Vegetables 1. (2001). doi:10.006/jfca.2001.0989

31. Britfon, G. Structure and properties of carotenoids in relation to function. *FASEB J.* **9,** 1551–1558 (1995).

32. Schneemann, K. *Vitamins*. 26776–28029 (Wiley, 2005).

33. Edge, R., Mcgarvey, D. J. & Truscott, T. G. The carotenoids as anti-oxidants -. **41,**

34. Britton, George, Liaaen-Jensen, Synnove, Pfander, H. *Carotenoids: Handbook*. 1–687 (Birkhauser Verlag, 2004).

35. UBIC Consulting. The World Beta-Carotene Market. 1–98 (2011).

36. Ribeiro, B. D., Barreto, D. W. & Coelho, M. A. Z. Technological Aspects of β-Carotene Production. *Food Bioprocess Technol.* **4,** 693–701 (2011).

37. Opinion, S. Scientific Opinion on the re-evaluation of mixed carotenes (E 160a (i)) and. **10,** 1–67 (2012).

38. Bioeva. Vitaminas e Suplementos. 1 (2001). at <http://biovea.com.pt/product_detail.aspx?PID=2776&OS=204&AG=Beta Carotene&cp=4&NAME=BETA-CAROTENO-25,000-IU-120-C□psulas-de-Gel>

39. SkinStore. Murad. (1997). at <http://www.skinstore.com/p-3226-murad-pure-skin-clarifying-dietary-supplement.aspx>

40. SkinStore. Amazing Grace. 1 (1997). at <http://www.skinstore.com/p-2538-philosophy-amazing-grace-shower-gel.aspx>

41. SkinStore. Pevonia. 1 (1997). at <http://www.skinstore.com/p-1476-pevonia-problematic-skin-lotion.aspx>

42. Halim, R., Danquah, M. K. & Webley, P. a. Extraction of oil from microalgae for biodiesel production: A review. *Biotechnol. Adv.* **30,** 709–32 (2012).

43. Siddiquee, M. N. & Rohani, S. Lipid extraction and biodiesel production from municipal sewage sludges: A review. *Renew. Sustain. Energy Rev.* **15,** 1067–1072 (2011).

44. However, A. in *Encycl. Chem. Technol.* 1–36 (John Wiley and Sons, 2007).

45. Sahena, F. *et al.* Application of supercritical CO2 in lipid extraction – A review. *J. Food Eng.* **95,** 240–253 (2009).

46. Nasir, N. F., Daud, W. R. W., Kamarudin, S. K. & Yaakob, Z. Process system engineering in biodiesel production: A review. *Renew. Sustain. Energy Rev.* **22,** 631–639 (2013).

47. Fruhwirth, G. O. & Hermetter, A. Production technology and characteristics of Styrian pumpkin seed oil. *Eur. J. Lipid Sci. Technol.* **110,** 637–644 (2008).

48. Shi, J., Mittal, G., Kim, E. & Xue, S. J. Solubility of Carotenoids in Supercritical CO2. *Food Rev. Int.* **23,** 341–371 (2007).

49. Mchugh, M. A. & Krukonis, V. J. *Supercritical Fluid Extraction*.

50. Mukhopadhyay, M. Extraction and processing with supercritical fluids. *J. Chem. Technol. Biotechnol.* **84,** 6–12 (2009).

51. Díaz-Reinoso, B., Moure, A., Domínguez, H. & Parajó, J. C. Supercritical CO2 extraction and purification of compounds with antioxidant activity. *J. Agric. Food Chem.* **54,** 2441–69 (2006).

52. Sovova, H., Stateva, R. P. & Galushko, A. A. Solubility of i -carotene in supercritical CO 2 and the effect of entrainers. **21,** 195–203 (2001).

53. Ambrogi, A., Cardarelli, D. A. & Eggers, R. SEPARATION OF NATURAL COLORANTS USING A COMBINED HIGH PRESSURE EXTRACTION-ADSORPTION PROCESS. **326,** 323–326 (2003).

54. Linstrom, P. J. NIST Livro de Química na Web. 1 (2011). at <26/02/2014>

55. Pronyk, C. & Mazza, G. Design and scale-up of pressurized fluid extractors for food and bioproducts. *J. Food Eng.* **95,** 215–226 (2009).

56. Lucien, F. P. & Foster, N. R. Solubilities of solid mixtures in supercritical carbon dioxide: a review. *J. Supercrit. Fluids* **17,** 111–134 (2000).

57. Corporation, C. P-H Diagram for Carbon Dioxide. 1 (1999). at <http://www.chemicalogic.com/Documents/co2_mollier_chart_met.pdf>

58. Munshi, P. & Bhaduri, S. Supercritical CO2 : a twenty-first century solvent for the chemical industry.

59. Licence, P., Ke, J., Sokolova, M., Ross, S. K. & Poliakoff, M. Chemical reactions in supercritical carbon dioxide: from laboratory to commercial plant. *Green Chem.* **5,** 99–104 (2003).

60. Fukuoka, S. *et al.* A novel non-phosgene polycarbonate production process using by-product CO2 as starting material. *Green Chem.* **5,** 497 (2003).

61. Oliveira, E. L. G., Silvestre, A. J. D. & Silva, C. M. Review of kinetic models for supercritical fluid extraction. *Chem. Eng. Res. Des.* **89,** 1104–1117 (2011).

62. Huang, Z., Shi, X.-H. & Jiang, W.-J. Theoretical models for supercritical fluid extraction. *J. Chromatogr. A* **1250,** 2–26 (2012).

63. Reverchon, E. Mathematical modeling of supercritical extraction of sage oil. *AIChE J.* **42,** 1765–1771 (1996).

64. Wang, L. & Weller, C. L. Recent advances in extraction of nutraceuticals from plants. *Trends Food Sci. Technol.* **17,** 300–312 (2006).

65. Del Valle, J. M., de la Fuente, J. C. & Cardarelli, D. a. Contributions to supercritical extraction of vegetable substrates in Latin America. *J. Food Eng.* **67,** 35–57 (2005).

66. Catchpole, O. J., Bernig, R. & King, M. B. Measurement and Correlation of Packed-Bed Axial Dispersion Coefficients in Supercritical Carbon Dioxide. *Ind. Eng. Chem. Res.* **35,** 824–828 (1996).

67. However, A. in *Encycl. Chem. Technol.* **11,** 1–57 (John Wiley and Sons, 2007).

68. Catchpole, O. J. & King, M. B. Measurement and Correlation of Binary Diffusion Coefficient in Near Critical Fluids. *Phys. Chem. Chem. Phys.* **14,** 16775–94 (2012).

69. Araus, K., Uquiche, E. & del Valle, J. M. Matrix effects in supercritical CO2 extraction of essential oils from plant material. *J. Food Eng.* **92,** 438–447 (2009).

70. Del Valle, J. M. & de la Fuente, J. C. Supercritical CO2 extraction of oilseeds: review of kinetic and equilibrium models. *Crit. Rev. Food Sci. Nutr.* **46,** 131–60 (2006).

71. Diaz, M. S. & Brignole, E. a. Modeling and optimization of supercritical fluid processes. *J. Supercrit. Fluids* **47,** 611–618 (2009).

72. G. Lutfullah, A.Zeb, T. Ahmad, S. Atta, F. K. B. Changes in the Quality of Sunflower and Soybean Oils Induced by High Doses of Gamma Radiations.pdf. *J. Chem. Soc.* **25,** 269–275 (2003).

6. Annex

6.1. Annex A

Figures 58 – 64 show the implemented mathematical model code for the oil extraction process.

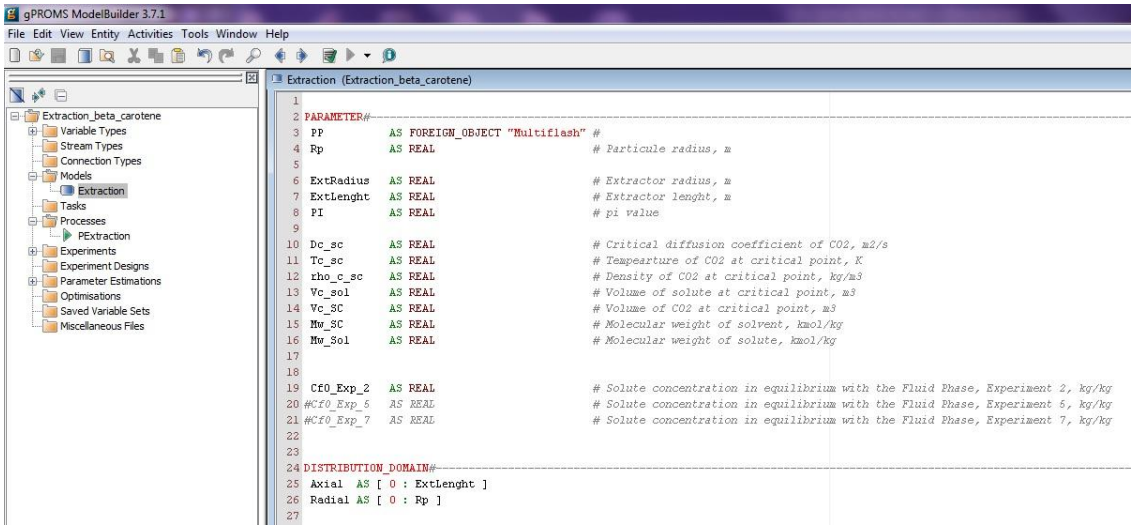

Figure 59 - Model section code - parameters and distribution domain section.

```
VARIABLE#
Cf,jf          AS distribution(axial)        OF concentration # Fluid phase concentration, g/g and solute mass flux from solid to fluid phase, g/g.s
Cs             AS distribution(axial,radial) OF concentration # Solid phase concentration, g/g
Cs0_Exp_2_5    AS concentration                               # Oil concentration in raw material, in Experiments 2-5, g/g
#Cs0_Exp_7     AS concentration                               # Oil concentration in raw material, in Experiments 7, g/g

Dax            AS diffusion_extractor                        # Axial dispersion coefficient, m2/s
De             AS diffusion_particle                         # Effective dispersion coefficient, m2/s
D12            AS binary_dif_coef                            # Binary diffusion coefficient, m2/s

u              AS velocity                                   # Fluid interstitial velocity , m/s
kf             AS mass_coefficient                           # Mass transfer coefficient, m2/s
k              AS partition                                  # Partion coefficient
rho_sc         AS density                                    # Supercritical CO2 density, kg/m3
Ebed           AS porosity                                   # Bed porosity
ap             AS area_particule                             # Particule effective area, m2
Ext_Area       AS area_extractor                             # Extractor base area, m2

Qm_Exp_2       AS flowrate                                   # Fluid flow rate, kg/s
#Qm_Exp_5      AS flowrate                                   # Fluid flow rate, kg/s
#Qm_Exp_7      AS flowrate                                   # Fluid flow rate, kg/s

T              AS temperature                                # Operating temperature, K
P              AS pressure                                   # Operating pressure, bar

Re             AS reynolds                                   # Reynolds number
Sc             AS schmidt                                    # Schmidt number
X              AS diffusion_particle
S              AS diffusion_particle
miu            AS viscosity                                  # scCO2 dynamic viscosity, Pa/s or kg/m.s


mass_p_Exp_2   AS mass_pumpkin                               # Pumpkin mass, kg
#mass_p_Exp_5  AS mass_pumpkin                               # Pumpkin mass, kg
#mass_p_Exp_7  AS mass_pumpkin                               # Pumpkin mass, kg

Y              AS yield                                      # Yield, %
oil            AS oil_out                                    # Oil extracted, g/g
```

Figure 60 - Model section code - variables section.

```
SET#-------------------------------------------------------------
 PP := "C:\Users\Jose\CO2.mfl";

BOUNDARY#--------------------------------------------------------
#------------------------- Extractor ------------------------
  # z = 0
    Dax*partial(Cf(0),axial)- u*Cf(0) = 0 ;
  # Z = L
    partial(Cf(ExtLenght),axial) = 0 ;

#------------------------- Particule ------------------------
  # r = 0
    partial(Cs(,0),radial) = 0 ;
  # r = R
    kf*(Cs(,Rp)/k - cf) = -De*partial(Cs(,Rp),radial) ;
```

Figure 61 - Model section code - set and boundary section.

```
EQUATION#--------------------------------------------------------------------------------------------------------
#------------------------ Parameters Extimation ------------------------------------------------------------------

#------------------------ Fluid Density and Viscosity ------------------------------------------------------------

  rho_sc = pp.liquiddensity(T+273.15,P*101303,1)   ;
  miu    = pp.liquidviscosity(T+273.15,P*101303,1) ;

#------------------------ Solute Diffusion Coefficient -----------------------------------------------------------
  Re = (2*Rp*u*rho_sc)/miu ;

  X = ((1 + (Vc_sol/Vc_SC)^(1/3))^2)/((1 + (Mw_SC/Mw_Sol))^(1/2)) ;

  S = 1.0 ;

  Dl2 = 5.152*Dc_sc*(T/Tc_sc)*((rho_sc/rho_c_sc)^(-2/3) - 0.4510)*(S/X) ; # Catchpole and King

  Dax = Dl2*((157.7*Re^2 + 0.284*Re + 0.199)/(Re+0.7)) ;                  # Catchpole_et_al, Re = 2-80, Sc = 15.77

#------------------------ Convective Mass Transfer Coefficient ---------------------------------------------------
  Sc = (miu/rho_sc)/Dl2 ;

  kf = (Dl2*(2.2 + 1.1*Re^(0.6)*Sc^(1/3)))/(2*Rp) ;                       # Wakao and Funazkri, Re = 3-10000

#------------------------ Extractor and Particule Area -----------------------------------------------------------
  Ext_Area = PI*ExtRadius^2 ;

  ap       = (6/(2*Rp))     ;
```

Figure 62 - Model section code - equations section (part 1).

```
#------------------------ Flow Rate, Velocity, Partition Coefficient and Solute Mass Flux -------

  Qm_Exp_2   = 100.0/(1000*60)                  ;
 #Qm_Exp_5   = 10.0/(1000*60)                   ;
 #Qm_Exp_7   = 32.8/(1000*60)                   ;


  u          = Qm_Exp_2/(rho_sc*Ext_Area*ebed)  ;

  k          = Cs0_Exp_2_5/Cf0_Exp_2            ;

  jf         = kf*(Cs(,Rp)/k - Cf)              ;

#------------------------ Mass Balance - Fluid Phase -------------------------------------------------
 FOR z := 0|+ TO ExtLenght|- DO
   $Cf(z) = Dax*partial(Cf(z),axial,axial) - u*partial(Cf(z),axial) + ap*(1-ebed)/ebed * jf(z) ;
 END

#------------------------ Mass Balance - Particule Phase ---------------------------------------------
 FOR z := 0 TO extLenght DO
  FOR r := 0|+ TO Rp|- DO
   $Cs(z,r) = (De/r^2)*partial(r^2*partial(Cs(z,r),radial),radial) ;
  END
 END

#------------------------ Oil Balance and Yield ------------------------------------------------------
 $oil = Cf(ExtLenght)*Qm_Exp_2 ;
 Y    = (oil/mass_p_Exp_2)*100 ;
```

Figure 63 - Model section code - equations section (part 2).

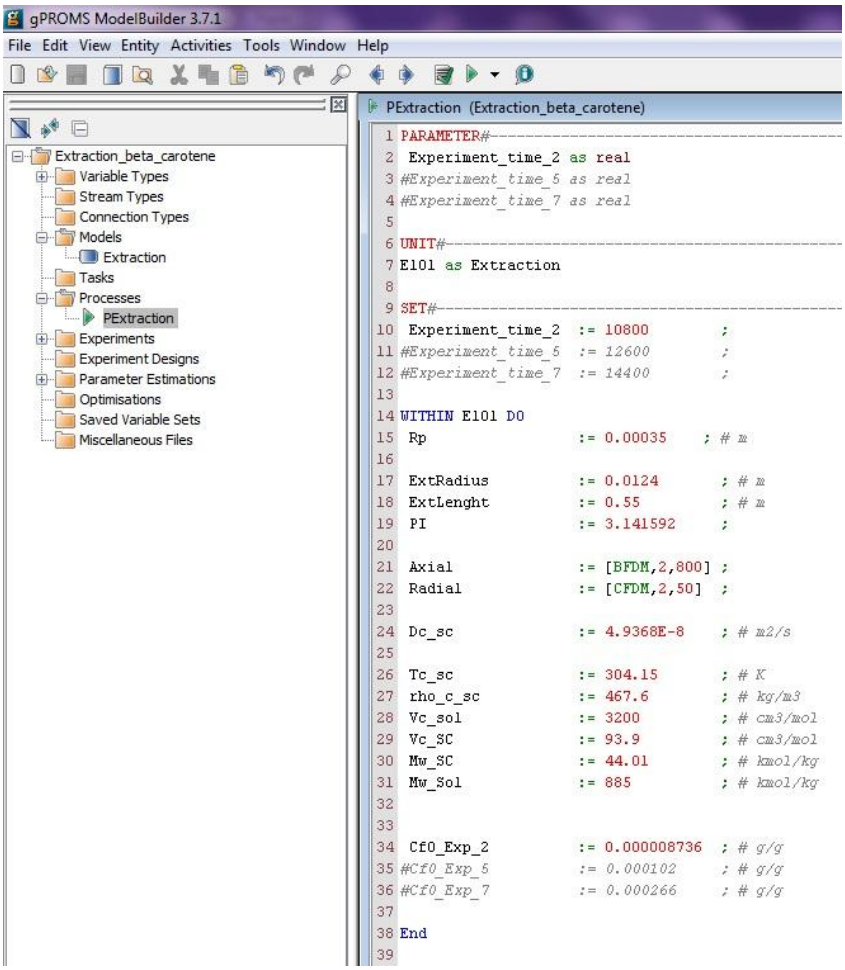

Figure 64 - Process section code - parameters, unit and set sections.

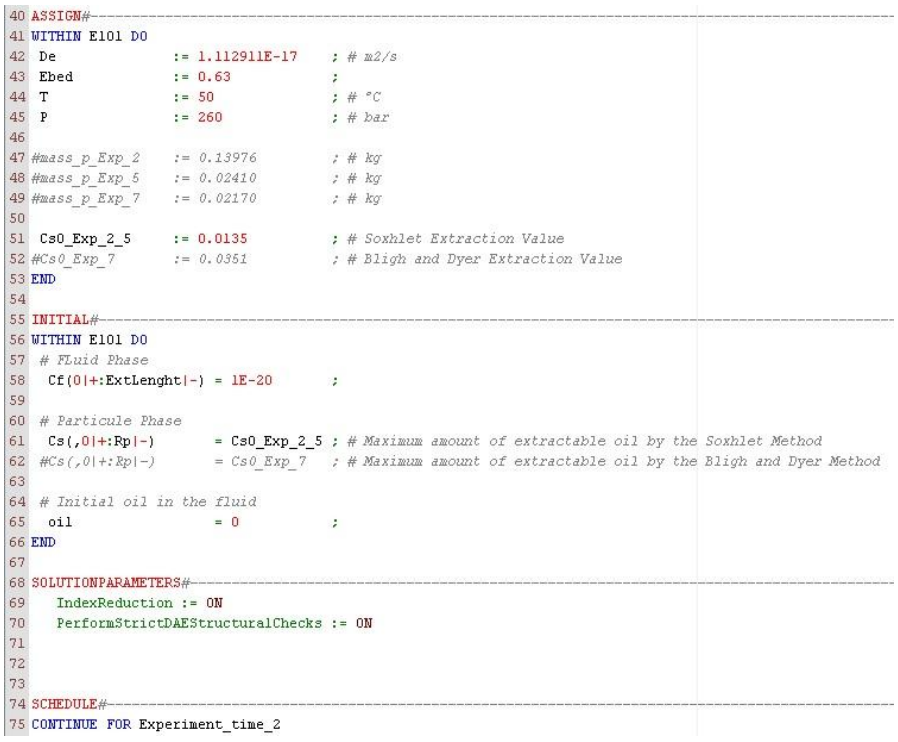

Figure 65 - Process section code - assign, initial conditions, solution parameters and schedule sections.

6.2. Annex B

Table 25 - Fatty acid profile of extracted oil with scCO2.

Name	Notation	Retention Time (min)	Peak Area	Peak Area/IS Peak Area	%
Myristic	C14:0	2,600	17840	0,3428	1,08
Palmitic	C16:0	3,230	399152	7,6700	24,15
Palmitoleic	C16:1	3,300	3801	0,0730	0,23
Stearic	C18:0	3,830	120727	2,3198	7,30
Oleic	C18:1	3,890	400564	7,6971	24,24
Linoleic	C18:2	4,040	337552	6,4863	20,42
Linolenic	C18:3	4,270	370218	7,1140	22,40
Eicosanoic	C20:0	4,350	2973	0,0571	0,18
Internal Standard (IS)					
Name	Notation	Retention Time (min)	Peak Area		
Heptadecanoic Acid	C17:0	3,530	52041		

6.3. Annex C

Figure 65, Figure 66 and Figure 67 show the calibration plots for experiment 1 to 5, experiment 6, 7, Soxhlet method and Bligh and Dyer method, and experiment 8, respectively. Calibration plots for mono-, di-, and triglycerides are shown in Figure 68 to 70, respectively.

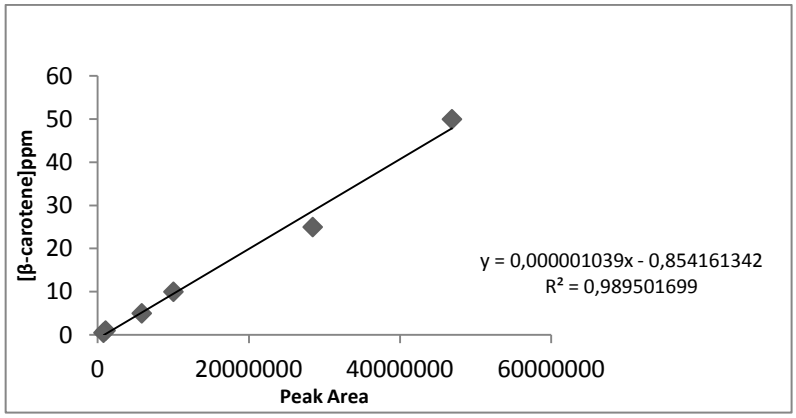

Figure 66 - Calibration plot for experiment 1 to 5.

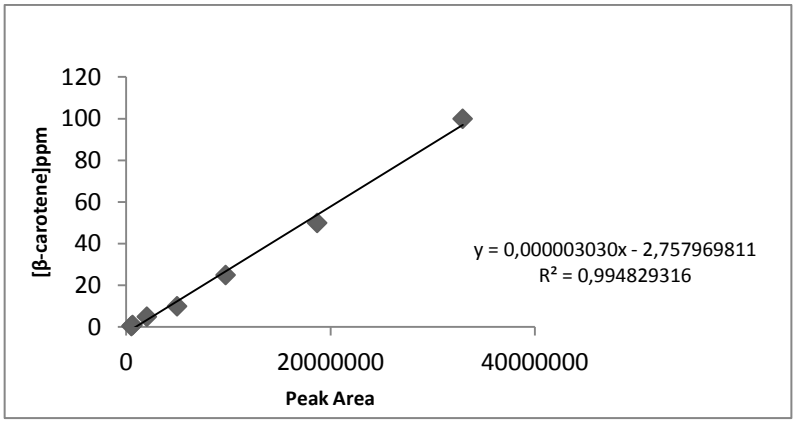

Figure 67 - Calibration plot for experiment 6, 7, Soxhlet method and Bligh and Dyer method.

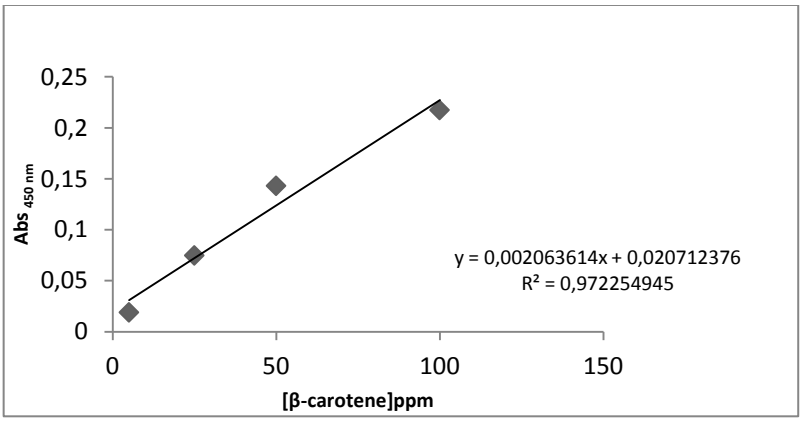

Figure 68 - Calibration plot for experiment 8.

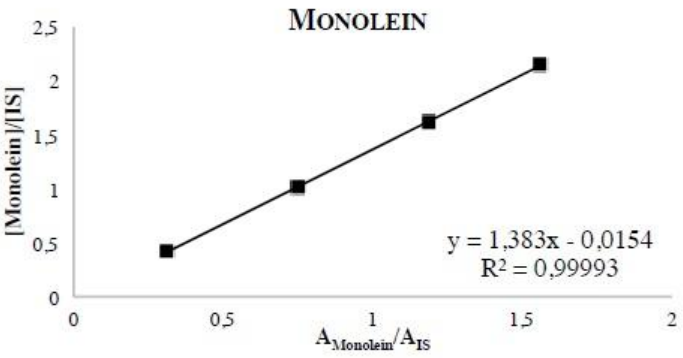

Figure 69 - Calibration plot for monoglycerides.

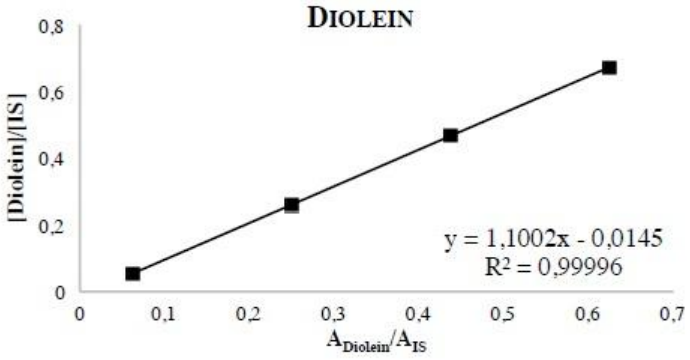

Figure 70 - Calibration plot for diglycerides.

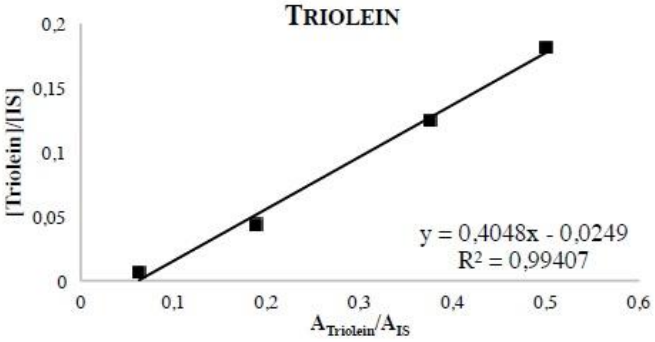

Figure 71 - Calibration plot for triglycerides.

6.4. Annex D

Table 26 - Fatty acid chemical structure.

Fatty Acid	Chemical Structure
Myristic Acid (C14:0)	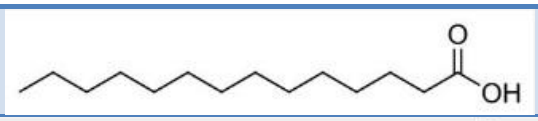
Palmitic Acid (C16:0)	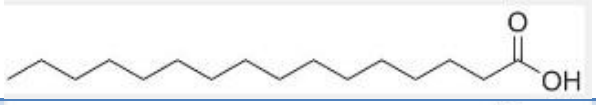
Palmitoleic Acid (C16:1)	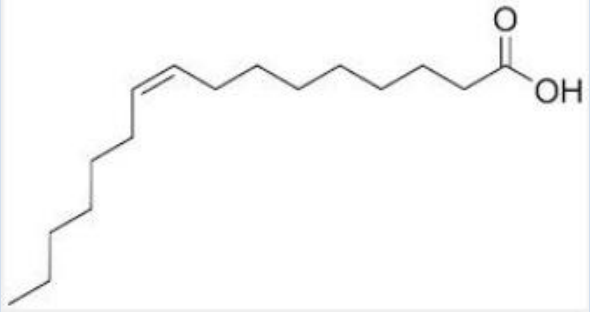
Heptadecanoic Acid (C17:0)	
Stearic Acid (C18:0)	
Oleic Acid (C18:1)	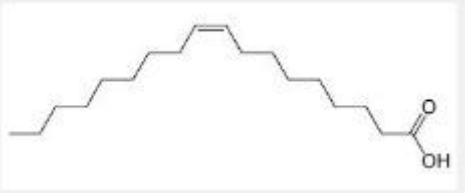
Linoleic Acid (C18:2)	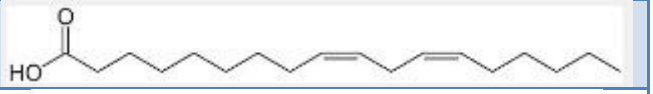
Linolenic Acid (C18:3)	
Eicosanoic Acid (C20:0)